Universidad Autónoma de Madrid

Facultad de Ciencias
Departamento de Física Teórica

Consejo Superior de Investigaciones Científicas

Instituto de Física Teórica
IFT UAM-CSIC

Applications of the Dirac operator in the adjoint representation to Yang-Mills Theories

Alfonso Sastre Bruno

Madrid, Junio 2010.

Universidad Autónoma de Madrid

Facultad de Ciencias
Departamento de Física Teórica

Consejo Superior de Investigaciones Científicas

Instituto de Física Teórica
IFT UAM-CSIC

Applications of the Dirac operator in the adjoint representation to Yang-Mills Theories

Memoria de Tesis Doctoral realizada por
D. Alfonso Sastre Bruno,
presentada ante el Departamento de Física Teórica
de la Universidad Autónoma de Madrid
para la obtención del Título de Doctor.

Trabajo dirigido por
Dr. D. Antonio González-Arroyo España,
Catedrático de Física Teórica de la Universidad Autónoma de Madrid,

y co-dirigida por
Dra. Dña. Margarita García Pérez,
Científica Titular del Instituto de Física Teórica UAM-CSIC.

Madrid, Junio 2010.

Contents

Prefacio

A lo largo del siglo XX se ha producido un gran avance en el entendimiento de la estructura interna de la materia. Actualmente toda la materia visible puede explicarse en términos de unas pocas partículas: quarks y leptones. La interacción de estas partículas puede ser explicada mediante solo cuatro fuerzas: la interacción gravitatoria, la interacción electromagnética, la interacción fuerte y la interacción débil. De modo que podemos explicar casi todos los fenómenos que observamos con solo unos pocos ingredientes.

Las interacciones electromagnética, débil y fuerte, actualmente se enmarcan en el denominado Modelo Estándar. El Modelo Estándar es una Teoría Cuántica de Campos, basada en la Simetría Gauge $SU(3) \times SU(2) \times U(1)$. Este modelo permite explicar la dinámica de las partículas fundamentales a escalas inferiores al núcleo atómico. A altas energías el uso de la Teoría de Perturbaciones ha permitido verificar con gran precisión muchas de las predicciones de la teoría. Sin embargo, existen problemas como el Confinamiento o la Ruptura Espontánea de la Simetría Quiral que no pueden ser tratados con estas técnicas, debido a su carácter no perturbativo. Una de las corrientes más extendidas, defiende que estos problemas están dominados por la dinámica generada por ciertas pseudo-partículas presentes en el vacío de la teoría. La naturaleza de estos objetos está determinada por las propiedades topológicas de la teoría.

Aunque las propiedades de muchas de estas pseudo-partículas son conocidas, es necesario calcular cual es su contribución a la Integral de Camino. Para estudiar estos problemas, se han desarrollado nuevos métodos de cálculo que incluyen estos efectos no perturbativos. El más extendido, se basa en definir la Teoría Cuántica de Campos en un espacio-tiempo discreto, denominado Retículo. La Teorías en el Retículo, permiten dar una definición rigurosa de la Integral de Camino. Aunque el número de grados de libertad permanece finito en estas teorías, su elevado número requiere de un tratamiento estadístico.

En la mayor parte de los cálculos realizados en Teorías en el Retículo, se generan configuraciones mediante métodos Monte Carlo. Estas configuraciones están dominadas por momentos de Fourier altos, los cuales enmascaran las estructuras extendidas que definen las propiedades topológicas de la configuración. Conocer la distribución en que estas estructuras aparecen, nos permitiría conectar los resultados obtenidos en el Retículo con modelos basados en la aproximación semi-clásica.

A lo largo de los últimos 30 años, se han desarrollado muchas técnicas para extraer información acerca de estas estructuras. Algunas de ellas se basan en modificar las configuraciones con algoritmos que reduzcan los modos de Fourier más altos. El problemas de estas técnicas es que modifican también los modos más bajos y por tanto las estructuras topológicas iniciales. En lo últimos años, se ha usado el operador de Dirac, como método para filtrar las configuraciones sin modificarlas. Este es posible por dos razones:

- El operador de Dirac es menos sensible a los modos altos de Fourier.
- El Teorema de Índice relaciona la carga topológica de las configuraciones gauge con

los modos cero del operador de Dirac.

Generalmente se ha empleado la representación fundamental para este propósito. En esta tesis se estudia el uso de estas técnicas con fermiones en la representación adjunta. La razón princpal, es que esta representación presenta una propiedad adicional: para soluciones clásicas de las ecuaciones gauge, se puede construir una solución de la ecuación de Dirac, cuya densidad corresponde con la densidad de acción gauge. Para encontrar esta solución, hemos definido un operador a partir de una determinada proyección del operador de Dirac. Hemos conseguido obtener una implementación de este operador en el Retículo basado en el operador de Neuberger. En orden de testar cuales son las limitaciones numéricas del método se han analizado un amplio rango de situaciones. Estos test incluyen problemas relacionados con:

- Efectos de la discretización.
- Efectos de volumen finito.
- Violaciones de la condición de solución clásica.
- Inclusión de ruido de alta frecuencia.

En todos estos casos hemos sido capaces de reproducir la densidad de acción gauge esperada.

Como paso previo al estudio en el Retículo, estudiamos de forma analítica algunas de las soluciones clásicas de la ecuación de Dirac en la adjunta. Esto nos permite conocer cuales son las estructuras que aparecen en este tipo de soluciones. A lo largo de este proceso, hemos obtenido las soluciones analíticas del operador de Dirac en la representación adjunta asociadas a unas pseudo-partículas denominadas Calorones. Estas soluciones son relevantes en el estudio de sistemas a temperatura finita y también en construcciones supersimétricas de las teorías gauge.

Las soluciones que hemos encontrado, pueden ser útiles en el estudio de teorías que incluyan fermiones en la representación adjunta. Este tipo de teorías son habituales en extensiones al Modelo Estándar. Dos claros ejemplos son la Supersimetría y los modelos de Tecnicolor. En los últimos años, se ha comenzado a usar esta representación para el estudio de la expansión a gran N.

La tesis esta estructurada de la siguiente forma: el formalismo necesario para el desarrollo de la tesis es introducido en los capítulos del 1 al 3. En el capítulo 1, se introducen las nociones básicas de la Teoría Cuántica, centrándonos en su formulación Euclídea y en la definición de la aproximación semi-clásica. El capítulo 2 esta dedicado a introducir el concepto de Teoría Gauge y su formulación matemática. Se desarrollan algunas de las soluciones clásicas conocidas para estas teorías. Estas soluciones son necesarias en el uso de la aproximación semi-clásica. A continuación se introduce la formulación de la TCC en el Retículo en el capítulo 3. Finalmente en el capítulo 4 se resumen las propiedades generales del espectro del operador Dirac en la representación adjunta. Los resultados obtenidos en la tesis se desarrollan en los capítulos 5 y 7. El capítulo 5 esta dedicado al estudio de soluciones de la ecuación de Dirac en la representación adjunta en presencia de

un Calorón. Hemos deducido las soluciones a esta ecuación para el grupo gauge SU(N), para varias condiciones de contorno en la dirección temporal. En el capítulo 6, se define una solución de operador de Dirac en la representación adjunta que reproduce la densidad del campo gauge presente. Se propone usar esta solución como método para obtener una imagen filtrada de las configuraciones gauge generadas por métodos Monte Carlo. La solución es obtenida minimizando un operador definido a partir del operador de Dirac. El método es testado para comprobar su eficiencia y limitaciones. En el capítulo 7 se resumen los resultados obtenidos. Los aspectos más técnicos son desarrollados en los apéndices.

Chapter 1

Basics in QFT

Quantum field theory (QFT) is a way to combine the quantum mechanics and the principle of relativity. Nowadays, QFT is the theoretical framework to understand Particle Physics. In this chapter we present the basic ideas of the formulation. Technical details will be omitted, the interested reader can find a complete review in any of the many books written about it.

1.1 The Euclidean Path integral formulation

The path integral approach to Quantum Mechanic was introduced by Feynmann [1]. In this formulation, the probability amplitude for a particle to move from point x to point y within the time interval t is

$$\langle y|e^{-iHt}|x\rangle = \int Dz e^{\frac{i}{\hbar}S[z]}, \tag{1.1}$$

where $S[z]$, is the action associated to z trajectory,

$$S[z] = \int_0^t \left(\frac{1}{2}m\dot{z}^2 - V(z)\right) dt'. \tag{1.2}$$

In this approach all classical paths contribute to the probability amplitude weighted by the phase term. The mathematical meaning of these integrals is not clear yet, due to the complex oscillating term. A better mathematical framework is obtained if the time direction, t is rotated to an imaginary time, τ, by

$$t \to -i\tau, \;\; \tau > 0. \tag{1.3}$$

The path integral is written as

$$\langle y|e^{-H\tau}|x\rangle = \int Dz e^{-\frac{1}{\hbar}S_E[z]}, \tag{1.4}$$

where S_E is the euclidean action,

$$S[z] = \int_0^\tau \left(\frac{1}{2}m\dot{z}^2 + V(z)\right) d\tau'. \tag{1.5}$$

The Euclidean PI is real and the oscillations are suppressed.

In the Euclidean Quantum Field Theory formulation paths, $x(\tau)$, are replaced by fields, $\phi(x)$, in R^4. The PI is written in term of these fields as

$$Z = \int D\phi e^{-\frac{1}{\hbar}S[\phi]} \tag{1.6}$$

and the mean value of an operator $\mathrm{O}(\phi)$ is given by

$$\langle \mathrm{O}(\phi) \rangle = \frac{1}{Z} \int D\phi \mathrm{O}(\phi) e^{-\frac{1}{\hbar}S[\phi]}. \tag{1.7}$$

The Euclidean QFT formulation is quite similar to the statistical mechanics at finite temperature, and many of the notation and techniques are inherited.

A large part of the most interesting QFT are written in terms of gauge and fermion fields (discussed in chapter 2). In term of these fields the path integral is written as

$$Z = \int D\bar{\psi} D\psi DA_\mu e^{-\frac{1}{\hbar}S[\bar{\psi},\psi,A_\mu]}, \tag{1.8}$$

$$\left\langle \mathrm{O}(\bar{\psi},\psi,A_\mu) \right\rangle = \frac{1}{Z} \int D\bar{\psi} D\psi DA_\mu \mathrm{O}(\bar{\psi},\psi,A_\mu) e^{-\frac{1}{\hbar}S[\bar{\psi},\psi,A_\mu]}. \tag{1.9}$$

The main problem is how to compute Eq. 1.9. The first problem is that the number of degrees of freedom in Quantum Field Theory is infinite, and some of the integrals involved are divergent. Part of the divergence come from the contribution of ultraviolet modes . The addition of a regulator restricts the largest modes, and the integral remains finite.

Once the divergence problem is under control, it is necessary to compute the integral 1.9. The most common method is Perturbation Theory, where Eq. 1.9 is expanded in terms of the coupling constants, and each term is regularized independently. This is a very useful method when the coupling constants are small and non-perturbative effects are not involved in the problem. In order to study non-perturbative aspects of the theory, the most powerful tool is the lattice formulation introduced by Wilson [2] and reviewed in chapter 3. A different approach is the semi-classical approximation explained in the following section.

1.2 The Semi-classical approximation

Quantum tunnelling is a phenomenon characteristic of Quantum Mechanics. It allows a particle to cross a potential barrier connecting different minima of the potential. In Classical Mechanics, this situation is forbidden since the kinetic energy of the particle becomes negative. After Wick rotation, this situation changes since the potential changes sign two vacua can be connected by an euclidean classical trajectory. The tunnelling amplitude is exponentially suppressed and it is given in terms of the action of the euclidean classical solutions. In this sense, there is a relation between the tunnelling process and classical solutions in Euclidean time.

In the Euclidean PI formulation, the contribution of each configuration is weighted by its action, Eq. 1.9. In this formulation, the action can be expanded around a classical solution

$$S \to S_{cl} + \delta S(\bar{\psi}, \psi, A_\mu)\,, \tag{1.10}$$

and the quantum correction can be computed by integrating the fluctuations around the classical solutions. If the fields are deformed by a small perturbation as

$$A_\mu \to A_\mu^{cl} + \delta A_\mu, \tag{1.11}$$

$$\psi \to \psi^{cl} + \delta\psi, \tag{1.12}$$

$$\bar{\psi} \to \bar{\psi}^{cl} + \delta\bar{\psi}, \tag{1.13}$$

the Lagrangian, to quadratic order in the fluctuations is given by

$$\begin{aligned} L(\bar{\psi}, \psi, A_\mu) &= L_{cl}(\bar{\psi}^{cl}, \psi^{cl}, A_\mu^{cl}) + \delta\bar{\psi} M_D \delta\psi \\ &+ \frac{1}{2}\delta A_\mu M_G \delta A_\mu + O(\delta\bar{\psi}, \delta\psi, \delta A_\mu)^3 \end{aligned} \tag{1.14}$$

The evaluation of the path integral involves the computation of the determinant of the M_D and M_G fluctuation operators. The technical aspects of the calculations will not be discussed here (see for example [3]). We only discuss the special case in which the operators M_D and M_G have zero-modes. These zero-modes are related with symmetries in the Lagrangian that allow to change the classical solution, without energy cost, i.e. to moduli in the space of classical solutions. If the explicit form of the zero-modes is known, they can be projected out from the determinant and parametrized by explicit integration of the so called collective coordinates. The probability amplitude of tunneling is written as

$$T \sim e^{-S_0/\hbar} \int D[Z] \det(M_D)(\det(M_G))^{-1/2} + O(\hbar^{-2}), \tag{1.15}$$

where $D[Z]$ represents the integration over the collective coordinates.

We will address along the thesis the discussion of a particular set of self-dual deformations of the classical solutions which are directly related to adjoint zero-modes of the Dirac operator that will be discussed in chapter 5.

Chapter 2

Gauge Theories

The Gauge principle is the framework to understand the dynamics elementary particles. Initially QFT developed in the attempt to construct a quantum theory of electrodynamics. Later, two new interactions were discovered and explained in a similar way. All these theories are encompassed in a mathematical framework called Gauge theories. In this chapter Gauge theory is introduced by imposing invariance of the fermionic action under local phase transformations.

Electromagnetic theory is rewritten in Gauge language in the first section. In the second one, Gauge theory is extended to the non-abelian group $SU(N)$ by adding Yang-Mills fields. In the last section some interesting solutions of the euclidean Yang-Mills equations are presented.

2.1 Electromagnetism as a gauge theory

The classical theory of electromagnetism is defined by the action

$$S = \int dx^4 \bar{\psi}(i\gamma^\mu \partial_\mu - m)\psi - \frac{1}{4e^2} F_{\mu\nu}F^{\mu\nu} + \bar{\psi}\gamma^\mu A_\mu \psi, \tag{2.1}$$

where gamma matrices satisfy the anti-commutation relations

$$\{\gamma_\mu, \gamma_\nu\} = 2\eta_{\mu\nu}. \tag{2.2}$$

The first term in Eq. 2.1 is the electron kinetic term, the second one is a function of the vector potential, $F_{\mu\nu} = \partial_\mu A_\nu - \partial_\nu A_\mu$, and the last one is the coupling term between the electron field and the vector potential. The field strength, $F_{\mu\nu}$, is invariant under transformations of the vector potential given by:

$$A_\mu(x) \to A_\mu(x) - \partial_\mu \omega(x). \tag{2.3}$$

The kinetic term of the matter field and the coupling term can be grouped by introducing a new operator D_μ as,

$$\bar{\psi}\gamma^\mu D_\mu \psi \equiv \bar{\psi}\gamma^\mu(\partial_\mu - iA_\mu)\psi, \tag{2.4}$$

the electron field can be transformed by

$$\psi \to e^{-i\omega(x)}\psi, \quad \bar{\psi} \to e^{i\omega(x)}\bar{\psi}, \tag{2.5}$$

and the new operator has the same transformation properties:

$$D_\mu\psi \to e^{-i\omega(x)}D_\mu\psi. \tag{2.6}$$

Accordingly the whole action is invariant under this transformation.

In this context, invariance of the theory under local phase transformations can be obtained by coupling it to an electromagnetic field. This fact can be generalized to more complex phase-space transformations by using non-abelian gauge theories [4], which are formulated in the next section for the group $SU(N)$.

2.2 Non-Abelian Gauge theory

Consider the action of a free fermion composed by N internal degrees of freedom of equal mass:

$$S = \int dx^4 \bar{\psi}\left(i\gamma^\mu\partial_\mu - m\right)\psi, \tag{2.7}$$

where ψ and $\bar{\psi}$ are N-vectors. This Lagrangian is invariant under the global transformation:

$$\psi(x) \to \Omega\psi(x); \quad \bar{\psi}(x) \to \bar{\psi}(x)\Omega^\dagger \tag{2.8}$$

where Ω is an element of $SU(N)$. This global symmetry can be extended to a local one by transforming the fermions fields as

$$\psi(x) \to \Omega(x)\psi(x); \quad \bar{\psi}(x) \to \bar{\psi}(x)\Omega^\dagger(x) \tag{2.9}$$

where now the matrix $\Omega(x)$ is space-time dependent. Using the fact that $SU(N)$ is a Lie group, any element $\Omega \in SU(N)$ can be written as $\Omega(x) = e^{-i\omega^a(x)T^a}$, where $\omega^a(x)$ are $\mathrm{N}^2 - 1$ real functions and T^a are the generators of the Lie algebra of the gauge group in the fundamental representation defined by

$$tr(T^aT^b) = \frac{1}{2}\delta^{ab}, \quad \left[T^a, T^b\right] = if^{abc}T^c, \tag{2.10}$$

where the structure constants, f^{abc}, are real and antisymmetric. By transforming the fermionic action according to Eq. 2.9, a new term appears in Eq. 2.7

$$S \to \int dx^4 \bar{\psi}(x)\left(i\gamma^\mu\partial_\mu - m\right)\psi(x) - i\bar{\psi}(x)\gamma_\mu\left(\Omega(x)\partial_\mu\Omega^\dagger(x)\right)\psi, \tag{2.11}$$

The additional term is quite similar to the coupling term in electromagnetism. We can develop further this parallelism. In order to do that, a new derivative operator, D_μ, is defined as

$$D_\mu(x) = \partial_\mu - iA_\mu(x), \tag{2.12}$$

where $A_\mu(x)$ is an element of the lie algebra of $SU(N)$. Let us impose that the new derivative transforms as

$$D_\mu\psi(x) \to \Omega D_\mu\psi(x). \tag{2.13}$$

Accordingly the A_μ fields must be transformed as

$$A_\mu \to \Omega A_\mu \Omega^\dagger + i\Omega\partial_\mu\Omega^\dagger. \tag{2.14}$$

In conclusion, like in the electromagnetic case, an invariant action under local transformations can be obtained by adding a vector field.

Finally, a new term must be added to the action in order to generate the dynamics of the Yang-Mills fields, A_μ. The action of these fields is constructed by imposing invariance under gauge and Lorentz transformations. The resulting action is given by

$$S_{YM} = \frac{1}{2g^2}\int d^4x \mathrm{Tr}(F_{\mu\nu}F^{\mu\nu}), \tag{2.15}$$

where $F_{\mu\nu} = \partial_\mu A_\nu - \partial_\nu A_\mu - i\left[A_\mu, A_\nu\right]$ and g is the coupling constant.

Until now, the formulation of Gauge theory has been done in Minkowski space. The Wick rotation, Eq. 1.3, involves the following changes

$$\{\gamma_\mu^E, \gamma_\nu^E\} = 2\delta_{\mu\nu}. \tag{2.16}$$

if the gamma matrices are selected as: $\gamma_\mu = \gamma_\mu^\dagger = \gamma_\mu^{-1}$. The euclidean gamma matrices can be obtained as

$$\gamma_4^E = \gamma^0; \;\; \gamma_i^E = -i\gamma^i. \tag{2.17}$$

In addition ∂_0 and A_0 are changed as

$$\partial_0 \to i\partial_4, \tag{2.18}$$
$$A_0 \to iA_4. \tag{2.19}$$

The euclidean action is given by

$$S_E = \int dx^4 \bar{\psi}\left(\gamma_\mu^E D_\mu + m\right)\psi + \frac{1}{2g^2}\mathrm{Tr}(F_{\mu\nu}F_{\mu\nu}). \tag{2.20}$$

An important part of the dynamics of elementary particles resides in the interaction of Yang-Mills fields. Therefore, the understanding of the pure Yang-Mills theory (without fermions) is a crucial first step for a complete understanding of the Standard Model dynamics. The contribution of these fields to the path integral is directly related with problems like: confinement, spontaneous chiral symmetry breaking ($S\chi SB$), asymptotic freedom.

2.2.1 A note about non-trivial topological configurations in Yang-Mills theory

Under Lorentz and gauge symmetry invariance, another term is allowed in Eq. 2.20,

$$S_Q = \frac{1}{2}\int d^4x \epsilon_{\mu\nu\sigma\rho}\mathrm{Tr}(F_{\mu\nu}F_{\sigma\rho}). \tag{2.21}$$

This term can be rewritten as a pure divergence

$$\frac{1}{2}\epsilon_{\mu\nu\sigma\rho}\mathrm{Tr}(F_{\mu\nu}F_{\sigma\rho}) = \partial_\mu K^\mu, \tag{2.22}$$

where $K_\mu = 2\epsilon_{\mu\nu\sigma\rho}\mathrm{Tr}(A_\nu\partial_\rho A_\sigma - \frac{2}{3}iA_\nu A_\rho A_\sigma)$. Hence, the value of the integral, Eq. 2.21, is determined by the value of K_μ at infinity. In order to obtain a finite action, the field strength must go to zero when $|x|$ goes to infinity. This condition implies that the gauge fields go to a pure gauge at infinity,

$$A_\mu(x) \to i\Omega^\dagger(x)\partial_\mu\Omega(x). \tag{2.23}$$

The possible values of these integrals are classified by the homotopy classes which are determined by the topological winding number $n \in Z$. Then, value of term S_Q is quantized by

$$S_Q = 8\pi^2 n. \tag{2.24}$$

A way to find classical solutions with a non-zero value of the topological charge begins from the relation:

$$0 \leq \frac{1}{4}\int d^4x \mathrm{Tr}(F_{\mu\nu} \pm \tilde{F}_{\mu\nu})^2 = \frac{1}{2}\int d^4x \mathrm{Tr}\left(F_{\mu\nu}^2 \pm F_{\mu\nu}\tilde{F}_{\mu\nu}\right). \tag{2.25}$$

The first term of the last integral is the Yang-Mills action, and the other one corresponds to the topological charge. So the last expression can be written as

$$S_{YM} \geq |S_Q| = 8\pi^2|n|. \tag{2.26}$$

The equality is fulfilled when A_μ is (anti)self-dual, $F_{\mu\nu} = \pm\tilde{F}_{\mu\nu}$. This is a very useful result, since the (anti)self-dual condition only involve first derivatives. So the problem is reduced to find solutions to the self-duality condition. Some of the known self-dual solutions for Yang-Mills theories are presented in the following section.

2.3 Classical Solutions in Yang-Mills theories

Finding the complete set of classical solutions of the Yang-Mills theory is an open problem. In this section some of the solutions found in the last years are presented. One of the most interesting example is the instanton [5]. This solution was used by t'Hooft to postulate a solution to the $U_A(1)$ problem [3]. Many other problems related with the QCD dynamics (confinement, SχSB, ...) have been addressed using these kind of solutions, but their

contribution is still unclear. As an example the realization of SχSB through the Banks-Casher relation [6] can be mentioned. The value of the chiral condensate is proportional to the quasizero-mode density of the Dirac operator. The Atiyah-Singer index theorem [7, 8] associates a zero-mode of the Dirac operator to each instanton. In this way, configurations with large number of instantons and anti-instantons are expected to have large number of quasizero-modes. Models like the Instanton Liquid [9, 10, 11] are based in these ideas.

Much progress has been attained since the discovery of the instanton. For instance, all the (anti)self-dual solutions for R^4 can be computed using the ADHM construction [7, 8]. Other interesting solutions can be obtained in other manifolds, like monopoles in R^3, vortices in $R^2 \times T^2$ or calorons in $R^3 \times S^1$. The latter are interesting in several ways. First, the manifold $R^3 \times S^1$ is used in the definition of Yang-Mills theories at finite temperature. In addition, instanton and monopole solutions can be related by tuning the size of periodic direction. For the gauge group $SU(2)$ and topological charge one, the solution was found by Harrington and Shepard in [12, 13] for trivial holonomy in the time direction, and it was generalised to non-trivial holonomy by Kraan-Van Baal [14, 15] and Lee [16] independently, and generalised to the gauge group $SU(N)$ in [17].

In the first part of this section the instanton solution is presented. Below, the ADHM construction is developed as the general formalism to obtain (anti)self-dual solutions of Yang-Mills equations. Expressions for the Dirac zero-modes in the fundamental representation are computed too. In addition, solutions on other interesting manifolds are presented. The first one are solutions on a torus. Finally, the construction of the $Q = 1$ solution in $R^3 \times S^1$, the $SU(N)$ caloron with non-trivial holonomy, is discussed.

2.3.1 The SU(2) Instanton solution.

The instanton is a non-perturbative solution to the euclidean Yang-Mills equation of motion with topological charge one. This solution was found in [5]. The instanton solution is obtained by solving the self-dual condition for $n = 1$. Then, the main problem is to solve the self-duality condition:

$$F_{\mu\nu} = \tilde{F}_{\mu\nu}. \tag{2.27}$$

while imposing that the gauge fields, A_μ are pure gauge configurations when $|x| \to \infty$ as:

$$A_\mu(x) \;=\; i\Omega(x)\partial_\mu\Omega^\dagger(x). \tag{2.28}$$

The explicit form of the instanton gauge field can be written as

$$A^a_\mu \;=\; 2\eta^{\mu\nu}_a \frac{x_\nu - X^0_\nu}{((x - X^0)^2 + \rho^2)}, \tag{2.29}$$

where a=1,...,3 and the $\eta^{\mu\nu}_a$ symbols are defined by the relation

$$\sigma_\mu\bar{\sigma}_\nu = \bar{\eta}^{\mu\nu}_\alpha\bar{\sigma}_\alpha, \tag{2.30}$$

where the sigma matrices are written in terms of the Pauli matrices as: $\sigma_\mu = (1, -i\tau_i)$ and $\bar{\sigma}_\mu = (1, i\tau_i)$. In addition the $\eta^{\mu\nu}_a$ symbols can be defined as

$$\bar{\sigma}_\mu\sigma_\nu = \eta^{\mu\nu}_\alpha\sigma_\alpha. \tag{2.31}$$

The field strength is given by

$$F^a_{\mu\nu} = -4\bar{\eta}^{\mu\nu}_a \frac{\rho^2}{((x-X^0)^2+\rho^2)^2}, \tag{2.32}$$

$$\tag{2.33}$$

and finally, the topological charge density is

$$Q(x) = \frac{6}{\pi^2}\frac{\rho^4}{((x-X^0)+\rho^2)^4}. \tag{2.34}$$

The instanton solution is a localized object defined by 5 parameters: position (X^0_μ) and size (ρ).

In the next section the general construction of a self-dual solution of charge Q in R^4 obtained in [7, 8] is presented.

2.3.2 The ADHM construction. Self-dual solutions in $\mathbb{R}^4$

In this section we will revise the main formulas of the ADHM construction [7, 8] of self-dual gauge fields. We will restrict ourselves to the case of gauge group SU(N).

The ADHM expression for an SU(N) gauge field with topological charge Q is given by:

$$A_\mu(x) = iN^\dagger \partial_\mu N\,, \tag{2.35}$$

where N is a $(2|Q|+N)\times N$ matrix satisfying $N^\dagger N = I\!\!I_N$. This vector is annihilated by the $(2|Q|+N)\times 2|Q|$ matrix M:

$$N^\dagger M = 0\,. \tag{2.36}$$

The second index of the matrix M is split into a index running from 1 to $|Q|$ and an spinorial index $\alpha = 1, 2$. This matrix has the form:

$$M = A + B\hat{x}\,, \tag{2.37}$$

where A and B are constant matrices of the same type as M, and $\hat{x} = x_\mu\sigma_\mu$ is an x-dependent quaternion which acts on the spinorial index.

One can show that A_μ constructed in such a way is self-dual provided the matrix $R = M^\dagger M$ is invertible and commutes with the σ_μ. Let us find out the implications of this condition for the matrices A and B. We have that both $B^\dagger B$ and $A^\dagger A$ must commute with σ_μ, and the matrix $B^\dagger A$ can be written as $S_\mu\sigma_\mu$ with S_μ hermitian. To express this equation in a more compact way we might introduce some notation, which will turn out to play an important role in what follows.

Given a $2m\times 2m$ matrix $S = S_\mu\sigma_\mu$, where S_μ are $m\times m$ complex matrices, we denote

$$\overline{S} = S_\mu\overline{\sigma}_\mu$$

The overline operation combined with the hermitian conjugate is a particularly interesting operation (star-operation):

$$S^\star \equiv \overline{S^\dagger} = S^\dagger_\mu\sigma_\mu\,, \tag{2.38}$$

which will turn out to be very useful in what follows. In particular, it satisfies

$$(SQ)^\star = S^\star Q\,, \tag{2.39}$$
$$(QS)^\star = QS^\star\,, \tag{2.40}$$

for any square matrix with quaternionic entries S, and an arbitrary quaternion Q. From here it follows, in the particular case of 2×2 matrices (m=1), that $(TS)^\star = T^\star S^\star$. The subspace of quaternions is characterised by the condition $Q^\star = Q$. Furthermore, if the 2×2 matrix is of dyadic form $S = \xi\zeta^\dagger$, then

$$S^\star = \xi_C\zeta_C^\dagger\,, \tag{2.41}$$

where the subscript C stands for the "charge-conjugate" introduced in the last section.

Using the previous notation, we can rewrite the ADHM conditions as

$$(B^\dagger A)^\star = B^\dagger A\,, \tag{2.42}$$

and

$$(M^\dagger M)^\star = M^\dagger M\,. \tag{2.43}$$

This type of equations will appear several times along the paper. If we write as before $S = S_\mu\sigma_\mu$, the condition $S^\star = S$ amounts to $S_\mu = S_\mu^\dagger$.

Another relation which plays an important role in the following derivations is that, given an arbitrary $2|Q|$ square matrix $S = S_\mu\sigma_\mu$, one obtains

$$\sigma_\mu S\sigma_\mu = \overline{\sigma}_\mu S\overline{\sigma}_\mu = -2\overline{S}\,.$$

Using this relation we can show that

$$(\partial_\mu(M^\dagger M) + (\partial_\mu M^\dagger)M)\overline{\sigma}_\mu = 0\,. \tag{2.44}$$

This formula will be important later. The proof is simple. We plug in the expression for M and perform the derivatives and obtain:

$$2\overline{\sigma}_\mu(B^\dagger M)\overline{\sigma}_\mu + M^\dagger B\sigma_\mu\overline{\sigma}_\mu\,.$$

Using $\sigma_\mu\overline{\sigma}_\mu = 4$ and Eq. (2.43) one easily verifies that it vanishes.

Let us now proceed to study the zero-modes of the Dirac operator in terms of the ADHM quantities introduced above. The expression for the normalised zero-modes in the fundamental representation, derived in Ref. [18, 19], is given by:

$$\boldsymbol{\psi} = \frac{1}{\pi}N^\dagger BR^{-1}\tau_2\,(B^\dagger B)^{\frac{1}{2}}. \tag{2.45}$$

The quantity $\boldsymbol{\psi}$ is a $N\times 2Q$ matrix, with the first index being the ordinary colour index. The second index decomposes into an spinorial one, and another labelling the Q different linearly independent solutions, in agreement with the index theorem.

2.3.3 Yang-Mills fields on a torus

Classical solutions of the Yang-Mills equations on a torus were introduced by 't Hooft [20] as a mechanism to understand Confinement. Nowadays, there are additional motivations to study classical solution in this manifold: the relation with R^4 for large volumes, lattice gauge theories are usually formulated on a torus, theories in extra dimensions, large N limit.

An interesting property is the existence of new topological solutions related with the boundary conditions. For gauge fields, this geometry allows to impose a more general boundary condition than periodicity. Some interesting results are presented here. A complete review can be found in [21].

The Yang-Mills action is invariant under gauge transformations, so the gauge fields are allowed to be periodic up to a gauge transformation as

$$A_\mu(x + L_\nu) = [\Omega_\nu(x)]\, A_\mu(x), \tag{2.46}$$

where $[\Omega_\nu(x)]$ is a gauge transformation. These matrices are known as *twist matrices*. If the condition is imposed in two directions,

$$A_\mu(x + L_\nu + L_\rho) = [\Omega_\rho(x+\nu)\Omega_\nu(x)]\, A_\mu(x) = [\Omega_\nu(x+\rho)\Omega_\rho(x)]\, A_\mu(x)\ , \tag{2.47}$$

for consistency the twist matrices must fulfil

$$\Omega_\rho(x + \hat{\nu})\Omega_\nu(x) = z_{\rho\nu}\Omega_\nu(x + \hat{\rho})\Omega_\rho(x), \tag{2.48}$$

where $z_{\rho\nu}$ are elements of the centre of the gauge group. They can be written as

$$z_{\mu\nu} = \exp\left\{2\pi i \frac{n_{\mu\nu}}{N}\right\}, \tag{2.49}$$

where $n_{\mu\nu}$ is an antisymmetric tensor of integers defined modulo N. This matrix is usually called *twist tensor* and can be decomposed into two 3-vectors

$$n_{ij} = \epsilon_{ijk} m_k \tag{2.50}$$

$$n_{0i} = k_i. \tag{2.51}$$

In section 2.2.1, topological properties were extracted by imposing that the field strength vanishes when $|x|$ goes to infinity. On the torus, the situation is quite different. In this case, the topological charge is determined by the twist matrices Ω_μ. In summary, the topological charge in presence of twist is given by

$$Q = -\frac{\vec{k}\cdot\vec{m}}{N} + n, \quad n \in Z. \tag{2.52}$$

In contrast with the ADHM construction on R^4, there is not an analogous construction for self-dual solutions on a torus. Some interesting results have been obtained for particular cases. For example, it can prove non-existence of $Q = 1$ solutions on periodic torus [22].

An interesting tool to study self-duals solutions on a torus is the Nahm transformation. It maps SU(N) solutions of charge Q on a torus to SU(Q) self-dual solutions of charge N on the dual torus. The mapping is obtained by constructing a Weyl operator $\bar{D}(x,z)$ as

$$\bar{D}(x,z) = \bar{\sigma}_\mu \left(D^\mu - 2\pi i z^\mu\right) \ , \tag{2.53}$$

where $z^\mu \in R^4$. As $A_\mu(x)$ has topological charge Q, from the Index theorem, there are Q fermion fields, $\Psi^\alpha(x,z)$, that fulfil,

$$\bar{D}(x,z)\Psi^\alpha(x,z) = 0. \tag{2.54}$$

For trivial twist ($\vec{k}\cdot\vec{n} = 0_{ModN}$) the Nahm transformed gauge field is obtained from these zero-modes by

$$\hat{A}^{\alpha\beta}(z) = i\int d^4x (\psi_z^\alpha(x))^\dagger \frac{\partial}{\partial z_\mu}\psi_z^\beta(x) \ . \tag{2.55}$$

A more general definition can be found in [23].

A situation where the Nahm transformation is specially interesting is the limit where some of the directions are non-compact $R^{4-n}\times T^n$. The dual torus in this cases corresponds with $\hat{T}^n$. So, the non-compact directions collapse to one point. The case $n = 0$ corresponds with the ADHM case, and the self-dual equations in the dual space are reduced to an algebraic problem. For $n = 1$, the problem is reduced to solve a derivative equation in one dimension. The manifold $R^3 \times S^1$ is relevant in the context of finite temperature, and it is the object of the following section.

Nahm-ADHM formalism

The ADHM formalism is valid for gauge fields on the sphere or in R^4 with appropriate boundary conditions at infinity. For other manifolds one can use the extension introduced by Nahm [24]. A particularly symmetric case is that of the 4-torus T^4. Essentially, one can embed the torus onto R^4 and impose the appropriate periodicity conditions. If we look at the torus configurations as solutions in R^4, it is clear that their topological charge Q would be infinite. Then one can interpret the corresponding matrix indices of the basic ADHM quantities, $M = A + B\hat{x}$ and N, as Fourier coefficients of functions or operators depending on 4 new *dual coordinates* z_μ. In particular, the matrix B can be chosen as minus the identity operator ($B = -I\!I$) and $A = \hat{D}_\mu\sigma_\mu/(2\pi i)$. The Nahm-dual covariant derivative $\hat{D}_\mu$ is given by

$$\hat{D}_\mu = \frac{\partial}{\partial z_\mu} - i\hat{A}_\mu(z)\,, \tag{2.56}$$

expressed in terms of the Nahm-dual gauge field $\hat{A}_\mu(z)$. The operator $A^\dagger$ becomes simply proportional to the Nahm-dual left-handed Weyl operator in the fundamental representation, and N is replaced by the zero-modes $\hat{\boldsymbol{\psi}}(z,x)$ of the modified Weyl equation

$$\overline{\sigma}_\mu(\hat{D}_\mu - 2\pi i x_\mu)\hat{\boldsymbol{\psi}}(z,x) = 0\,. \tag{2.57}$$

With this interpretation all the standard ADHM conditions and formulas adopt a simple interpretation. For example, the condition that R commutes with quaternions, leads to the self-duality of the Nahm-dual gauge field. The Weitzenböck formula then gives

$$R = -\frac{\hat{D}_\mu \hat{D}_\mu - 4\pi i x_\mu \hat{D}_\mu - 4\pi^2 x^2}{4\pi^2}\,, \tag{2.58}$$

which obviously commutes with quaternions. Its invertibility follows from the invertibility of the covariant Laplacian in Nahm-dual space.

The formulas work both ways, so that the Nahm-dual field can be obtained from the original self-dual field by the standard formula

$$\hat{A}_\mu(z) = i \int dx\, \boldsymbol{\psi}^\dagger(x,z) \frac{\partial}{\partial z_\mu} \boldsymbol{\psi}(x,z)\,, \tag{2.59}$$

in terms of the normalised zero-modes $\boldsymbol{\psi}(x,z)$ of the modified Weyl equation in the fundamental representation:

$$\overline{\sigma}_\mu (D_\mu - 2\pi i z_\mu)\boldsymbol{\psi}(x,z) = 0\,. \tag{2.60}$$

These zero-modes can also be expressed in terms of Nahm-dual quantities by replacing in Eq. (2.45) the quantities by their equivalents

$$\boldsymbol{\psi}(x,z) = -\frac{e^{2\pi i z x}}{\pi} \int d^4 z'\, \hat{\boldsymbol{\psi}}^\dagger(z',x) \hat{G}(z',z;x)\tau_2 \tag{2.61}$$

where $\hat{G}(z',z;x)$ is the Green function of the operator R.

In Eq. (2.59) we have omitted the indices labelling the different solutions of the Weyl equation. The index theorem tells us that there are Q linearly independent solutions, implying that $\hat{A}_\mu(z)$ is an SU(Q) gauge field. It can be shown that the new field has topological charge N. Thus, we obtain a mapping between SU(N) and SU(Q) self-dual gauge fields, which is an involution [22]. The Nahm-dual gauge field lives in the dual torus, parametrised by z_μ, whose periods are the inverse of those that define the original torus.

2.3.4 Instantons at finite temperature. Self-dual solutions in $\mathbb{R}^3 \times S^1$

The study of Yang-Mills theory at finite temperature is related with cosmological problems and with high energy heavy ion collisions. An extended review of the role of instantons at finite temperature can be found in [25].

The finite temperature behaviour of any theory is specified by the partition function

$$Z = Tr(e^{-\beta H}) \tag{2.62}$$

where H is the Hamiltonian of the system and β is the inverse of the temperature. This formulation can be related with a Euclidean QFT (see section 1) in three dimensions restricted to fields satisfying the periodicity conditions,

$$A_\mu(\vec{x}, \tau+\beta) = A_\mu(\vec{x},\tau), \tag{2.63}$$

$$\psi(\vec{x}, \tau+\beta) = -\psi(\vec{x},\tau). \tag{2.64}$$

then, it is equivalent to study Euclidean QFT in $R^3 \times S^1$ and finite-temperature field theory in R^3. In this sense, it is interesting to ask how the instanton solutions studied in the previous section are modified. As it was mentioned in the introduction of this section, this case was solved by Harrington and Shepard [12, 13] for $Q = 1$. This solution can be obtained from a multi-instanton configuration in R^4, with instanton positions in the X_4 direction given by:

$$X_k^4 = X_0^4 + k\beta \tag{2.65}$$

where $k \in Z$. This sum can be performed and the solution is given by

$$A_\mu = -\bar{\sigma}_{\mu\nu}\partial_\nu\phi \tag{2.66}$$

where $\bar{\sigma}_{\mu\nu} = \frac{1}{2}(\bar{\sigma}_\mu\sigma_\nu - \sigma_\nu\bar{\sigma}_\mu)$ and

$$\phi(x) = 1 + \frac{\pi\lambda^2}{\beta|x - X^0|}\frac{\sinh(\frac{2\pi|\vec{x}-\vec{X}^0|}{\beta})}{\cosh(\frac{2\pi|x-X^0|}{\beta}) - \cos(\frac{2\pi|x_4-X_0^4}{\beta})} \tag{2.67}$$

In the last part of this chapter, this solution is generalized to the case where the Polyakov loop (holonomy) at infinity is not trivial,

$$\lim_{|x|\to\infty} P\exp(\int_0^\beta A_0(x, x_4)dx_4) = \Omega P_\infty \Omega^\dagger \,, \tag{2.68}$$

where $P_\infty = \exp(i2\pi \text{ diag } (Z_1, ..., Z_n))$ are the eigenvalues of the Polyakov loop. For the initial caloron above Z_i=0,1.

SU(N) calorons

In this section we will modify the formalism introduced in 2.3.3 to make it valid for the case of calorons. These are self-dual gauge fields living in $R^3 \times S^1$. The non-compact directions introduce modifications to the Nahm construction on the torus, which we will now specify. If we try to construct the Nahm-dual gauge field by the same formulas as before, we should study the solutions of the Weyl equation in the fundamental representation:

$$\overline{\sigma}_\mu(D_\mu - 2\pi i z_\mu)\boldsymbol{\psi}(x, z) = 0\,. \tag{2.69}$$

The non-compactness of the spatial directions is helpful in trivialising the dependence of $\boldsymbol{\psi}(x, z)$ on z_i, which reduces to simple phase factors of the form $\exp(2\pi i x_i z_i)$. With this, the Nahm-dual gauge field $\hat{A}_\mu(z)$ depends on a single variable z_0. There is, however, a problem that arises at specific values of z_0 for which some of the zero-modes become non-normalisable. This case depends on how fields decay at large distances and this is related to the holonomy. The latter is characterised by the eigenvalues of the Polyakov loop at spatial infinity, i.e.:

$$\begin{aligned} P_\infty = \exp\{i\,2\pi\,\text{diag}(Z_1, Z_2, \cdots, Z_N)\}\,, \text{with} \\ 0 \le Z_1 \le Z_2 \le \cdots Z_N < 1,\ \sum_{a=1}^{N} Z_a \in \mathcal{Z}\,, \end{aligned} \tag{2.70}$$

where we have made use of gauge invariance to bring the Polyakov loop to diagonal form and order the Z_a in increasing values from 0 to 1. Indeed, non-normalisable solutions can only occur when z_0 coincides with one of the Z_a. Since the Nahm construction is local this means that the Nahm-dual fields would be self-dual except at these isolated points in z_0 [14, 15, 17].

Nahm data for Q=1 calorons

The case of $Q = 1$ calorons is particularly simple, since then the Nahm-dual field $\hat{A}_\mu(z)$ is abelian and, as already mentioned, depends on a single variable $z_0 \equiv z$. It is furthermore periodic with period 1.

In this case, the whole scheme can be fitted into the ADHM formalism by identifying, the matrix $\widetilde{A}$, appearing in the Christ-Stanton-Weinberg canonical form, with the Weyl-Dirac operator associated to the Nahm-dual field:

$$\widetilde{A} = \frac{1}{2\pi i}\left(\partial_z - i\sigma_\mu \hat{A}_\mu(z)\right) . \tag{2.71}$$

Since the Nahm-dual gauge field is self-dual except when z equals one of the Z_a, the ADHM condition of commutation of R with the quaternions, can be interpreted as the condition of self-duality of $\hat{A}_\mu(z)$ up to delta function singularities at Z_a. These follow from the $q(z)$ having the form:

$$q(z) = \sum_{b=1}^{N} \delta(z - Z_b)\, \zeta^b \,, \tag{2.72}$$

where ζ^b is a $2 \times N$ matrix, with spinor index α and SU(N) index i, such that $\zeta^b_{\alpha i} \propto \delta_{bi}$. For the case of SU(N) [17, 26] the Nahm-dual gauge field has the following form ($\widehat{A}_0 = 0$):

$$\widehat{A}_i = -2\pi \sum_{a=1}^{N} X_i^a \chi_a(z) \,, \tag{2.73}$$

which is discontinuous and constant at N intervals. The symbol $\chi_a(z)$ stands for the characteristic function of the interval (Z_{a-1}, Z_a), assumed to be periodic in z with period 1. As we will see, each interval is associated to one of the N constituent monopoles of the caloron, and $\vec{X}^a$ will represent its position in 3-space. The length of the intervals $(Z_a - Z_{a-1}) \equiv m_a/(2\pi)$ define the masses of the constituent monopoles $M_a = 2\pi m_a/g^2$. Since these intervals (their closure) provide a covering of the whole period, then $\sum_a m_a = 2\pi$.

The ADHM condition implies the following one for the spinors ζ^b:

$$\zeta^{\dagger b}\tau_i\zeta^b = \frac{1}{\pi}(X_i^{b+1} - X_i^b) \equiv \frac{1}{\pi}\Delta X_i^b \,. \tag{2.74}$$

Notice, that if we sum over all values of b both sides of the equation the right-hand side vanishes identically, so that there are only N-1 independent spinors ζ^b, which determine the relative positions of the monopoles. The overall position of the centre of mass provides the remaining parameters of the solution.

Chapter 3

Lattice Gauge Theory

The lattice formulation allows a non-perturbative approach to QFT through a non-pertubative regulator, the lattice spacing. The main idea, introduced by Wilson [2], is using a discretized space-time. This fact provides a natural ultraviolet cut-off in the theory. Nowadays, no violations of the continuous symmetries of the Lorentz group have been observed, so the discretization should be removed in order to obtain a well-defined continuum limit.

Lattice field theory is the most used approach in the study of the non-perturvative dynamics of gauge theories. The hadronic spectrum has been computed in good agreement with the experimental data as well as other interesting problems as confinement or SχSB which are also addressed with these techniques.

In the lattice formulation, the path integral is mathematically well-defined. The integration measure is formally defined for a field ϕ as

$$D\phi = \prod_n d\phi(n). \tag{3.1}$$

Although the number of degrees of freedom is finite in the discretized theory, the evaluation of the path integral is unapproachable even if the number of lattice points is small. That suggests a statistical treatment. For example, the mean value of an observable, Eq. 1.9 is computed as

$$\langle O \rangle = \frac{1}{N} \sum_n O_n \ , \tag{3.2}$$

where O_n are realizations of O generated according to the distribution function of the path integral,

$$DU_\mu D\bar{\psi}_n D\psi e^{-S(U_\mu,\psi,\bar{\psi})}. \tag{3.3}$$

The generation of a representative ensemble of configurations is crucial for the efficiency of the method. Many efforts have been done by improving the lattice action definitions and the Monte Carlo methods used. In our computation the heat-bath algorithm proposed by Creutz [27] is used in chapter 6. We are restricted to the quenched approximation, where the fermion dynamics are not taken into account.

A numerical treatment allows to obtain the mean value of the observables. However, there are situations where it will be interesting to try to understand if some of the solutions dominate the value of the integral, just as in the semi-classical approximation.

Following the schema of chapter 2, the discretization of a the free fermion action is done. The discretization of fermionic fields presents some formal problems that will be briefly detailed. The overlap-Neuberger operator is taken as the best choice for our work. Below, in section 3.2, it is implemented the gauge invariance in the lattice by using links fields.

3.1 Fermions on the lattice

As mentioned in the final part of the introduction of this chapter, the discretization of femionic fields presents some formal problems. These problems already arise at the level of the free theory. Let us consider the action of a free fermion with mass M as in Eq. 2.7

$$S = \int d^4x \bar{\psi}(\gamma^\mu \partial_\mu - M)\psi. \tag{3.4}$$

Defining the lattice fields as

$$M \rightarrow \frac{1}{a} M_L, \tag{3.5}$$

$$\psi(x) \rightarrow \frac{1}{a^{3/2}} \psi_L(n), \tag{3.6}$$

$$\partial_\mu \psi(x) \rightarrow \frac{1}{a^{5/2}} \partial_\mu \psi_L(n), \tag{3.7}$$

where the lattice derivative is defined by

$$\partial_\mu \psi_L(n) \rightarrow \frac{1}{2} \left(\psi_L(n + \hat{\mu}) - \psi_L(n - \hat{\mu}) \right). \tag{3.8}$$

Replacing the integral by a sum over all lattice points, the lattice action reads

$$S = \sum_{n,m} \bar{\psi}_L(n) \mathcal{M}(n,m) \psi_L(m), \tag{3.9}$$

where $\mathcal{M}(n,m) = \frac{1}{2}\gamma_\mu(\delta_{n,m+\hat{\mu}} - \delta_{n,m-\hat{\mu}}) + M_L \delta_{n,m}$. The propagator can be computed as

$$S(k) = \frac{M_L - i\gamma_\mu \sin(ak^\mu)/a}{M_L^2 + \sum_\mu \sin^2(ak_\mu)/a^2}. \tag{3.10}$$

This propagator has sixteen poles in four dimensions within the Brillouin zone. So, the naïve discretization produces sixteen particles for each fermion of the continuum theory in the lattice version. This fact is known as the *doublers* [2]. Several solutions have been formulated in order to remove the extra particles. The first one was done by Wilson [2], by including an additional term in the action

$$S_W = \sum_{n,m} \bar{\psi}_L(n)(\gamma_\mu \partial_\mu - M_L)_{nm} \psi_L(m) - \frac{r}{2} \sum_n \bar{\psi}_L(n)(\partial_\mu^2)_{nm} \psi_L(m). \tag{3.11}$$

where r is a real number usually taken to 1. This term eliminates the doublers problem, but the action breaks chiral symmetry explicitly in the massless limit. This problem is related with a more fundamental question. In 1981 Nielsen and Ninomiya [28] showed that it is not possible to define a fermionic action in the lattice which simultaneously fulfils: no doublers, chiral symmetry and locality. There is an alternative way to break the chiral symmetry in the lattice proposed by Ginsparg and Wilson (GW) [29]. The GW operators are restricted for satisfying the relation

$$\gamma_5 D + D\gamma_5 = aD\gamma_5 D. \tag{3.12}$$

It was known that any matrix of the form

$$D_{ov} = \frac{1}{a}(1 - V), \tag{3.13}$$

where V is an unitary matrix and fulfils $V^\dagger = \gamma_5 V \gamma_5$. However, it was only in 1998 when Neuberger [30, 31] found and explicit solution. The Neuberger-Dirac operator is constructed by taking

$$V = (1 - aD_W)\left((1 - aD_W)^\dagger(1 - aD_W)\right)^{-1/2}. \tag{3.14}$$

The naïve continuum limit can be obtained from this equation as

$$D_{ov} = \not{D} + \frac{a}{2}\not{D}^\dagger \not{D} + O(a^2). \tag{3.15}$$

The Neuberger-Dirac operator is usually written in terms of the sign function, ϵ, as

$$D_{ov} = \frac{1}{2}\left(1 + \gamma_5 \epsilon(H_W(-M_L))\right), \tag{3.16}$$

where M_L is the mass of the Wilson-Dirac operator, $H_W(M_L) = \gamma_5 D_W(M_L)$ and $D_W(M)$ is the Wilson-Dirac operator.

The Neuberger-Dirac operator has no doublers, it fulfils the GW relation, but it is not strictly local (it decays exponentially at large distances with a rate $1/a$ [32]). The last point is related with the sign operator. This operator is the main obstacle to be able to implement the overlap operator in a computer. The rational expansion proposed by Neuberger in [33] is used in all our numerical calculations.

A final note about the Neuberger operator is that the operator $(\gamma_5 D)^2$ is diagonal in chirality. In order to prove it, it is only necessary to check

$$P_\pm (\gamma_5 D)^2 P_\mp = 0, \tag{3.17}$$

by using $\gamma_5 P_\pm = P_\pm \gamma_5 = \pm P_\pm$, $P_\pm P_\mp = 0$ and $\epsilon^2 = 1$. So, each chiral sector can be computed independently as

$$H_\pm^2 = P_\pm H^2 P_\pm = \frac{1}{4} P_\pm \gamma_5 (1 + \gamma_5 \epsilon)\gamma_5 (1 + \gamma_5 \epsilon) P_\pm = \frac{1}{2} P_\pm (1 \pm \epsilon) P_\pm, \tag{3.18}$$

and it is just needed to apply the sign operator once.

3.2 Gauge fields on the Lattice

In chapter 2, Yang-Mills fields are introduced by imposing the gauge symmetry. In order to do it on the lattice, we are going to proceed in a similar way. We impose invariance of the action under gauge transformations:

$$\Psi_L(n) \rightarrow \Omega(n)\Psi_L(n), \tag{3.19}$$

$$D_\mu\Psi_L(n) \rightarrow \Omega(n)D_\mu\Psi_L(n). \tag{3.20}$$

It is necessary to define the covariant derivative on the lattice. Just as in the continuum case, it can be done by introducing an extra field, called *link*, as

$$D_\mu\psi_L(n) = U_\mu(n)\psi_L(n+\mu) - \psi_L(n), \tag{3.21}$$

where $U_\mu(n) \in SU(N)$ that transforms through

$$U_\mu(n) \rightarrow \Omega(n)U_\mu(n)\Omega^\dagger(n+\mu). \tag{3.22}$$

The connection of these matrices with the gauge fields can be understood in the sense of parallel transport. The parallel transport between two lattice points, n and $n+\hat{\mu}$, is defined by the path-ordered product as

$$U_\mu(n) = P\exp\left\{-i\int_n^{n+\hat{\mu}} dzA_\mu(z)\right\}, \tag{3.23}$$

where $A_\mu(z)$ are the Yang-Mills fields. The adjoint matrix $U_\mu^\dagger(n)$ corresponds to the same path in the opposite direction. A larger path in the lattice can be defined as an ordered product of links. For example, in order to connect the points n and $n+2\nu+\mu$ we can define a path like

$$\gamma(n, n+2\nu+\mu) = U_\nu(n)U_\nu(n+\hat{\nu})U_\mu(n+2\hat{\nu}). \tag{3.24}$$

According with Eq. 3.22, a gauge transformation of this path can be done by

$$\gamma(n, n+2\nu+\mu) \rightarrow \Omega(n)\gamma(n, n+2\nu+\mu)\Omega^\dagger(n, n+2\nu+\mu). \tag{3.25}$$

This property is very useful to define a gauge invariant action for the link fields. Gauge invariant quantities can be obtained by taking the trace of closed paths. The simplest action was found by Wilson [2], by using the smallest closed path defined on the lattice as

$$S_W = \beta\sum_n\left(1 - \frac{1}{N}\mathrm{Re}\ tr(P_{\mu\nu}(n))\right), \tag{3.26}$$

where the *plaquette*, $P_{\mu\nu}$, is defined by

$$P_{\mu\nu}(n) = U_\mu(n)U_\nu(n+\hat{\mu})U_\mu^\dagger(n+\hat{\nu})U_\nu^\dagger(n). \tag{3.27}$$

As expected, the naïve continuum limit of this action has the correct form

$$S_W = \frac{\beta}{2N}\sum_x \frac{a^4}{2} tr(F_{\mu\nu}^2) + \mathrm{O}(a^6) \to \frac{\beta}{2N}\int d^4x \frac{1}{2} tr(F_{\mu\nu}^2) + \mathrm{O}(a^6). \tag{3.28}$$

Improved actions with lower corrections can be obtained by including more complex paths to the lattice action definition.

For completeness, the modification of the Wilson-Dirac operator in presence of gauge fields is presented,

$$\begin{aligned} D_W(M_L)\psi_L(n) &= (4r + M_L)\,\hat{\psi}_L(n) \\ &+ \frac{1}{2}\sum_\mu \gamma_\mu \left(U_\mu(n)\psi_L(n+\hat{\mu}) - U_\mu^\dagger(n)\psi_L(n-\hat{\mu}) \right) \\ &- \frac{r}{2}\sum_\mu \left(U_\mu(n)\psi_L(n+\hat{\mu}) + U_\mu^\dagger(n)\psi_L(n-\hat{\mu}) \right). \end{aligned} \tag{3.29}$$

Chapter 4

Spectrum of fermions in the adjoint representation

In this section we present a brief review of the spectral properties of the adjoint Dirac operator. The eigenvalue equation is given by

$$\not{D}\psi_k = i\lambda_k\psi_k, \tag{4.1}$$

where $\lambda_k \in R$ and $\not{D}$ is defined by

$$\not{D} = \gamma_\mu \left(\partial_\mu - iA_\mu\right). \tag{4.2}$$

The gauge field is written in terms of the generators of the SU(N) group as $A_\mu = A^a_\mu T^a$. In the adjoint represention the generators can be expressed in terms of the structure constants: $(T^a)_{bc} = -if_{abc}$. In this representation, the covariant derivative is real. Using this fact and the definition of the γ_μ matrices, it can be proved that for one solution, ψ_λ, another linearly independent one can be constructed as

$$\psi^C_k = \gamma_5 C\psi^*_k, \tag{4.3}$$

where $C = \gamma_0\gamma_2$, with opposite eigenvalue. These eigenvectors can be grouped as complex 2×4 matrices, $\Psi_k = (\psi_k, \psi^C_k)$. These matrices define a representation of a 2-vector field of quaternions. In this notation, a rotation in the subspace defined by ψ_k and ψ^C_k, is represented as follows

$$\Psi_k \to \Psi_k Q \tag{4.4}$$

where Q is a constant quaternion. The eigenvector equation is given by

$$\not{D}\Psi_k = \Psi_k(\lambda_k\sigma_3), \tag{4.5}$$

note that in this representation, the eigenvalues are quaternions.

In addition, the eigenvector with eigenvalue $\lambda_k\sigma_3$ ($\lambda_k \neq 0$) is related to the one with $-\lambda_k\sigma_3$ through $\Psi_{-k} = \gamma_5\Psi_k$. Both eigenvectors are orthogonal. The zero-modes ($\lambda_k = 0$) can be selected as eigenvectors with defined chirality,

$$\gamma_5 \Psi_\pm = \pm \Psi_\pm. \tag{4.6}$$

More information about the structure of the eigenvectors can be obtained if the Dirac operator is written in terms of Weyl operators as a 2×2 matrix

$$\not{D} = \begin{pmatrix} 0 & \hat{D} \\ \bar{D} & 0 \end{pmatrix}, \tag{4.7}$$

where $\hat{D} = \sigma_\mu D_\mu$ and $\bar{D}_\mu = \bar{\sigma}_\mu D_\mu$, and the eigenvectors are given by

$$\Psi_k = \begin{pmatrix} \Psi_k^+ \\ \Psi_k^- \end{pmatrix}, \tag{4.8}$$

where $\psi_k^\pm = \psi_{k\mu}^\pm \sigma_\mu$. The adjoint of the Dirac operator can be written as $\not{D}^\dagger = \gamma_5 \not{D} \gamma_5$. The hermitian operator $\not{D}^\dagger \not{D}$ is given by

$$\not{D}^\dagger \not{D} = \begin{pmatrix} -\hat{D}\bar{D} & 0 \\ 0 & -\bar{D}\hat{D} \end{pmatrix}. \tag{4.9}$$

The eigenvectors $\Psi_k^\pm$ can be computed as

$$-\hat{D}\bar{D}\Psi_k^+ = \Psi_k^+(\lambda_k^2 \sigma_0), \tag{4.10}$$

$$-\bar{D}\hat{D}\Psi_k^- = \Psi_k^-(\lambda_k^2 \sigma_0). \tag{4.11}$$

If $\lambda_k \neq 0$, both eigenvectors are related by

$$\Psi_k^- = \bar{D}\Psi_k^+, \ \Psi_k^+ = \hat{D}\Psi_k^-. \tag{4.12}$$

The eigenvectors of the Dirac operator can be written in terms of Ψ_k^+ as

$$\Psi_k = \begin{pmatrix} \Psi_k^+ \\ -\bar{D}\Psi_k^+ \lambda_k^{-1} \sigma_0 \end{pmatrix}. \tag{4.13}$$

In section 3.1 the GW operators were introduced in order to obtain an operator with good chiral properties on the lattice. These operators are defined by the relation

$$\{\gamma_5, D\} = D\gamma_5 D. \tag{4.14}$$

The spectrum of these operators presents some modifications with respect to the Dirac operator. The first difference is that the eigenvalues are complex numbers (in quaternionic notation, the eigenvalues are expressed as $\lambda_k = \lambda_0 \sigma + \lambda_3 \sigma_3$). Using the relation

$$D^\dagger = \gamma_5 D \gamma_5, \tag{4.15}$$

it is easy to show that if an eigenvector Ψ_n, has eigenvalues λ_k, then the eigenvector $\Psi_k^5 \equiv \gamma_5 \Psi_k$ has eigenvalue $\bar{\lambda}_k$. The form of these eigenvalues can be obtained from Eq. 4.14. We start from the eigenvector equation,

$$D\Psi_k = \Psi_k \lambda_k. \tag{4.16}$$

If the operator D is replaced by

$$D = -\gamma_5 D \gamma_5 + D\gamma_5 D \gamma_5, \tag{4.17}$$

and we multiply by γ_5, Eq. 4.16 reads

$$-D(\gamma_5 \Psi_k) + aD^\dagger D(\gamma_5 \Psi_k) = (\gamma_5 \Psi_k)\lambda_k. \tag{4.18}$$

If we act with the $D^\dagger D$ operator over $\gamma_5 \Psi_k$ and use the relation between the eigenvalues of Ψ_k^5 and Ψ_k, the eigenvalues are restricted by

$$\bar{\lambda}_k = -\lambda_k + a|\lambda_k|^2. \tag{4.19}$$

The form of the GW eigenvalues can be written as

$$\lambda_\pm = |\lambda| \left(\frac{a|\lambda|}{2} \sigma_0 \pm \sqrt{1 - \frac{a^2|\lambda|^2}{4}} \sigma_3 \right). \tag{4.20}$$

Finally, we analyse the spectrum of the hermitian operator $H = (\gamma_5 \not{D})$. The square of this operator is defined positive and it will be used in our numerical analysis in order to compute the spectrum of the Dirac operator. The eigenvector equation of this operator is given by

$$H\chi_k = \chi_k(\lambda_k \sigma_0), \tag{4.21}$$

where χ_k are 2-vector quaternions. For zero-modes, $\chi_k = \Psi_k$. If $\lambda_k \neq 0$, the eigenvectors of H are related with the eigenvectors of the Dirac operator through

$$\chi_k = \frac{1}{\sqrt{2}}(\Psi_k + \Psi_k^5 \sigma_3). \tag{4.22}$$

As for the Dirac operator, eigenvectors with opposite eigenvalues are related by

$$H\chi_k^5 = -\lambda_k \chi_5, \;\; \chi_k^5 = \gamma_5 \chi_k. \tag{4.23}$$

Chapter 5

Adjoint Caloron Zero-Modes

In recent years there has been renewed interest in the study of gauge theories on $R^3 \times S^1$ in situations that could be amenable to semi-classical treatment. This refers not only to thermal QCD but also to other QCD-like theories seemingly exhibiting exotic phase diagrams which depend on the representation and the boundary conditions for the fermionic fields. As an example, arguments are given to support the idea that adjoint QCD remains confined for any value of the S^1 cycle when fermions are endowed with periodic boundary conditions [34, 35, 36, 37, 38, 39, 40]. This temperature independence, interpreted in the spirit of the Eguchi-Kawai reduction [41, 42, 43, 44], could allow for an analytical approach to confinement in this theory. Here, as well as in ordinary thermal QCD or in supersymmetric gluodynamics, the relevant semi-classical objects are BPS monopoles and finite temperature instantons (calorons). Remarkably, these two objects cannot be considered as independent entities. For non-trivial values of the Polyakov loop at infinity and high temperatures, calorons split into N (for SU(N)) constituent BPS monopoles[14, 15, 16, 45], with the well known Harrington-Shepard caloron [12, 13] corresponding to the case in which N-1 of them become massless. Non-trivial holonomy calorons provide therefore a particular realisation of the idea of instanton quarks [46, 47, 48, 49, 50, 51], instrumental to many semi-classical attempts at explaining confinement in QCD. Constituent monopoles within calorons have been successfully used for obtaining, yet another, weak coupling computation of the gluino condensate in 4D $\mathcal{N} = 1$ supersymmetric Yang-Mills theory [34, 35]. The success of this approach relies on the relevance of non-trivial holonomy configurations when the theory is defined on $R^3 \times S^1$ with periodic boundary conditions for the adjoint fermions. On the contrary, in thermal QCD an old one-loop result by Gross, Pisarski and Yaffe [25] indicates the thermodynamic suppression of such configurations and consequently seems to point towards the irrelevance of non-trivial holonomy calorons for finite temperature QCD. Nevertheless, this result has recently been challenged on the basis of non-perturbative calculations [52, 53, 54, 55] and lattice simulations [56, 57, 58, 59, 60, 61, 62, 63, 64, 65] . Although the issue is far from being settled, see e.g. [66], it has revived the interest in applying semi-classical techniques to the analysis of QCD in a thermal set up. Last but nor least, non-trivial holonomy calorons could as well be of relevance for settling issues at stake such as that of supersymmetry breaking at finite temperature [67, 68, 69, 70, 71, 72, 73], or

the previously discussed phase structure of adjoint QCD or other QCD-like gauge theories.

An essential ingredient in the semi-classical analysis of these theories are the zero-modes of the Dirac operator in the background of the caloron gauge field. Those in the fundamental representation have been previously obtained, first for $Q = 1$ SU(2) calorons [74], and later generalised for SU(N) [75, 76]. Remarkably they are supported on a single BPS monopole selected through the choice of boundary conditions for the fermions on the thermal cycle. In the present chapter we will focus on the derivation of the zero-modes of the Dirac operator in the adjoint representation, relevant for supersymmetric gluodynamics as well as for adjoint QCD.

This chapter is organised as follows. In section 5.1 we introduce some basic properties of adjoint zero-modes and discuss their relation to self-dual deformations of the gauge field. The general construction of the adjoint modes as deformations of the ADHM gauge field is described in 5.2. The ADHM formalism has been devised to provide self-dual gauge fields on the sphere or R^4. To deal with more general manifolds one can make use of the Nahm-ADHM formalism. A general introduction was presented in section 2.3.3, starting with the simplest case of the 4-torus. We discuss there how the Nahm transform provides a mapping between the original self-dual gauge field and a self-dual gauge field living on the dual torus. We show how the adjoint zero-modes of the original Dirac operator are mapped onto those of the dual Dirac operator. In some cases the latter is much simpler than the original one and the Dirac equation can be easily solved. This constitutes the basis of the construction. It provides adjoint zero-modes with periodic boundary conditions in time. Anti-periodic modes are derived by making use of the so called replica trick which is described in section 5.3. The idea is to replicate the original thermal cycle and solve for the Dirac equation on the replicated torus. The periodic zero-modes thus obtained can be easily decomposed into periodic and anti-periodic zero-modes for the original, unreplicated torus. The application of these ideas to the case of calorons is presented in section 2.3.4. Explicit solutions for periodic and anti-periodic zero-modes are derived in section 5.5 where we also discuss the generalisation of our formulas to other periodicity conditions for the adjoint fermions. Section 5.6 presents some illustrative examples and discusses in detail some general properties of the solutions such as periodicity, normalisability and concordance with the expected number of zero-modes as dictated by the index theorem. Finally, we end in section 5.7 with a brief summary of the results and a recollection of possible applications. The most technical details concerning the derivation of the adjoint zero-modes in sections 2.3.4 and 5.5 are deferred to an Appendix.

5.1 Generalities about adjoint zero-modes

In the previous chapter, we reviewed the properties of the spectrum of the Dirac operator in the adjoint representation. In this section we pay special attention to the zero-modes,

$$\gamma_\mu D_\mu \Psi = 0\,, \tag{5.1}$$

This equation factorises into two Weyl equations for the two chiral components. The equation for the left-handed (or positive chirality $\gamma_5\Psi = \Psi$) component is

$$\overline{\sigma}_\mu D_\mu \Psi_+ = 0\,, \tag{5.2}$$

Self-dual gauge fields A^a_μ are those for which the field strength $F_{\mu\nu} = i[D_\mu, D_\nu]$ satisfies

$$\bar{\eta}^{\mu\nu}_i F_{\mu\nu} = 0\,, \tag{5.3}$$

for all $i = 1, 2, 3$. In analysing the solutions of the Weyl equations for self-dual gauge fields, it is important to consider the possible zero-modes $\kappa(x)$ of the covariant Laplacian $D_\mu D_\mu$. It is clear that the only zero-modes are functions that are simultaneously annihilated by all the D_μ ($D_\mu\kappa(x) = 0$). This implies that

$$[F_{\mu\nu}(x), \kappa(x)] = 0\,. \tag{5.4}$$

Except for very particular abelian-like gauge fields, this equation will have no solution other than the trivial one $\kappa(x) = 0$. From this result it is easy to conclude that the right-handed Weyl equation will have no zero-modes. From here one can make use of the index theorem [7, 8] to extract the number of zero-modes of the left-handed Weyl equation. Notice also, that the absence of zero-modes would guarantee the invertibility of the covariant Laplacian.

Another very important result concerning adjoint zero-modes of self-dual gauge fields is to realise the connection among self-dual deformations and solutions of the left-handed Weyl equation. Given a self-dual deformation δA_μ, one can choose a representative within the gauge trajectory satisfying the background gauge condition

$$D_\mu \delta A_\mu = 0\,. \tag{5.5}$$

The existence and uniqueness (up to non-trivial gauge transformations not connected with the identity) of this representative relies on the invertibility of the covariant Laplacian. Now, it is simple to see that the condition of self-duality, plus the background gauge condition amount to

$$\overline{\sigma}_\mu D_\mu \Psi = 0\,, \tag{5.6}$$

where $\Psi = \delta A_\mu \sigma_\mu$. The relation works both ways, so that there is a one-to-one correspondence between self-dual deformations and left-handed zero-modes. This relation combined with the index theorem was used in Refs. [77, 78, 79] to count the (dimensionality) number of moduli parameters of the manifold of self-dual gauge fields.

Notice that if we transform one solution of Eq. (5.6) by right multiplication by a quaternion $\Psi \longrightarrow \Psi Q$ the corresponding deformation transforms as

$$\delta A_\mu \longrightarrow q_\nu \bar{\eta}^{\mu\rho}_\nu \delta A_\rho = q_\nu \eta^{\nu\rho}_\mu \delta A_\rho\,, \tag{5.7}$$

where $Q = q_\mu \overline{\sigma}_\mu$.

A particular class of deformations is associated to symmetries (conformal transformations of the metric) that do not leave the solution invariant. Particularly interesting is

the case of translations. Translation in the ρ direction gives a deformation $\partial_\rho A_\mu$, which in general does not satisfy the background field gauge. However, if we write

$$\delta A_\mu = \partial_\rho A_\mu + D_\mu(-A_\rho) = F_{\rho\mu}\,, \tag{5.8}$$

the gauge condition is satisfied. This gives rise to the famous supersymmetric zero-mode present in conformally flat manifolds.

5.2 Adjoint Zero-modes in the ADHM construction

The adjoint zero-modes can be derived by exploiting their relation with self-dual deformations. These can be obtained by deforming the matrix M and the vector N of the ADHM construction [80]. It takes the form

$$\begin{aligned} \delta A_\mu &= i\delta N^\dagger \partial_\mu N + iN^\dagger \partial_\mu \delta N\,, & (5.9)\\ \delta N^\dagger M &= -N^\dagger \delta M\,, & (5.10)\\ \delta N^\dagger N + N^\dagger \delta N &= 0\,. & (5.11) \end{aligned}$$

Given a deformation δM, the variation of δN is determined from Eq. (5.10). The solution is not unique since the left-kernel of M is non-trivial. This allows us to choose a solution $\widetilde{\delta} N$ satisfying

$$\widetilde{\delta} N^\dagger N = 0\,, \tag{5.12}$$

which is also compatible with Eq. (5.11). A general solution would then be

$$\delta N = \widetilde{\delta} N - iN\omega\,, \tag{5.13}$$

with w a hermitian matrix. Using the form of the orthogonal projector to the kernel of M:

$$P = MR^{-1}M^\dagger\,, \tag{5.14}$$

we might write

$$\widetilde{\delta} N^\dagger = \widetilde{\delta} N^\dagger P = -N^\dagger \delta M R^{-1} M^\dagger\,. \tag{5.15}$$

Plugging this expression into Eq. (5.9) we arrive at:

$$\widetilde{\delta} A_\mu = iN^\dagger \left(\delta M R^{-1}\partial_\mu M^\dagger - \partial_\mu M R^{-1}\delta M^\dagger\right) N \equiv iN^\dagger (H_\mu - H_\mu^\dagger) N\,, \tag{5.16}$$

where we have moved the partial derivatives around in an obvious way. If instead of this solution we would have used the general one Eq. (5.13), the result would be

$$\delta A_\mu = \widetilde{\delta} A_\mu + D_\mu \omega\,, \tag{5.17}$$

a gauge transform of the previous one. The quantity H_μ appearing in Eq. (5.16) can be written as

$$H_\mu = \delta M \overline{\sigma}_\mu R^{-1} B^\dagger\,. \tag{5.18}$$

From here it is clear, by using the formula

$$\overline{\sigma}_\nu \overline{\sigma}_\mu = \eta_\mu^{\nu\rho} \overline{\sigma}_\rho \,, \tag{5.19}$$

that multiplying δM on the right by an arbitrary quaternion $Q = q_\nu \overline{\sigma}_\nu$ transforms the deformation as in Eq. (5.7), namely another one corresponding to the 2-dimensional space of adjoint zero-modes mentioned in the previous section.

We have obtained the expression of the self-dual deformation in terms of δM, the deformation of the M matrix. Notice that these deformations are not arbitrary, but should preserve the form $\delta M = \delta A + \delta B \hat{x}$ and preserve the invertibility (trivial) and the condition of commuting with quaternions. The latter condition can be re-expressed as

$$T - T^\star = \overline{T - T^\star} \,, \tag{5.20}$$

where $T = M^\dagger \delta M$.

Now we should verify whether Eq. (5.16) satisfies the background gauge condition. Acting with the covariant derivative and after some algebra we obtain

$$D_\mu \widetilde{\delta} A_\mu = i4 N^\dagger \left(\delta B \, R^{-1} B^\dagger - B R^{-1} \delta B^\dagger - B R^{-1} (M^\dagger \delta M - \delta M^\dagger M)_0 R^{-1} B^\dagger \right) N \,, \tag{5.21}$$

where the sub-index 0 amounts to extracting the part commuting with quaternions:

$$(S)_0 \equiv \frac{1}{2}(S + \overline{S}) = \frac{1}{4} \sigma_\mu S \overline{\sigma}_\mu \,. \tag{5.22}$$

We leave to the reader the details of reaching to Eq. (5.21). As an aid, we mention that we have used the form of the matrices M and δM, the previous relations Eq. (2.44) and Eq. (5.22), and the following formula for the covariant derivative of an object of the form $\omega = N^\dagger H N$:

$$\begin{aligned} &D_\mu \omega = N^\dagger \partial_\mu \left((\mathbb{I} - P) H (\mathbb{I} - P) \right) N = \\ &N^\dagger \left(\partial_\mu H - \partial_\mu M R^{-1} M^\dagger H - H M R^{-1} \partial_\mu M^\dagger \right) N \,. \end{aligned} \tag{5.23}$$

From Eq. (5.21), we conclude that the covariant derivative vanishes provided:

$$\delta B \, R^{-1} B^\dagger - B R^{-1} \delta B^\dagger = 0 \,, \tag{5.24}$$

$$(M^\dagger \delta M - \delta M^\dagger M)_0 = 0 \,. \tag{5.25}$$

The last equation can be combined with the condition on the deformations δM, Eq. (5.20), to conclude:

$$T = T^\star \,, \tag{5.26}$$

where $T = M^\dagger \delta M$.

Up to now we have not used the freedom to redefine M without altering the form of the gauge field A_μ. There are two types of transformations of this kind. The first is to replace $M \longrightarrow ML$ with invertible, constant and commuting with quaternions L. The second transformation is to modify $M \longrightarrow VM$ with V unitary and constant. The same

transformation has to be done to N ($N \longrightarrow VN$). Using these transformations Christ, Weinberg and Stanton [81] were able to show that the M matrix can be brought to the following canonical form:

$$M = \begin{pmatrix} q^\dagger \\ \widetilde{A} - \hat{x} \end{pmatrix} . \tag{5.27}$$

Then we have

$$N = \begin{pmatrix} I\!I_N \\ -u \end{pmatrix} F^{-1/2} , \tag{5.28}$$

where u is given by

$$u \equiv \widetilde{M}^{-1\dagger} q = B^\dagger N F^{1/2} , \tag{5.29}$$

with $\widetilde{M} = \widetilde{A} - \hat{x}$. The $N \times N$ matrix F is fixed by the normalisation condition ($N^\dagger N = I\!I_N$):

$$F = I\!I_N + u^\dagger u . \tag{5.30}$$

We will now give the expression of the gauge field and the vector potential in this canonical form. Introducing $\omega = R^{-1} q$, one can show that

$$u = \widetilde{M} \omega F . \tag{5.31}$$

Another useful expression is

$$R^{-1} u = \frac{1}{2} (\hat{\partial} R^{-1}) q F = \frac{1}{2} \hat{\partial} \omega F , \tag{5.32}$$

where $\hat{\partial} \equiv \sigma_\mu \partial_\mu$.

With this notation the main expressions for the ADHM fields are given by:

$$F^{1/2} A_\mu(x) F^{1/2} = i u^\dagger \partial_\mu u - i F^{1/2} \partial_\mu F^{1/2} \equiv F^{1/2} \mathcal{A}_\mu F^{1/2} - i F^{1/2} \partial_\mu F^{1/2} , \tag{5.33}$$

where

$$\mathcal{A}_\mu = \frac{i}{2} F^{1/2} q^\dagger \bar{\sigma}^\mu \hat{\partial} \omega F^{1/2} . \tag{5.34}$$

The (chromo-)electric field is given by

$$E_i = -F^{-1/2} u^\dagger \tau_i \hat{\partial} \omega F^{1/2} , \tag{5.35}$$

and the zero-modes of the Dirac operator in the fundamental representation by:

$$\boldsymbol{\psi} = \frac{1}{2\pi} F^{1/2} \left(\hat{\partial} \omega \right)^\dagger \tau_2 . \tag{5.36}$$

Now we go back to our main goal of obtaining the adjoint zero-modes. Notice that $\delta B = 0$ so that the first condition implying the background gauge Eq. (5.24) is automatically satisfied. The form of the self-dual deformation can be obtained by using

$$\delta M^\dagger \, N = (\delta q - \delta \widetilde{A}^\dagger u) F^{-1/2} , \tag{5.37}$$

and replacing it in our general formula Eq. (5.16):

$$\delta A_\mu = \frac{i}{2} F^{-1/2} (\delta q^\dagger - u^\dagger \delta \widetilde{A}) \bar{\sigma}^\mu \hat{\partial} \omega F^{1/2} + h.c.\,. \tag{5.38}$$

The condition that this is a self-dual deformation in the background Lorentz gauge, is simply Eq. (5.26) where

$$T \equiv M^\dagger \delta M = q \delta q^\dagger + \widetilde{A}^\dagger \delta \widetilde{A} - \bar{x} \delta \widetilde{A}\,. \tag{5.39}$$

The part proportional to $\bar{x}$ must satisfy the equation by itself ($\delta \widetilde{A} = (\delta \widetilde{A})^\star$). The remaining part can be rewritten as

$$\widetilde{A}^\dagger \delta \widetilde{A} - (\widetilde{A}^\dagger \delta \widetilde{A})^\star = -q \delta q^\dagger + (q \delta q^\dagger)^\star\,. \tag{5.40}$$

Considering deformations, the aforementioned mapping implies $\delta M = -\delta \hat{A}_\mu \sigma_\mu / 2\pi$. Plugging this onto Eq. (5.26) we get

$$\bar{\sigma}_\mu \hat{D}_\mu \hat{\Psi} = 0\,, \tag{5.41}$$

where $\hat{\Psi} = \sigma_\mu \delta \hat{A}_\mu$, which is the left-chirality adjoint Dirac equation. Thus, adjoint zero-modes map onto adjoint Nahm-dual zero-modes and viceversa. A explicit formula can be read off from Eq. (5.16):

$$\delta A^{ij}_\mu(x) = \frac{i}{2} \int d^4 z\, e^{-2\pi i z x}\, \boldsymbol{\psi}^{ia}(x,z) \tau_2 \sigma_\mu \overline{\sigma}_\nu \delta \hat{A}^{ab}_\nu(z) \hat{\boldsymbol{\psi}}^{bj}(z,x) + \text{h. c.} \tag{5.42}$$

where colour ($i = 1 \ldots N$) and dual-colour ($a = 1 \ldots Q$) indices are explicitly shown and repeated indices summed over (spinorial indices are not displayed).

All general properties of the ADHM construction are preserved, and in particular the fact that the mapping operates among the 2-dimensional spaces formed by each mode and its CP transform.

5.3 Replicas

There are a set of interesting relations which arise by embedding a self-dual solution on the 4-torus onto that of a *replicated* torus with periods being multiples of the original one. We call the new solution a replicated solution or replica. The replicated solution has a topological charge which is a multiple of the topological charge of the original one Q. Consider for example replicating the solution in one direction by a factor L, then the topological charge of the replica is QL. If we now take the Nahm transform of this solution it corresponds to an SU(LQ) self-dual configuration. How does this solution relate to the Nahm transform of the original configuration This question was addressed an answered in [82]. The answer is the following one:

$$\hat{A}^R_\mu(z) = \text{diag}\{\hat{A}_\mu(z), \hat{A}_\mu(z + \frac{1}{L}), \ldots, \hat{A}_\mu(z + \frac{L-1}{L})\}\,, \tag{5.43}$$

where the symbol diag constructs an $L \times L$ diagonal matrix with its arguments. An important point to take into account is that the Nahm transform of the replicated solution lives in a torus (the dual-torus) which is a fraction $\frac{1}{L}$ of the size of that of the original one. The transition matrices can be read off from Eq. (5.43). In particular, if $\hat{A}_\mu(z)$ is strictly periodic with period 1, we have

$$\hat{A}^R_\mu(z + \frac{1}{L}) = P \hat{A}^R_\mu(z) P^\dagger \,, \tag{5.44}$$

where P is the $L \times L$ 't Hooft matrix ($P_{ij} = \delta_{j\, i+1}$).

Adjoint zero-modes of the Dirac equation in the background field of the replicated solutions can be derived once again from self-dual deformations satisfying Eq. (5.26). They are connected to deformations of the SU(LQ) Nahm transform satisfying the left-chirality adjoint Dirac equation on the dual-torus, i.e. Eq. (5.41). The adjoint zero-modes derived in this way are periodic in the replicated torus but do not necessarily satisfy the same boundary conditions on the original one. If applied to doubly replicated tori ($L = 2$), this trick allows to obtain adjoint zero-modes which are anti-periodic in one direction.

5.3.1 Nahm data for the replicated caloron

Given the form of the Nahm data, we can use the Nahm-ADHM formulas Eqs. (5.33)-(5.38) to construct the caloron vector potential, the field strength, and the fundamental and adjoint zero-modes. All these general expressions are written in terms the matrix functions u, F and ω. A detailed evaluation of these quantities for the $Q = 1$ caloron case is presented in the Appendix A.

Here we will focus on deriving explicit formulas for the adjoint zero-modes satisfying the periodicity conditions:

$$\Psi(\vec{x}, x_0 + 1) = \pm P_\infty \Psi(\vec{x}, x_0) P_\infty^{-1} \,, \tag{5.45}$$

in the gauge in which the caloron vector potential transforms as:

$$A_\mu(\vec{x}, x_0 + 1) = P_\infty A_\mu(\vec{x}, x_0) P_\infty^{-1} \,. \tag{5.46}$$

In order to derive the anti-periodic modes we will make use of the replica trick presented in the previous section, In this subsection we will specialise the construction of replicas for the case of the caloron. Let us concentrate upon the study of the duplicate solution ($L = 2$). The idea is that of regarding the ordinary caloron solution presented previously as living in a double torus in the time-direction. The topological charge, being an additive quantity, is now equal to two. The Nahm-dual field is a U(2) field, whose structure follows from Eq. (5.43). We have

$$\hat{A}^R_\mu(z) = \begin{pmatrix} \hat{A}_\mu(z) & 0 \\ 0 & \hat{A}_\mu(z + \frac{1}{2}) \end{pmatrix} , \tag{5.47}$$

where $\hat{A}_\mu(z)$ is the Nahm data of the ordinary caloron, and $\hat{A}^R_\mu(z)$ is the Nahm data of the replicated caloron.

We still have to fix the corresponding q for such a replica solution. We will argue that the solution is actually given by

$$q^R(z) = \begin{pmatrix} q(z) \\ q(z+\frac{1}{2}) \end{pmatrix} . \tag{5.48}$$

Notice that each of the components of q^R and $\hat{A}^R$ are periodic with unit period, but the whole set is periodic with period 1/2 with a twist matrix given by τ_1:

$$\hat{A}^R_\mu(z+\frac{1}{2}) = \tau_1 \hat{A}^R_\mu(z)\tau_1 . \tag{5.49}$$

The quantity q transforms by periodicity as follows:

$$q^R(z+1/2) = \tau_1 q^R(z) . \tag{5.50}$$

From here it is possible to use the general formulas of the ADHM construction to verify that indeed we obtain a replicated solution. In particular we have that $u^R(z)$ is given by:

$$u^R(z) = \begin{pmatrix} u(z) \\ u(z+\frac{1}{2}) \end{pmatrix} , \tag{5.51}$$

in terms of the quantity $u(z)$ for the normal (unreplicated) caloron. Now

$$F^R - 1 = \int_0^{\frac{1}{2}} dz u^{R\dagger}(z) u^R(z) = \int_0^1 dz\, u^\dagger(z) u(z) , \tag{5.52}$$

which coincides with $F-1$ for the caloron.

5.4 Deformations of SU(2) calorons

Before discussing to general $SU(N)$ case, we are going to solve the antiperiodic solutions in the $SU(2)$ case. For this group, the antiperiodic solutions have two special properties. The first is is that one of the masses is larger or equal to π. This situation has important consequence in the Atiya-Singer index theorem, in the far-field limit [83, 84]. This question will be clarify in the section 5.6.3. The second question is related with the existence of a solution without δq terms. Although in the periodic case, this solution is given by the supersymmetric zero-mode, in the antiperiodic case, a special relation between the holonomy properties and the position of the monopoles is necessary. A particular case occurs when all monopoles are aligned. In $SU(2)$ only two monopoles appear, so they are aligned. This case is quite simpler than the general case. The analysis of the asymptotic behaviour of this solution and a numerical comparative with the solution obtained in a lattice construction will be presented.

After suitable rotations, translations and gauge transformations the caloron Nahm data can be taken to be [14, 15]

$$q^{(0)}(z) = \rho(P_+\,\delta(z-\delta_1) + P_-\,\delta(z+\delta_1)) , \tag{5.53}$$

where $P_\pm = (1 \pm \tau_3)/2$. The parameter δ_1 parametrizes the holonomy, becoming trivial for 0 and $\frac{1}{2}$. Without loss of generality we will assume in what follows that $\delta_1 \leq \delta_2 \equiv \frac{1}{2} - \delta_1$. In the previous formula the delta functions have to be taken as periodic functions in z with unit period. The Nahm-dual gauge field of the caloron is given by

$$\hat{A}^{(0)}_\mu(z) = -2\pi\delta_{\mu 3}(X^1_3\chi_1(z) + X^2_3\chi_2(z))\,, \tag{5.54}$$

where X^a_3 is the position of the ath constituent monopole on the z-axis. They can be obtained from the relations $m_1X^1_3 + m_2X^2_3 = 0$, and $X^2_3 - X^1_3 = \pi\rho^2$, where $m_a = 4\pi\delta_a$ are proportional to the constituent monopole masses. The function χ_1 is the characteristic function of the interval $[-\delta_1, \delta_1]$ and χ_2 that of its complementary.

Now we proceed to study the self-dual deformations of this replicated caloron satisfying the background field condition. We will make use of our general formula Eq. (5.38). The conditions following that equation when translated to our case become

$$\hat{\bar{D}}\psi^R \equiv \frac{d\psi^R}{dz} - i\bar{\sigma}_\mu[\hat{A}^R_\mu, \psi^R] = 4\pi^2 i\left(q^R_\mu \delta q^{\dagger R}_\nu - \delta q^R_\nu q^{\dagger R}_\mu\right)\bar{\sigma}_\mu\sigma_\nu\,, \tag{5.55}$$

where $\psi^R = \delta\hat{A}^R_\mu\sigma_\mu = -\delta\widetilde{A}^R/(2\pi)$. The quantities δq^R_ν are two-component column vector whose elements are linear combinations of delta functions with complex coefficients. The holonomy fixes that the argument of the delta functions must be $z \pm \delta_1$ and $z \pm \delta_1 + \frac{1}{2}$. Notice that, as anticipated previously, up to the delta functions in the right-hand side, the equation adopts the form of the Weyl equation for adjoint zero-modes in Nahm dual space.

Our next step will then be that of finding the solution of Eq. (5.55). Notice that both ψ^R and $\delta q^R \equiv \delta q^R_\nu\bar{\sigma}_\nu$ are the unknowns. Without much effort one can demonstrate that given a solution one can obtain other solutions by the operation $\psi^R \to \psi^R Q$, $\delta q^R \to Q^\dagger \delta q^R$, with Q an arbitrary constant quaternion. This transformation is associated to the double degeneracy of adjoint zero-modes. We must also point out certain subtleties necessary to understand Eq. (5.55) and their solutions. The main idea is that the equation must be understood as one relating two operators acting on the space two-component functions of the form Eq. (5.51).

The right-hand side of Eq. (5.55) acts by multiplication. Thus, the left-hand side must be equivalent, when acting over our space of functions, to the multiplication by a linear combination of delta functions. This imposes non-trivial conditions on the form of δq^R. In what follows we will give the possible values for δq^R that follow from the previous analysis, as well as the resulting form for the equation for ψ^R, skipping all the details of the derivation.

Before showing the equations, we recall that ψ^R is a 2×2 matrix in (Nahm-dual) colour space

$$\psi^R(z) = \begin{pmatrix} \psi_{11}(z) & \psi_{12}(z) \\ \psi_{21}(z) & \psi_{22}(z) \end{pmatrix}. \tag{5.56}$$

The boundary conditions specify that it is enough to know the form of ψ_{11} and ψ_{12} (the other components can be obtained by translating in z by 1/2). The equations for ψ_{11} coincide with those for the $Q = 1$ caloron, and therefore can be associated with

deformations that are periodic in time. Thus, our sought time-antiperiodic zero-modes should follow from the equation

$$\partial_z\psi_{12}+\tau_3(\Delta\hat{A})\psi_{12}=4\pi^2\rho\Big\{\begin{array}{ll} P_+ & \Big(\quad \delta(z-\delta_1)-\delta(z-\delta_2)\Big) \\ +P_- & \Big(\quad \delta(z+\delta_2)-\delta(z+\delta_1)\Big)\Big\}\,Q\,, \end{array} \tag{5.57}$$

where the function $\Delta\hat{A}$ is given by

$$\Delta\hat{A}\equiv\hat{A}_3^{(0)}(z)-\hat{A}_3^{(0)}(z+1/2)=2\pi^2\rho^2(\chi(-\delta_1,\delta_1)-\chi(\delta_2,1-\delta_2))\,. \tag{5.58}$$

The arbitrary quaternion Q reflects the degeneracy of solutions mentioned earlier. Keeping that in mind one only needs to solve the equation for $Q=0$ and $Q=1$. A particular solution is all that is needed, since the general solution can be obtained by linear combinations of these ones with quaternionic coefficients. The counting matches the predictions of the index theorem. As for the periodic case there are essentially two CP-pairs of zero-modes.

After these considerations we proceed to show the two particular solutions that we will need. The first one corresponds to the inhomogeneous equation ($Q=1$) and is given by

$$\psi_{12}=4\pi^2\rho\,(P_+\chi(\delta_1,\delta_2)+P_-\chi(1-\delta_2,1-\delta_1))\;. \tag{5.59}$$

The value of δq^R associated to it is

$$\delta q^R=iP_+\begin{pmatrix}\delta(z+\delta_2)\\ \delta(z-\delta_1)\end{pmatrix}-iP_-\begin{pmatrix}\delta(z-\delta_2)\\ \delta(z+\delta_1)\end{pmatrix} \tag{5.60}$$

These expressions can now be introduced into the general formula Eq. (5.38) to obtain the first solution

$$\begin{aligned}\delta A_\mu^{(1)}&=-\frac{1}{2}\Big(P_+\bar{\sigma}_\mu\hat{\partial}\omega(-\delta_2)-P_-\bar{\sigma}_\mu\hat{\partial}\omega(\delta_2)\Big)\\ &-i\pi\rho\Big(\int_{\delta_1}^{\delta_2}u^\dagger(z+\frac{1}{2})P_-\bar{\sigma}_\mu\hat{\partial}\omega(z)+\int_{1-\delta_2}^{1-\delta_1}u^\dagger(z+\frac{1}{2})P_+\bar{\sigma}_\mu\hat{\partial}\omega(z)\Big)+\text{h.c.}\,.\end{aligned} \tag{5.61}$$

The quantities u and ω are the ones associated to the $Q=1$ caloron. The analytic expressions needed to do the calculation were explicitly given in [85].

Now we investigate the other solution, associated to $\delta q^R=0$. One has to solve the homogeneous equation (5.57) for vanishing right hand side. A particular solution is given by

$$\psi_{12}(z)=\exp\{-\tau_3\int_0^z dz'\,\Delta\hat{A}(z')\}\equiv\phi_s(z)-\tau_3\phi_a(z)\,. \tag{5.62}$$

Since $\Delta\hat{A}(z')$ is constant at intervals, the integral in the exponent is trivial to perform. We leave the explicit form of $\phi_s(z)$ and $\phi_a(z)$ to the reader. It is interesting to point out nonetheless, that $\phi_s(z)$ is periodic in z with period $\frac{1}{2}$ and $\phi_a(z)$ antiperiodic.

From the previous expression we can compute the corresponding self-dual deformation using Eq. (5.38). The result is given by

$$\delta A_\mu^{(2)} = \frac{-i}{4\pi}\int_0^1 dz\ (u^\dagger(z+\frac{1}{2})(\phi_s(z)+\tau_3\phi_a(z))\bar{\sigma}_\mu\hat{\partial}\omega(z)) + \text{h.c.}\,. \tag{5.63}$$

Again, the integration over z can be performed analytically using the formulas of the Appendix A.

We have arrived to the general solution our problem. The adjoint zero-modes of the (self-dual) caloron which are antiperiodic in time are

$$\Psi = \frac{1}{2}\delta A_\mu^{(1)}\gamma_\mu(\mathbf{I}+\gamma_5)V_1 + \frac{1}{2}\delta A_\mu^{(2)}\gamma_\mu(\mathbf{I}+\gamma_5)V_2\,, \tag{5.64}$$

where V_a are arbitrary constant spinors and $\delta A_\mu^{(a)}$ are given in Eqs.(5.61)-(5.63).

It is interesting to mention that the general investigation of the possible values of δq^R has led to another solution having a fairly simple form. The expression of the left-handed Weyl spinor, $\Psi^{(3)} \equiv \Psi_a^{(3)}\tau_a$, is:

$$\Psi_a^{(3)} = \sigma_\mu\partial_\mu T^a\sigma_a V\,, \tag{5.65}$$

where a labels a colour component, σ_α acts on the spin indices and V denotes an arbitrary constant 2-spinor. The functions T_a depend on the colour index as: $T^1 = T^2 = -1/F$ and $T^3 = P_+\chi + P_-\bar{\chi}$. The function χ is essentially the function with the same name given in Ref. [14, 15]. Curiously this solution interpolates between the non-supersymmetric periodic adjoint zero-mode for $m_1 = 0$ ($\delta_1 = 0$) and one of our antiperiodic solutions (Eq. (5.61)) for $m_1 = m_2$ ($\delta_1 = 1/4$). Using the formulas of the next section it can be proven that the solution is neither periodic no antiperiodic for other values of the mass m_1.

Far-field limit and Normalization

The reader might question whether our general solution Eq. (5.64) is normalizable. One can investigate the behaviour at points whose distance to the location of the constituent monopoles (r_1 and r_2) is much larger that β and that $\pi\rho^2$. For the unequal mass case the zero-mode density goes to zero exponentially as $e^{-(m_2-m_1)r_2}$. The equal mass case ($m_1 = m_2 = \pi$) is more subtle since both solutions decay in power-like fashion. The non-homogeneous solution Eq. (5.61) coincides with the additional solution Eq. (5.65) in this case. In the limit under consideration χ goes to zero exponentially and $F = (r_1 + r_2 + \pi\rho^2)/(r_1 + r_2 - \pi\rho^2)$. Thus the density behaves as $1/r^4$.

An alternative approach to normalizability of the solutions is to compute the norm of the solutions. In fact there exist a general formula [14, 26] which allows one to compute the norm and the scalar products of the solutions in terms of Nahm-data directly. This is also useful in checking if the real dimensionality of the space of solutions is 8 (4 complex

dimensions, 2 quaternionic dimensions), as indicated by the index theorem. Using this formula we obtain

$$\left|\delta A_\mu^{(1)}\right|^2 = 4\pi^2 + 8\pi^4\rho^2\left(\delta_2 - \delta_1\right), \tag{5.66}$$

$$\left|\delta A_\mu^{(2)}\right|^2 = \frac{\sinh(4\pi^2\rho^2\delta_1)}{2\pi^2\rho^2} + (\delta_2 - \delta_1)\cosh(4\pi^2\rho^2\delta_1), \tag{5.67}$$

$$\left\langle \delta A_\mu^{(1)}, \delta A_\mu^{(2)} \right\rangle = 2\pi^2\rho\, e^{-2\pi^2\rho^2\delta_1}\left(\delta_2 - \delta_1\right). \tag{5.68}$$

Profile of the zero-mode density

In this subsection we will describe the qualitative properties of the zero-mode densities. For that purpose we developed two independent programs to draw these profiles. Both programs give matching results. In Fig. 5.1 we give the contour plot in a z-y plane of the solution $\delta A_\mu^{(2)}$ (top) and an orthogonal CP-pair (bottom) for $\rho = 1$ (giving an intermediate size caloron separation) and two representative values of the masses. The z axis is the line joining the constituent monopoles and is represented horizontally. The vertical axis denotes the y axis (the density is axially symmetric).

For the equal mass case ($m_1 = m_2 = \pi$) the mode following from Eq. (5.63) has an approximately constant higher density along the line joining both calorons (top left). This can be interpreted as a string. In contrast, the other solution associated to Eq. (5.61) has a region of small density located along the line joining the two monopoles (bottom left). As the masses become unequal, the most massive monopole dominates the densities. The right contour plots show the situation for $\delta_1 = 0.23$.

Limiting cases

The caloron is an interesting solution which interpolates between the gauge potential of an instanton and that of a BPS monopole. It is interesting then to see how our antiperiodic zero-modes behave in these extreme cases. We will first concentrate in the situation corresponding to the trivial holonomy, Harrington-Shepard, caloron: $\delta_1 = 0$. In that case one of the constituent monopoles is massless and pushed to infinity. The ρ parameter of the solution does no longer control the separation between the monopoles but is still a free parameter. For small ρ the HS caloron approaches an ordinary, zero temperature, instanton. From our general formulas, it is easy to check that in that limit and close to the center of the caloron the time periodicity becomes irrelevant and the two zero mode CP-pairs approach the periodic zero modes of the instanton. In the opposite, $\rho \to \infty$, limit the HS caloron becomes a BPS monopole with time independent action density. Despite the time independence of the background there are still 4 non-trivial antiperiodic zero-modes. They can be easily derived from Eqs. (5.61) and (5.63) by taking the appropriate $\delta_1 = 0$ and $\rho \to \infty$ limits. Up to a gauge transformation we obtain:

$$\delta A_\mu^{(1)\prime}(x) = \eta_{3\mu}^\alpha\, \pi\rho\left(\bar{e}_1^2(x)\, E_\alpha^{\rm bps}(r) - \bar{e}_2^2(x)\,\tilde{E}_\alpha(r)\right) + \text{h.c.}, \tag{5.69}$$

$$\delta A_\mu^{(2)}(x) = \frac{1}{4\pi}\left(\bar{e}_2^2(x)\, E_\mu^{\rm bps}(r) + \bar{e}_1^2(x)\,\tilde{E}_\mu(r)\right) + \text{h.c.}, \tag{5.70}$$

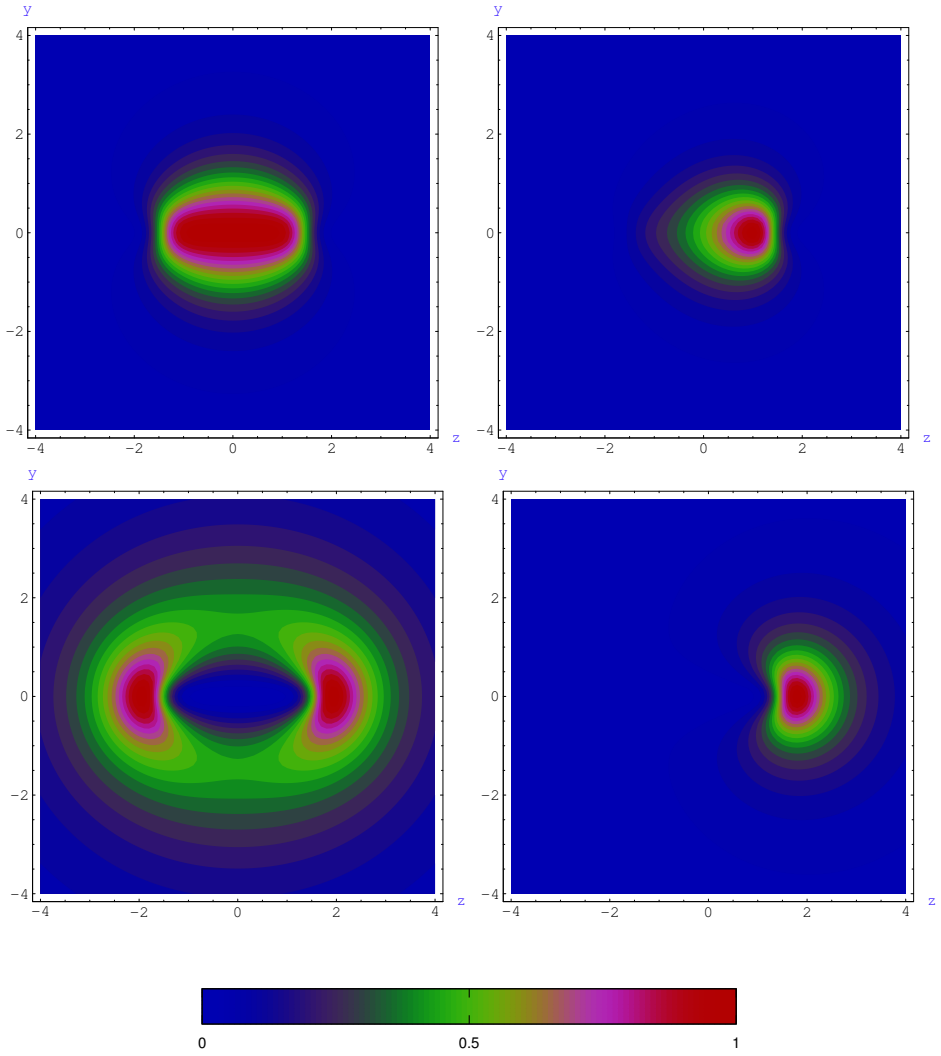

Figure 5.1: Contour plots of the density of the two antiperiodic zero modes in the $y-z$ plane. Constituent monopoles are localized at $y=0$ and separated along the z axis which is drawn horizontally. Left: For $m_1 = m_2 = \pi$ and $\rho = 1$. Right: For $\delta_1 = 0.23$ and $\rho = 1$.

where $\delta A_\mu^{(2)}$ is directly derived from Eq. (5.63) and $\delta A_\mu^{(1)'}$ is the combination of Eqs. (5.61) and (5.63) orthogonal to $\delta A_\mu^{(2)}$. In the expression above, $E_\alpha^{\rm bps}$ is the electric field of the BPS monopole:

$$E_\alpha^{\rm bps}(x) = -i\,\frac{g^2(2\pi r)-1}{2r^2}\,P_\alpha^+ - i\,\frac{\pi g'(2\pi r)}{r}\,P_\alpha^-\,, \tag{5.71}$$

and we have introduced the time independent quantity:

$$\tilde{E}_\alpha(x) = \frac{\tanh(\pi r)}{2\cosh(\pi r)}\left(i\,\frac{g(\pi r)-\cosh(\pi r)}{r^2}\,P_\alpha^+ - i\,\frac{\pi g'(\pi r)}{r}\,P_\alpha^-\right), \tag{5.72}$$

with $g(u) = u/\sinh(u)$, $g'(u)$ its derivative with respect to u, and $P_\mu^\pm = (\bar\sigma_\mu \pm \hat n \bar\sigma_\mu \hat n)/2$, $\hat n = x_i\tau_i/r$. The antiperiodicity of the solution is encoded in the time dependent quaternions $\bar e_1^2$ and $\bar e_2^2$ defined through:

$$e^{-i\pi x_\mu \bar\sigma_\mu} = i(e_1^2(x) + i e_2^2(x))\,. \tag{5.73}$$

For non-trivial holonomy there is also an interesting limit in which the caloron solution tends to the BPS monopole. It corresponds to making the separation of the constituent monopoles tend to infinity ($\rho \to \infty$). Our adjoint zero-modes lead to those of the BPS monopole if the appropriate limit is taken ($r_1 << \pi\rho^2$, $\rho >> 1$). For example, for the equal mass case ($m_1 = m_2 = \pi$) the first solution Eq. (5.61) follows quite simply by applying the appropriate limit to Eq. (5.65). Computing the density we obtain:

$$2(h'^2(\pi r) + 1 - 2h'(\pi r)\cos\theta) + g^2(\pi r) + g'^2(\pi r) + 2g(\pi r)g'(\pi r)\cos\theta \tag{5.74}$$

where $h'(u)$ is the derivative of $h(u) \equiv u\coth(u)$. This profile has axial symmetry depending explicitly on the azimuthal angle θ. Notice also that the solution is non-normalizable.

Comparison with numerical results

We have crosschecked our results with a direct evaluation of adjoint zero-modes on the torus obtained by lattice methods using Neuberger's overlap operator [30, 31] in the adjoint representation. One expects that the spatial profile of the torus solutions approaches our analytical formulas as the box size becomes much larger than all scales of the problem (β and $\pi\rho^2$). To make a quantitative comparison we computed the zero-mode density integrated in time along the line $x = y = 0$ joining both constituent monopoles. It is not possible a priori to construct numerical zero-modes with a prescribed value of ρ and δ_1, although some tuning is possible [74]. For the numerical comparison displayed in Fig. 5.2 we slightly tuned by hand these parameters to improve the agreement ($\rho = 0.79$, $\delta_1 = 0.172$). A technical point which one has to address is how to guarantee that the same linear combinations are selected for the numerical and analytical data. We chose to define the two linearly independent modes by imposing that at the center of mass ($x = y = z = 0$) one has maximal and the other minimal density (integrated over time).

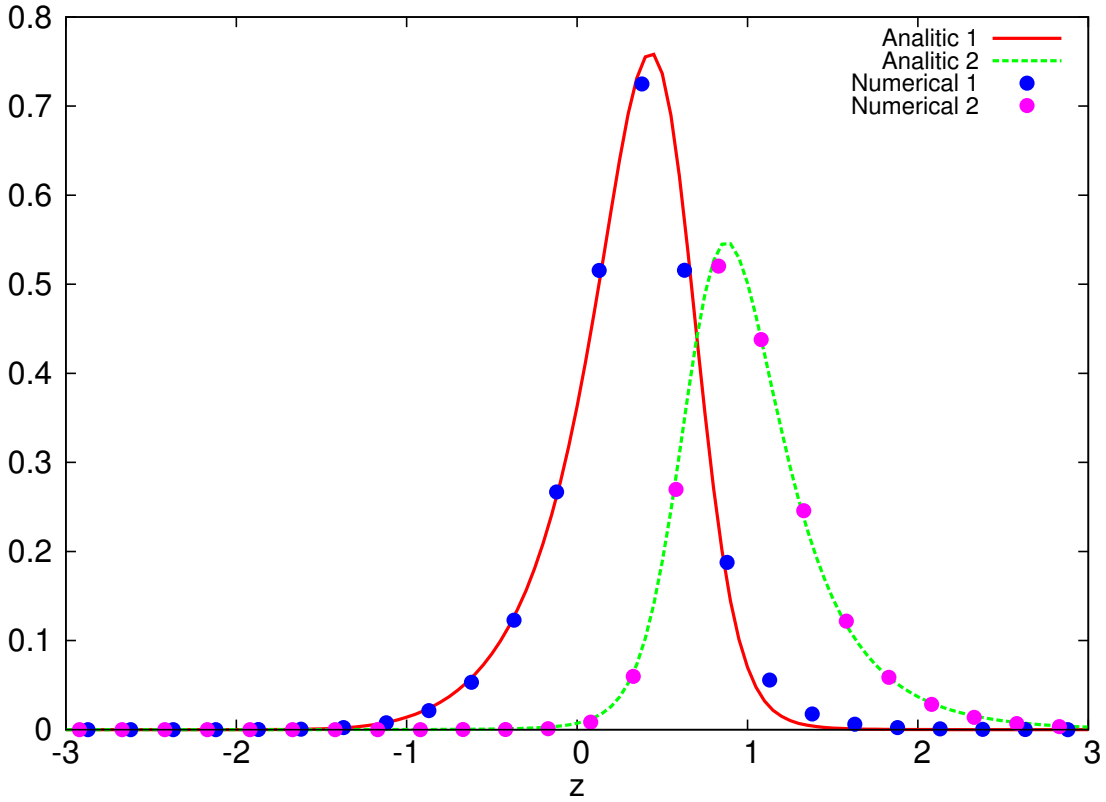

Figure 5.2: Comparison between numerical (circles) and analytic (lines) zero modes for $\rho = 0.79$ and $\delta_1 = 0.172$. We display the density of the zero modes, integrated in time, along the line joining the two monopoles.

5.5 Deformations of SU(N) calorons

In order to obtain adjoint zero-modes we must analyse self-dual deformations of the caloron vector potential. As described in section 5.2, this is achieved by deforming the corresponding ADHM-Nahm data. Imposing in addition the background gauge condition, we are led to Eq. (5.26), i.e:

$$M^\dagger \delta M = (M^\dagger \delta M)^\star \,. \tag{5.75}$$

Plugging into this formula the expression of M and δM in terms of Nahm data, leads to

$$\bar{\sigma}_\mu \hat{D}_\mu \hat{\Psi} = 4\pi^2 i (q\delta q^\dagger - (q\delta q^\dagger)^\star)\,, \tag{5.76}$$

where $\hat{\Psi} = \delta \hat{A}_\mu \sigma_\mu$ and $\hat{D}_\mu = \delta_{0\mu}\partial_z - i\hat{A}_\mu$ is the Nahm-dual covariant derivative in the adjoint representation. The previous equation should determine both $\hat{\Psi}$ and δq. The latter should have the same delta-function singularity structure as q, since that is fixed by the holonomy.

If one wants to obtain periodic and anti-periodic zero-modes one can apply the same procedure to the duplicated caloron which has $Q = 2$ topological charge. The formula now becomes

$$\bar{\sigma}_\mu \hat{D}^R_\mu \hat{\Psi}^R = 4\pi^2 i (q^R \delta q^{R\dagger} - (q^R \delta q^{R\dagger})^\star)\,, \tag{5.77}$$

where the super-index R specifies that the Nahm-dual of the replicated caloron is used. This is an U(2) gauge field living in a 1-dimensional torus (circle) of period $\frac{1}{2}$, and which is self-dual except at isolated singularities. The deformations take the form

$$\hat{\Psi}^R = \begin{pmatrix} \hat{\Psi}_{11} & \hat{\Psi}_{12} \\ \hat{\Psi}_{21} & \hat{\Psi}_{22} \end{pmatrix}. \tag{5.78}$$

The transition matrix is given by the first Pauli matrix τ_1. Thus, the boundary condition is $\hat{\Psi}^R(z+\frac{1}{2}) = \tau_1 \hat{\Psi}^R(z)\tau_1$ which implies that the components satisfy

$$\hat{\Psi}_{21}(z) = \hat{\Psi}_{12}(z+\frac{1}{2}); \quad \hat{\Psi}_{22}(z) = \hat{\Psi}_{11}(z+\frac{1}{2})\,. \tag{5.79}$$

The same conditions hold for q^R and δq^R

$$\delta q^R(z) = \begin{pmatrix} \delta\tilde{q}(z) \\ \delta\tilde{q}(z+\frac{1}{2}) \end{pmatrix}. \tag{5.80}$$

To solve Eq. (5.77) several considerations are important. The first is that δq^R is a linear combination of delta functions with singularities at Z_a and $Z_{\bar{a}} = Z_a + \frac{1}{2}$, which correspond to the same point on the dual-circle, which has period 1/2. The general form of the upper component is:

$$(\delta\tilde{q})_{\alpha i}(z) = \sum_{a=1}^{N} \left(\varphi^a_{\alpha i}\delta(z-Z_a) + \varphi^{\bar{a}}_{\alpha i}\delta(z-Z_{\bar{a}})\right)\,, \tag{5.81}$$

Furthermore, Eq. (5.77) has to be understood as an identity among operators acting over two-component vectors functions of the form:

$$\begin{pmatrix} \phi(z) \\ \phi(z+\frac{1}{2}) \end{pmatrix} . \tag{5.82}$$

Finally, it is easy to prove that each solution is associated to a 1-dim linear space in quaternions. More explicitly, given a solution $(\hat{\Psi}^R, \delta q^{R\dagger})$ a new solution is given by $(\hat{\Psi}^R Q, \delta q^{R\dagger} Q)$ for any constant quaternion Q.

In solving Eq. (5.77) one must start by determining the form of the δq^R coefficients φ, and later by solving the linear inhomogeneous equation for $\hat{\Psi}$ with fixed singularity structure.

Let us focus on the delta function structure of both sides of the equation. The singularity structure of the left-hand side is of the following form:

$$\sum_b \left[\begin{pmatrix} S_b & T_b \\ T'_b & S'_b \end{pmatrix} \delta(z - Z_b) + \begin{pmatrix} S'_b & T'_b \\ T_b & S_b \end{pmatrix} \delta(z - Z_{\bar{b}}) \right] . \tag{5.83}$$

This acts by multiplication on the appropriate space of two-component functions. On the other hand, the right-hand side of Eq. (5.77) is a linear combination of tensor products of two delta function singularities at points Z_a and $Z_{\bar{a}}$:

$$\sum_{A\,B} Q_{AB} \begin{pmatrix} \delta(z - Z_A)\,\delta(z' - Z_B) & \delta(z - Z_A)\,\delta(z' - Z_{\bar{B}}) \\ \delta(z - Z_{\bar{A}})\,\delta(z' - Z_B) & \delta(z - Z_{\bar{A}})\,\delta(z' - Z_{\bar{B}}) \end{pmatrix} , \tag{5.84}$$

where A takes 2N values which run over the values of a and $\bar{a}$, corresponding to Z_a and $Z_{\bar{a}}$ respectively. At first sight this seems quite different to the structure displayed in Eq. (5.83). However, the matching between both expressions has to be deduced by identifying the result of acting onto a vector of the appropriate space. The delta function on z' acts over the argument function and the result is then integrated over z' in the interval $[0, \frac{1}{2}]$. By comparing this action with the result of acting with Eq. (5.83) we deduce that all coefficients Q_{AB} must vanish except Q_{aa}, $Q_{a\bar{a}}$, $Q_{\bar{a}a}$ and $Q_{\bar{a}\bar{a}}$ for a running from 1 to N. In more detail we conclude that $S'_a = 0$ and

$$\delta_{ab} S_a = Q_{ab} = 4\pi^2 i \left(\zeta^a \varphi^{b\dagger} - \zeta^b_C \varphi^{a\dagger}_C \right) , \tag{5.85}$$

$$\delta_{ab} T_b = 4\pi^2 i (\zeta^a \varphi^{\bar{b}\dagger}) , \tag{5.86}$$

$$\delta_{ab} T'_b = -4\pi^2 i (\zeta^b_C \varphi^{\bar{a}\dagger}_C) , \tag{5.87}$$

where the label C stands for "charge conjugate" ($\zeta_C = \sigma_2 \bar{\zeta}$).

It is convenient to realise that the set of equations involving S_a coincide with those obtained for non-replicated calorons. Thus, it is to be expected that the corresponding zero-modes are periodic. On the other hand the equations for T and T' occur only for the replicated caloron and should be associated to anti-periodic zero-modes. This is indeed the case as we will see in the next two subsections dealing with both cases respectively.

Once the Nahm-dual deformations are obtained we can use our general formula Eq. (5.38) to obtain the ordinary deformations and adjoint zero-modes:

$$\delta A_\mu = \frac{i}{2} F^{-1/2} \int_0^{1/2} dz \left(\delta q^{R\dagger} + \frac{1}{2\pi} u^{R\dagger}(z) \hat{\Psi}^R(z) \right) \overline{\sigma}_\mu \hat{\partial} \omega^R(z) F^{1/2} + \text{h.c.}\,. \tag{5.88}$$

This formula can be simplified using the periodicity properties of the replicated functions. This will we done in the following two subsections.

5.5.1 Periodic adjoint zero-modes

In this section we will deal with the 11 component of Eq. (5.77), and we will show that it gives rise to the periodic zero-modes. The resulting equation is

$$\partial_z \hat{\Psi}_{11} = \sum_a \delta(z - Z_a) S_a \,, \tag{5.89}$$

where S_a is the solution of Eq. (5.85). Notice that $\hat{\Psi}_{11}$ is constant at intervals, so that in order to have a solution which is periodic in z with period 1, one must have:

$$\sum_a S_a = 0 \,. \tag{5.90}$$

Now we should find the solution of Eq. (5.85). Excluding exceptional values of ζ^a, which will be discussed at the end of this section, we can write

$$\varphi^a = \bar{Q}_a \zeta^a \,, \tag{5.91}$$

where Q_a are quaternions. This is easily seen to be a solution of Eq. (5.85), and furthermore

$$S_a = \mathcal{Q}_a Q_a \,, \tag{5.92}$$

where the quaternion $\mathcal{Q}_a$ is defined as

$$\mathcal{Q}_a = 4\pi^2 i (\zeta^a \zeta^{a\dagger} - \zeta^a_C \zeta^{a\dagger}_C) = -4\pi \sigma_i \Delta X^a_i \,. \tag{5.93}$$

Notice that the Q_a are not independent, since they must satisfy Eq. (5.90).

$$\sum_{a=1}^{N} \mathcal{Q}_a Q_a = 0 \,. \tag{5.94}$$

We point that the solution Eq. (5.91) coincides with the result of performing a variation of the ζ parameters describing the non-replicated caloron solution. For non-vanishing ζ^a a general variation can be written as

$$\delta \zeta^a = \bar{Q}_a \zeta^a \,. \tag{5.95}$$

Thus, the corresponding adjoint zero-modes are expected to be periodic in z. The connection between the ζ-parameters and the position of the constituent monopoles, given by

Eq. (2.74), automatically relates the deformation of these parameters with the modification of relative position of the monopoles. This relation also implies that the ζ^a are not all independent. Summing both sides of Eq. (2.74) for all values of b implies that

$$\sum_b \zeta^b \zeta^{b\dagger} = \lambda \mathbf{I}\,, \tag{5.96}$$

which can be recast in the form

$$\sum_b \zeta^b \zeta^{b\dagger} = (\sum_b \zeta^b \zeta^{b\dagger})^\star\,. \tag{5.97}$$

Obviously, the deformed values $\zeta^a + \delta\zeta^a$ must also satisfy this equation, so they are not independent. It is a trivial exercise, that we leave to the reader, to verify that Eq. (5.94) automatically enforces this constraint.

We now turn back to solving Eq. (5.94). The first trivial solution amounts to taking $Q_a = 0\ \forall a$. Then $\delta q = 0$ and Ψ_{11} is just a constant quaternion. This is easily seen to correspond to the supersymmetric zero-mode, whose density coincides with the action density of the caloron. It is obviously associated to an overall translation of the solution, i.e. to a change of the centre of mass of the monopoles.

The remaining zero-modes are associated to non-vanishing $\delta\zeta^a$. To solve the constraint equation we simply rewrite

$$Q_a = \frac{\mathcal{Q}^{a\dagger}}{\mathcal{Q}^a \mathcal{Q}^{a\dagger}} S_a = \frac{\sigma_i(\Delta X_i^a)}{4\pi ||\Delta \vec{X}^a||^2} S_a\,, \tag{5.98}$$

in terms of the quaternions S_a, which must add up to zero (Eq. (5.90)).

Now that we have been able to find the variations δq and $\delta\tilde{A}$ which satisfy the background Lorentz gauge, we can simply apply our general formulas for the adjoint modes:

$$\delta A_\mu(x) = \frac{i}{2} F^{-\frac{1}{2}} \Big\{ \int_0^1 dz \delta\tilde{q}(z)^\dagger \bar{\sigma}_\mu \hat{\partial}\omega(z) + \frac{1}{2\pi} \int_0^1 dz u^\dagger(z) \hat{\Psi}_{11}(z) \bar{\sigma}_\mu \hat{\partial}\omega(z) \Big\} F^{\frac{1}{2}} + \text{h.c.}\,. \tag{5.99}$$

For the supersymmetric mode we have $\delta\tilde{q} = 0$ and $\hat{\Psi}_{11} = 2\pi\mathbf{I}$. Thus, one obtains $\delta A_0 = 0$ and

$$\delta A_i = E_i = \sum_{a=1}^N E_i^{(a)}\,, \tag{5.100}$$

as expected. The second equality expresses the decomposition of the electric field into the contribution of each constituent monopole given by

$$E_\mu^{(a)} = \frac{i}{2} F^{-1/2} \int_{Z_{a-1}}^{Z_a} dz\, u^\dagger(z) \overline{\sigma}^\mu \hat{\partial}\omega(z) F^{1/2} + \text{h.c.}\,, \tag{5.101}$$

where the quantities $u(z)$ and $\omega(z)$ are the ADHM functions for the SU(N) calorons given in the Appendix. Furthermore, the integrals can be performed analytically. Details are given in the Appendix.

For the remaining modes one can choose a basis as follows. Take all $S_b = 0$ except for two: $S_{a-1} = 2\pi$ and $S_a = -2\pi$. This gives

$$\delta A_\mu^{(a)}(x) = E_\mu^{(a)}(x) + \widetilde{E}_\mu^{(a)}(x)\,, \tag{5.102}$$

where the first term is given by Eq. (5.101) and follows from the term involving $\hat{\Psi}_{11}$ in the deformation formula. The remaining piece $\widetilde{E}_\mu^{(a)}$ is associated to the δq piece and has a similar form to that of the vector potential:

$$\widetilde{E}_\mu^{(a)} = -\frac{i}{4}\eta_\nu^{i\mu}\left(\frac{\Delta X_i^a}{||\Delta\vec{X}^a||^2}(\mathcal{G}_\nu^a - \mathcal{G}_\nu^{a\dagger}) - \frac{\Delta X_i^{a-1}}{||\Delta\vec{X}^{a-1}||^2}(\mathcal{G}_\nu^{a-1} - \mathcal{G}_\nu^{a-1\dagger})\right)\,, \tag{5.103}$$

where

$$\mathcal{G}_\alpha^b = F^{-1/2}\zeta^{\dagger b}\overline{\sigma}_\alpha\hat{\partial}\mathcal{W}_b F^{1/2}\,, \tag{5.104}$$

with $\mathcal{W}_b = \omega(Z_b)$, and where all the quantities appearing in the formulas are computed in the Appendix.

Notice that the $\delta A_\mu^{(a)}(x)$ provide a full basis of the space of periodic deformations. In particular, the supersymmetric mode follows by addition of all these deformations.

Special cases

In our general discussion of solutions of Eq. (5.85) we excluded several special cases. One of them is that of vanishing ζ^a, corresponding to $X_i^{a+1} = X_i^a$ (coinciding monopole positions). However, there is another special case which we excluded and gives rise to additional solutions. This occurs whenever ζ^a is proportional to ζ_C^b for two different indices a and b. This condition leads to $\vec{X}^{a+1} - \vec{X}^a$ being anti-parallel to $\vec{X}^{b+1} - \vec{X}^b$. When this situation occurs there are new solutions to Eq. (5.85) having $S_a = 0$ and therefore $\hat{\Psi}_{11} = 0$ but $\delta q \neq 0$. Using the freedom to choose a representative in the one-dimensional quaternionic space we might take the solution to be

$$\varphi_{\alpha i}^a = \delta_{ib}\zeta_{\alpha a}^a \qquad \varphi_{\alpha i}^b = -\delta_{ia}\zeta_{\alpha a}^b\,. \tag{5.105}$$

Plugging this solution onto the general formula for adjoint zero-modes we obtain:

$$\delta A_\mu = \frac{i}{2}F^{-1/2}TF^{1/2}(\mathcal{G}_\mu^a + \mathcal{G}_\mu^b) + \text{h.c.}\,, \tag{5.106}$$

where T is an $N \times N$ matrix whose only non-zero elements are $T_{ab} = -T_{ba} = 1$. As we will see in Section 5.6 this solution does not satisfy neither periodic nor anti-periodic boundary conditions except for $Z_a = Z_b$ (periodic) and $|Z_a - Z_b| = \frac{1}{2}$ (anti-periodic). One of the cases analysed in Section 5.6 will be of this type.

5.5.2 Anti-periodic adjoint zero-modes

To obtain the anti-periodic modes one has to solve the 12 component of Eq. (5.77) with the singularity structure determined by Eq. (5.86)-(5.87). Excluding the case in which

$\zeta^a = 0$, corresponding to monopoles having coincident locations, the solution is given by $\varphi^{\bar{a}} = \bar{Q}_{\bar{a}}\zeta^a$, where $Q_{\bar{a}}$ is an arbitrary quaternion. The equation now becomes

$$\left(\bar{\sigma}_\mu \hat{D}^R_\mu \hat{\Psi}^R\right)_{12} = 4\pi^2 i \sum_{a=1}^{N} \left(\zeta^a \zeta^{a\dagger} \delta(z - Z_a) - \zeta^a_C \zeta^{a\dagger}_C \delta(z - \bar{Z}_a)\right) Q_{\bar{a}}\,. \tag{5.107}$$

After evaluating the commutator, the left-hand side of the previous equation becomes

$$\left(\partial_z - i\overline{\sigma}_i\,[\hat{A}_i(z) - \hat{A}_i(z + \frac{1}{2})]\right) \hat{\Psi}_{12}\,. \tag{5.108}$$

We recall that $\hat{A}_i$ is constant at intervals separating the singular points located at Z_a and $Z_{\bar{a}}$. Excluding the exceptional case of coinciding values (which can be treated as a limiting case), there are altogether 2N intervals separating two contiguous singular points. Furthermore, by the construction, we know that there are N of these singularities in the semicircle $[0, \frac{1}{2})$, and the remaining ones are displaced by $\frac{1}{2}$. Let us reorder the values in increasing order of z (from 0 to 1) and use capital letter subscripts as labels, running over positive integers modulo 2N. The value of $(\hat{A}_i(z) - \hat{A}_i(z + \frac{1}{2}))$ in the interval separating Z_{A-1} and Z_A is constant and will be labelled $-2\pi\Delta X^A_i$. On the other hand, the coefficient of the delta function $\delta(z - Z_A)$ on the left hand-side of Eq. (5.107) will be labelled $L_A Q_{\bar{A}}$, with $Q_{\bar{A}}$ a quaternion. From the periodicity properties under translations in z by $\frac{1}{2}$, we deduce $\Delta X^{A+N}_i = -\Delta X^A_i$, $L_{A+N} = L^\star_A$ and $Q_{\overline{A+N}} = Q_{\bar{A}}$.

With this notation it is easy to integrate $\hat{\Psi}_{12}$ in the interval (Z_{A-1}, Z_A), giving

$$\hat{\Psi}_{12}(z) = \exp\{-i2\pi(z - Z_{A-1})\overline{\sigma}_i \Delta X^A_i\}\kappa^{A-1}_+, \quad \text{for } z \in (Z_{A-1}, Z_A)\,. \tag{5.109}$$

At the edge of the interval this gives

$$\kappa^A_- \equiv \lim_{z \to Z_A} \hat{\Psi}_{12}(z) \equiv \mathcal{U}_{A\,A-1}\kappa^{A-1}_+\,. \tag{5.110}$$

To match the solution at the different intervals one must use

$$\kappa^A_+ - \kappa^A_- = L_A Q_{\bar{A}}\,. \tag{5.111}$$

Finally, by imposing periodicity (with period 1) in z, we obtain

$$\kappa^{2N+1}_- = W^\star_1 W_1 \kappa^1_- + \sum_{A=1}^{2N} \mathcal{U}_{2N+1\,A} L_A Q_{\bar{A}} = \kappa^1_-\,, \tag{5.112}$$

where we have introduced the following 2×2 matrices

$$\mathcal{U}_{BA} = \mathrm{Texp}\{i \int_{Z_A}^{Z_B} dz'\, \bar{\sigma}_i (\hat{A}_i(z') - \hat{A}_i(z' + \frac{1}{2}))\}\,, \tag{5.113}$$

where Texp is the clockwise-ordered exponential, and $B > A$. These matrices are like parallel transporters satisfying

$$\mathcal{U}_{CA} = \mathcal{U}_{CB}\mathcal{U}_{BA}\,. \tag{5.114}$$

The symbol W_A denotes $\mathcal{U}_{A+N\,A}$. The elementary *links* $\mathcal{U}_{A\,A-1}$, appearing in Eq. (5.110), are simple exponentials having two important properties: they are hermitian and have unit determinant. Thus, they are elements of SL(2,C), namely of the type corresponding to boosts in the $(\frac{1}{2},0)$ representation of the Lorentz group. In addition, we have $\mathcal{U}^{-1}_{A\,A-1} = \mathcal{U}^{\star}_{A\,A-1}$. Obviously, all matrices $\mathcal{U}_{BA}$ have unit determinant, but in general they cease to be hermitian. From the periodicity in z it follows that

$$\mathcal{U}_{B+N\,A+N} = \mathcal{U}^{\star}_{BA}\,. \tag{5.115}$$

In solving Eq. (5.112) one has to distinguish two cases. This depends on whether $\mathbf{I} - W_1^{\star}W_1$ is invertible or not. Since $W_1^{\star}W_1$ has unit determinant, the previous matrix is either invertible or zero. The second possibility is exceptional although it affects some particular arrangements of the monopoles. Thus, in the remaining of this section we would concentrate on the generic case, corresponding to invertibility of Eq. (5.112), which allows the determination of κ_+^A in terms of $Q_{\bar{A}}$. Later in this section we will clarify the conditions under which invertibility does not hold and provide the construction of adjoint zero-modes in that case as well.

To obtain a basis of the space of solutions we will proceed as follows. We construct the particular solutions for which all the $Q_{\bar{b}}$ are set to zero except for one $b = a$, and such that $Q_{\bar{a}} = 1$. Thus, the only discontinuities in the solution take place at $z = Z_a$ and $z = Z_{\bar{a}}$. The equation can then be solved in the two intervals separating these two singularities. We have

$$\hat{\Psi}^{(a)}_{12}(z) = \mathrm{Texp}\{i\int_{Z_a}^{z} dz'\,\overline{\sigma}_i(\hat{A}_i(z') - \hat{A}_i(z'+\frac{1}{2}))\}\kappa_+^a \quad \text{for } Z_a \le z \le Z_{\bar{a}}\,, \tag{5.116}$$

$$\hat{\Psi}^{(a)}_{12}(z) = \mathrm{Texp}\{i\int_{Z_{\bar{a}}}^{z} dz'\,\overline{\sigma}_i(\hat{A}_i(z') - \hat{A}_i(z'+\frac{1}{2}))\}\kappa_+^{a\star} \quad \text{for } Z_{\bar{a}} \le z \le Z_a\,. \tag{5.117}$$

The integrations have to be done clockwise along the unit circle. Now we should match the discontinuities from both sides of the equation. This gives simply a particular case of Eq. (5.112):

$$(\mathbf{I} - W_a^{\star}W_a)\kappa_+^a = i4\pi^2(\zeta^a\zeta^{a\dagger} - W_a^{\star}\zeta_C^a\zeta_C^{a\dagger})\,. \tag{5.118}$$

We might now collect the value of δq and $\hat{\Psi}_{12}(z)$ for this solution. Plugging these values in the general formula for the adjoint zero-modes for the replicated caloron we obtain a particular anti-periodic self-dual deformation:

$$\delta A_\mu^{(\bar{a})} = \frac{i}{2}F^{-\frac{1}{2}}\zeta^{a\dagger}\overline{\sigma}_\mu\hat{\partial}\mathcal{W}_{\bar{a}}F^{\frac{1}{2}} + \frac{i}{4\pi}F^{-\frac{1}{2}}\int_0^1 dz\,u^{\dagger}(z+\frac{1}{2})\hat{\Psi}^{(a)}_{12}(z+\frac{1}{2})\overline{\sigma}_\mu\hat{\partial}\omega(z)F^{\frac{1}{2}}\,, \tag{5.119}$$

where $\mathcal{W}_{\bar{a}} = \omega(Z_{\bar{a}})$.

The general anti-periodic zero-mode can be obtained by a linear combination with quaternionic coefficients of these N linearly independent solutions:

$$\Psi(x) \equiv \delta A_\mu \sigma_\mu = \sum_{a=1}^{N}\delta A_\mu^{(\bar{a})}\sigma_\mu Q_{\bar{a}}\,. \tag{5.120}$$

The counting agrees with the prediction of the index theorem. In the Appendix we show how to compute the integrals in Eq. (5.119) analytically.

Special cases

Our previous construction has focused in the solution of the problem for the generic case, but there are several particular cases which are interesting and do not fall into the previous category. In particular, we have to address the case for which $W_a^\star W_a = \mathbf{I}$. First we should explain in which cases does this situation arise, and then find the general solution for Nahm-dual deformations for it.

Given the properties of the $\mathcal{U}_{BA}$ matrices introduced earlier, one easily concludes that the necessary and sufficient condition for $W_a^\star W_a = \mathbf{I}$, is that W_a are hermitian. This happens for all values of a or for none. The hermiticity condition on W_a amounts, via the connection to the Lorentz group, to the problem of whether there exist a product of N boosts which is itself a boost. Obviously, this occurs whenever the boosts are collinear. In our case this occurs when all monopoles lie along a straight line, and in cases where the appropriate relative positions of monopoles are aligned. We do not know the answer to the general case but we have investigated the SU(3) and SU(4) cases and found that this in indeed the only solution for SU(3). For SU(4) a necessary condition is that the monopole relative positions must be coplanar and there are indeed an infinite set of solutions which are not collinear in which we will encounter such a situation.

In order to perform the construction of adjoint zero-modes in this case we examine the form of Eq. (5.112) in our case. We get

$$0 = \sum_{A=1}^{2N} \mathcal{U}_{2N+1\,A} L_A Q_{\bar{A}} = \sum_{A=1}^{N} (W_1^\star \mathcal{U}_{N+1\,A} L_A + \mathcal{U}^\star_{N+1\,A} L^\star_A)\, Q_{\bar{A}}\,. \tag{5.121}$$

To make this equation more clear we introduce the square root S of W_1 ($S^2 = W_1$), with the property $SS^\star = \mathbf{I}$. This is possible given the properties of W_1. Multiplying the previous equation by S we arrive at

$$0 = \sum_{A=1}^{N} \mathcal{Q}_{\bar{A}} Q_{\bar{A}}\,, \tag{5.122}$$

where the quaternion $\mathcal{Q}_{\bar{A}}$ is given by

$$\mathcal{Q}_{\bar{A}} = S^\star \mathcal{U}_{N+1\,A} L_A + (S^\star \mathcal{U}_{N+1\,A} L_A)^\star\,. \tag{5.123}$$

Eq. (5.122) is similar to the one appearing for the periodic deformations, and the conclusions are similar. There are N-1 independent solutions with $Q_{\bar{A}} \neq 0$ in addition to the homogeneous $Q_{\bar{A}} = 0$ one.

The subsequent steps to obtain the explicit form of $\hat{\Psi}_{12}$ and $\delta\tilde{q}$ for each solution of Eq. (5.122) are straightforward and we will skip them.

5.5.3 Adjoint zero-modes with more general boundary conditions

It is easy to generalise our construction to obtain adjoint zero-modes of the Dirac operator with more general periodicity conditions. These solutions turn out to be useful in several

contexts. For instance, they have been used to define the so-called dual quark condensate [86], which has been recently used to the study of the SU(2) gauge theory with adjoint fermions [87]. They could also prove to be useful in probing the topological content of the QCD vacuum [88, 89], in analogy with the case of fundamental zero-modes [56]-[65] .

In this section, we will indicate how to make use of the replica procedure described in section 5.3 to obtain solutions of the adjoint Dirac equation with periodicity given by

$$\Psi(\vec{x}, x_0 + 1) = e^{i\frac{2\pi n}{L}} P_\infty \Psi(\vec{x}, x_0) P_\infty^{-1}, \quad n, L \in \mathcal{Z} \,. \tag{5.124}$$

The construction is a straightforward generalisation of the one for anti-periodic zero-modes. It is based on replicating the caloron L times in the time direction, and solving the adjoint Nahm-dual Dirac equation, Eq. (5.77), for the replicated solution. The Nahm-dual gauge connection is given by Eq. (5.43), with transition matrices given in terms of the 't Hooft matrix P:

$$\hat{A}_\mu^R(z + \frac{n}{L}) = P^n \hat{A}_\mu^R(z) P^{n\dagger} \,. \tag{5.125}$$

In what concerns $q^R(z)$, it is given by

$$q^R(z) = \begin{pmatrix} q(z) \\ q(z + \frac{1}{L}) \\ . \\ . \\ q(z + \frac{L-1}{L}) \end{pmatrix} , \tag{5.126}$$

The deformations $\hat{\Psi}^R$ take the form of the $L \times L$ generalisation of Eq. (5.78), with periodicity condition identical to that of $\hat{A}_\mu^R(z)$ given above. The structure of δq^R is also a straightforward generalisation of Eq. (5.80). It is given by an L vector with components made up of a linear combination of delta functions with singularities at $Z_{a,q} \equiv Z_a + q/L$, with $q = 0, \cdots, L-1$. The top component for example can be written as:

$$(\delta\tilde{q})_{\alpha i}(z) = \sum_{a=1}^{N} \sum_{q=0}^{L-1} \varphi_{\alpha i}^{a,q} \, \delta(z - Z_{a,q}) \,. \tag{5.127}$$

To obtain solutions with periodicity given by Eq. (5.124) one has to solve the equations involving the $\hat{\Psi}_{1n}$ component of $\hat{\Psi}^R$. As in the case of the duplicated caloron, on must first determine the singularity structure of Eq. (5.77). The left hand side of the equation is of the form:

$$\sum_{b=1}^{N} \sum_{q=0}^{L-1} \delta(z - Z_{b,q}) \, P^q \begin{pmatrix} S_{b,0} & T_{b,0}^1 & \cdots & T_{b,0}^{L-1} \\ T_{b,1}^1 & S_{b,1} & \cdots & T_{b,1}^{L-1} \\ . & . & \cdots & . \\ T_{b,L-1}^1 & T_{b,L-1}^2 & \cdots & S_{b,L-1} \end{pmatrix} P^{q\dagger} \,. \tag{5.128}$$

An analysis analogous to that for the duplicated caloron allows to conclude that $S_{b,q}$ and $T^l_{b,q}$ are all zero except for $S_{b,0}$, $T^q_{b,0}$ and $T^{L-q}_{b,q}$ for which:

$$\begin{aligned}
\delta_{ab} S_{a,0} &= 4\pi^2 i \left(\zeta^a \varphi^{b,0\dagger} - \zeta^b_C \varphi^{a,0\dagger}_C \right) && (5.129)\\
\delta_{ab} T^q_{b,0} &= 4\pi^2 i \, (\zeta^a \varphi^{b,q\,\dagger}), \quad q = 1, \cdots, L-1 && (5.130)\\
\delta_{ab} T^{L-q}_{b,q} &= -4\pi^2 i \, (\zeta^b_C \varphi^{a,q\,\dagger}_C), \quad q = 1, \cdots, L-1 \, . && (5.131)
\end{aligned}$$

Note that the equation involving $S_{a,0}$ is identical to the one for the periodic zero-mode. The sought solutions with periodicity given by Eq. (5.124) involve instead the equations depending on $T^n_{b,0}$ and $T^{L-n}_{b,n}$. As for anti-periodic zero-modes, excluding the case in which $\zeta^a = 0$, the solution is given by setting all $\varphi^{a,q}$ to zero except for $q = n$ for which: $\varphi^{a,n} = \bar{Q}_{a,n}\zeta^a$, with an arbitrary quaternion $Q_{a,n}$. The final equation becomes:

$$\begin{aligned}
&\left(\partial_z - i\overline{\sigma}_i \, [\hat{A}_i(z) - \hat{A}_i(z + \frac{n}{L})] \right) \hat{\Psi}_{1n} = T^n_{a,0} \, \delta(z - Z_{a,0}) + T^{L-n}_{a,n} \, \delta(z - Z_{a,n}) \\
&\equiv 4\pi^2 i \sum_{a=1}^{N} \left((\zeta^a \zeta^{a\,\dagger}) \, \delta(z - Z_{a,0}) - \zeta^a_C \zeta^{a\,\dagger}_C \, \delta(z - Z_{a,n}) \right) Q_{a,n} \, . \qquad (5.132)
\end{aligned}$$

This equation is very similar to the one for the anti-periodic case and can be solved using the same techniques. Once the solution has been obtained the adjoint zero-modes with the required periodicity can be extracted from appropriate combinations of:

$$\delta H^n_\mu = \frac{i}{2} F^{-\frac{1}{2}} \sum_{a=1}^{N} \zeta^{a\dagger} Q_{a,n} \overline{\sigma}_\mu \hat{\partial} \mathcal{W}_{a,n} F^{\frac{1}{2}} + \frac{i}{4\pi} F^{-\frac{1}{2}} \int_0^1 dz \, u^\dagger(z - \frac{n}{L}) \hat{\Psi}_{1n}(z - \frac{n}{L}) \, \overline{\sigma}_\mu \hat{\partial} \omega(z) F^{\frac{1}{2}} \, , \qquad (5.133)$$

where $\mathcal{W}_{a,n} = \omega(Z_{a,n})$.

5.6 Analyses of the solutions

In this section we will study several properties of the solutions constructed in the previous sections. In particular, we will verify their assumed periodicity properties and discuss their orthogonality and normalisability. We will show several explicit examples that illustrate the density profiles of the solutions and their relation to the gauge field density and the position and masses of the constituent monopoles.

5.6.1 Periodicity

Here we will argue that the solutions presented in the previous sections have the required (anti)periodicity in time. This can be easily derived taking into account the transformation properties of u and w under a time shift by one period. Using the formulas for u and w derived in the Appendix, it can be checked that:

$$u(z, x_0 + 1) = e^{i2\pi z} \, u(z, x_0) \, P_\infty^{-1} \, , \qquad (5.134)$$

and that an identical expression holds for $w(z, x_0)$. Using in addition that δq and the Nahm data do not depend on x_0, and that $F = I\!I_N + u^\dagger u$, the appropriate periodicity is obtained for periodic, Eq. (5.99), and anti-periodic, Eq. (5.119), solutions. To show that the term in δq satisfies the required periodicity in time, one must realise that

$$\zeta^{a\dagger} e^{2\pi i Z_a} = P_\infty \zeta^{a\dagger} \tag{5.135}$$

These formulas also serve to substantiate the claim that the adjoint zero-modes associated to Eq. (5.133) satisfy the boundary conditions given in Eq. (5.124). The additional zero-modes given in Eq. (5.106) fail to satisfy simple boundary conditions unless $P_\infty^{-1} T P_\infty = \pm T$.

5.6.2 Normalisability

To analyse the normalisability of our solutions one can make use of the general formulas for the norm and the scalar products of the solutions derived in [14, 26] in terms of the Nahm data. Following [26] one can compute the scalar products of the zero-modes in terms of the quaternionic quantities:

$$\begin{aligned}
\langle \Psi, \Psi' \rangle \;\equiv\; & \int d\vec{x} \int_0^1 dt \, \mathrm{Tr}\Big(\Psi^\dagger(x) \Psi'(x) \Big) = \int_0^1 dz \, \Big(\hat{\Psi}^\dagger_{11}(z) \, \hat{\Psi}'_{11}(z) + \hat{\Psi}^\dagger_{12}(z) \, \hat{\Psi}'_{12}(z) \Big) \\
+ \;& 4\pi^2 \int_0^{\frac{1}{2}} dz \int_0^{\frac{1}{2}} dz' \Big(\delta\tilde{q}(z) \, \delta\tilde{q}'^\dagger(z') \;+\; (\delta\tilde{q}(z) \, \delta\tilde{q}'^\dagger(z'))^\star \Big) \\
+ \;& 4\pi^2 \int_{\frac{1}{2}}^1 dz \int_{\frac{1}{2}}^1 dz' \Big(\delta\tilde{q}(z) \, \delta\tilde{q}'^\dagger(z') \;+\; (\delta\tilde{q}(z) \, \delta\tilde{q}'^\dagger(z'))^\star \Big)
\end{aligned} \tag{5.136}$$

where $\Psi = \delta A_\mu \sigma_\mu$, Tr denotes the trace over colour indices, and $\delta\tilde{q}$ is given by Eq. (5.81). Notice that, given the shift by $\frac{1}{2}$ in the singularity position in $\delta\tilde{q}$ for periodic and anti-periodic solutions, the formula automatically gives the orthogonality of both sets of solutions. In the following two subsections we will analyse the scalar products within each set separately (periodic and anti-periodic).

Periodic zero-modes

The generic periodic zero-modes correspond to solutions where $\hat{\Psi}_{12} = 0$ and $\delta\tilde{q}(z) = \sum_{a=1}^N \varphi^a \delta(z - Z_a)$. Accordingly:

$$\langle \Psi, \Psi' \rangle = \int_0^1 dz \, \Big(\hat{\Psi}^\dagger_{11}(z) \, \hat{\Psi}'_{11}(z) \Big) + \, 4\pi^2 \sum_{a=1}^N \Big(\varphi^a \varphi'^{a\dagger} + (\varphi^a \varphi'^{a\dagger})^\star \Big) , \tag{5.137}$$

where we have used the fact that $\varphi^a \varphi'^{b\dagger}$ is proportional to $\delta_{a,b}$ for our choice of variations: $\varphi^a = \bar{Q}_a \zeta^a$, $\varphi'^a = \bar{Q}'_a \zeta^a$.

Let us start with the supersymmetric CP-pair of zero-modes Eq. (5.100), given by $\varphi^a = 0$, $\forall a$, and $\hat{\Psi}_{11}(z)$ a constant quaternion. From eq. (5.137) it follows that the solution

is normalisable with norm $4\pi^2$. This can also be derived using the already discussed proportionality between the density of the supersymmetric zero-modes and the action density of the caloron, i.e. $\delta A_0 = 0$ and $\delta A_i = E_i$, with E_i the electric field of the self-dual caloron.

We now proceed to analyse the normalisability of the remaining zero-modes. Consider the solution given by $\Psi^{(a)} = \delta A_\mu^{(a)} \sigma_\mu$, with $\delta A_\mu^{(a)} = E_\mu^{(a)} + \widetilde{E}_\mu^{(a)}$ as in Eq (5.102). They correspond to setting $\hat{\Psi}_{11}^{(a)} = 2\pi\chi_a(z)$, and all φ^b equal to zero except for $b = a-1$ and $b = a$, for which they are given by Eqs. (5.91) and (5.98), with $S_{a-1} = -S_a = 2\pi$. Using formula (5.137) we obtain the following expression for the scalar products:

$$\langle \Psi^{(a)},\, \Psi^{(b)} \rangle = 2\pi\, m_a\, \delta_{ab} + \frac{\pi}{||\Delta\vec{X}^a||}\,(\delta_{ab} - \delta_{a+1\,b}) + \frac{\pi}{||\Delta\vec{X}^{a-1}||}\,(\delta_{ab} - \delta_{a-1\,b})\,. \qquad (5.138)$$

The set becomes orthogonal in the limit in which the N constituent monopoles of the caloron are infinitely separated, i.e. $||\Delta\vec{X}^a|| \to \infty$, for all a. As mentioned in section 5.5.1, the supersymmetric zero-modes can be obtained as the linear combination $\Psi = \sum_{a=1}^N \Psi^{(a)}$. This correctly reproduces the fact that in the limit of large separation the energy density of the caloron decomposes in the sum of N BPS monopoles with respective masses equal to $2\pi m_a/g^2$. Each of them carries a CP-pair of periodic zero-modes given by $\Psi^{(a)} = (\psi^{(a)}, \psi_C^{(a)})$, in accordance to the Callias index theorem for BPS monopoles [90].

Anti-periodic zero-modes

In a similar way we can derive the expression for the scalar products of the anti-periodic zero-modes. They correspond to solutions with $\hat{\Psi}_{11} = 0$ and $\delta\tilde{q}(z) = \sum_{a=1}^N \varphi^{\bar{a}}\delta(z - Z_{\bar{a}})$, with $\varphi^{\bar{a}} = \bar{Q}_{\bar{a}}\zeta^a$. The general formula for the scalar products reduces in this case to:

$$\langle \Psi, \Psi' \rangle = \int_0^1 dz \left(\hat{\Psi}_{12}^\dagger(z)\, \hat{\Psi}'_{12}(z) \right) + 4\pi^2 \sum_{a=1}^N \left(\varphi^{\bar{a}} \varphi'^{\bar{a}\dagger} + (\varphi^{\bar{a}} \varphi'^{\bar{a}\dagger})^\star \right). \qquad (5.139)$$

We will only provide here an explicit expression for the generic case presented in section 5.5.2, non-generic situations are left to the reader. The generic solutions are given by $\Psi^{(\bar{a})} = \delta A_\mu^{(\bar{a})} \sigma_\mu$, with $\delta A_\mu^{(\bar{a})}$ as in Eq. (5.119). They are obtained by setting all $\varphi^{\bar{b}}$ to zero except for $\varphi^{\bar{a}} = \zeta^a$, and by taking $\hat{\Psi}_{12}$ as in Eqs. (5.116), (5.117). Inserting these expressions into the formula for the the scalar products, we obtain:

$$\langle \Psi^{(\bar{a})},\, \Psi^{(\bar{b})} \rangle = 4\pi\, ||\Delta\vec{X}^a||\, \delta_{ab} + \sum_{A=1}^{2N} \frac{\delta_A}{g(2\pi\delta_A\, ||\Delta\vec{X}^A||)}\, O_A^{a\dagger}\, e^{-i2\pi\bar{\sigma}_i \delta_A \Delta X_i^A}\, O_A^b\,, \qquad (5.140)$$

where $\delta_A = Z_A - Z_{A-1}$, and

$$\begin{aligned} O_A^c &= \mathrm{Texp}\{i \int_{Z_c}^{Z_{A-1}} dz'\, \overline{\sigma}_i (\hat{A}_i(z') - \hat{A}_i(z' + \frac{1}{2}))\} \kappa_+^c, \quad \text{for } (Z_{A-1}, Z_A) \subset (Z_c, Z_{\bar{c}})\,, \\ O_A^c &= \mathrm{Texp}\{i \int_{Z_{\bar{c}}}^{Z_{A-1}} dz'\, \overline{\sigma}_i (\hat{A}_i(z') - \hat{A}_i(z' + \frac{1}{2}))\} \kappa_+^{c\star}, \quad \text{for } (Z_{A-1}, Z_A) \subset (Z_{\bar{c}}, Z_c)\,. \end{aligned}$$

5.6.3 Zero-mode density profiles

We proceed now to discuss some illustrative examples of periodic and anti-periodic zero-modes for different gauge groups. In order to obtain the density profiles we have developed two independent numerical codes which work for general SU(N) gauge group and give matching results. We will discuss separately the cases corresponding to different periodicity.

Periodic zero-modes

Figure 5.3 displays results for the gauge group SU(3) and for three different choices of the monopole masses: $m_1 = m_2 = m_3 = 2\pi/3$; $m_1 = m_2 = \pi/2$, $m_3 = \pi$; and $m_1 = m_2 = \pi/3$, $m_3 = 4\pi/3$. In all cases the monopoles are located on the vertices of an equilateral triangle of side 2. We plot both the density of the supersymmetric CP-pair of zero-modes and the 3 CP-pairs denoted previously by $\Psi^{(a)}$. The figure exemplifies how in the regime in which $||\Delta\vec{X}^a|| > 1$, $\forall a$, the action density of the caloron, given by the density profile of the supersymmetric zero-mode, decomposes into three constituent BPS monopoles. Each of

them carries a CP-pair of adjoint zero-modes given in this limit by the solutions parametrised by $\Psi^{(a)}$.

In the opposite limit in which $||\Delta\vec{X}^a|| << 1$, $\forall a$, the caloron becomes an ordinary BPST instanton and the action density recovers spherical symmetry. For the equal mass case and with monopoles located on the vertices of an equilateral triangle, the symmetry properties allow us to obtain three orthogonal modes, given by the supersymmetric mode and two other linear combinations. The latter are obtained in terms of the following linear combinations of the Nahm data

$$\hat{\Psi}^{(1)}_{11} + \hat{\Psi}^{(2)}_{11}\, e^{-\frac{2}{3}\pi\sigma_3} + \hat{\Psi}^{(3)}_{11}\, e^{\frac{2}{3}\pi\sigma_3}\,,$$
$$\hat{\Psi}^{(1)}_{11} + \hat{\Psi}^{(2)}_{11}\, e^{\frac{2}{3}\pi\sigma_3} + \hat{\Psi}^{(3)}_{11}\, e^{-\frac{2}{3}\pi\sigma_3}\,,$$

with analogous combinations for the $\delta\tilde{q}^\dagger$ terms. The resulting density profiles, for an equilateral triangle of side 0.1, are presented in figure 5.4. Figure 5.5 displays the periodic zero-modes for gauge group SU(4) and for equal mass monopoles arranged on the vertices of a square of side 2. Again each non-supersymmetric CP-pair of zero-modes has support on a single constituent monopole. The limit of small separation reproduces again the situation for the BPST instanton.

Anti-periodic zero-modes

In this subsection we will focus on describing a few representative examples of anti-periodic zero-modes for SU(3) and SU(4). We have already discussed in section 5.5.2 that one has to distinguish two main cases depending on the invertibility of $\mathbf{I} - W_1^\star W_1$. We will only focus on the generic situation which correspond to the invertible case. This covers all the possible cases for SU(3) although not for SU(4).

Let us start with the SU(3) case for which the three CP-pairs of solutions, i.e. $\Psi^{(\bar{a})} \equiv \delta A^{(\bar{a})}_\mu \sigma_\mu$, are given by Eqs. (5.116)-(5.119). The first thing that singles out anti-periodic

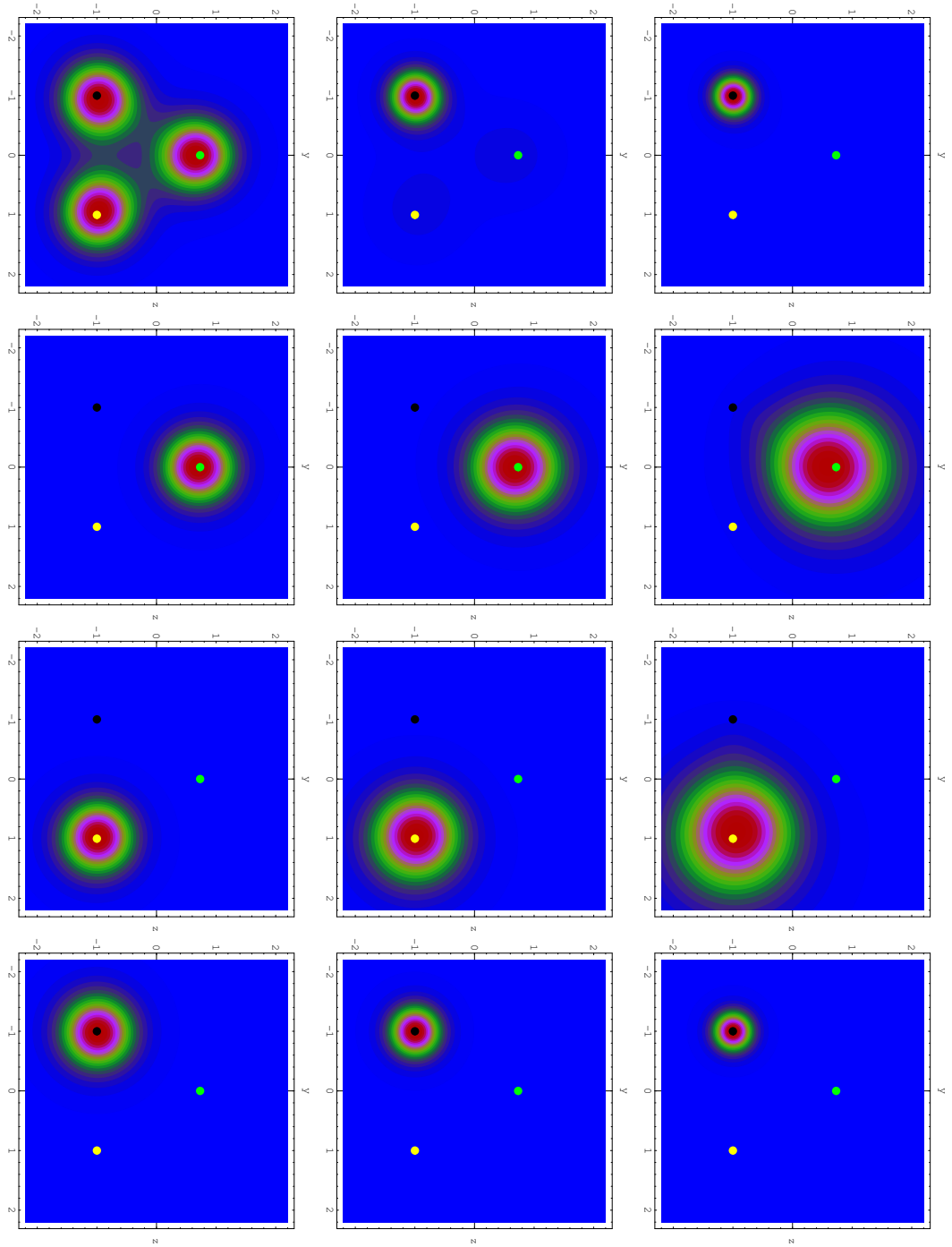

Figure 5.3: Contour plots of the periodic zero-mode densities in the $x = t = 0$ plane for gauge group SU(3). The three columns display, from left to right, the zero-modes corresponding to monopole masses: $m_1 = m_2 = m_3 = 2\pi/3$; $m_1 = m_2 = \pi/2$, $m_3 = \pi$; and $m_1 = m_2 = \pi/3$, $m_3 = 4\pi/3$. The top row displays the supersymmetric zero-modes and the lower three the non-supersymmetric modes, i.e. $\delta A_\mu^{(a)}$ as in Eq. (5.102), with, from top to bottom, $a = 1, 2, 3$. Monopoles are localised on the vertices of an equilateral triangle of side 2, on the $x = t = 0$ plane. The small filled circles indicate the monopole positions, starting from the top monopole in each plot and in clockwise sense: $\vec{X}^1$-green, $\vec{X}^2$-yellow, $\vec{X}^3$-black.

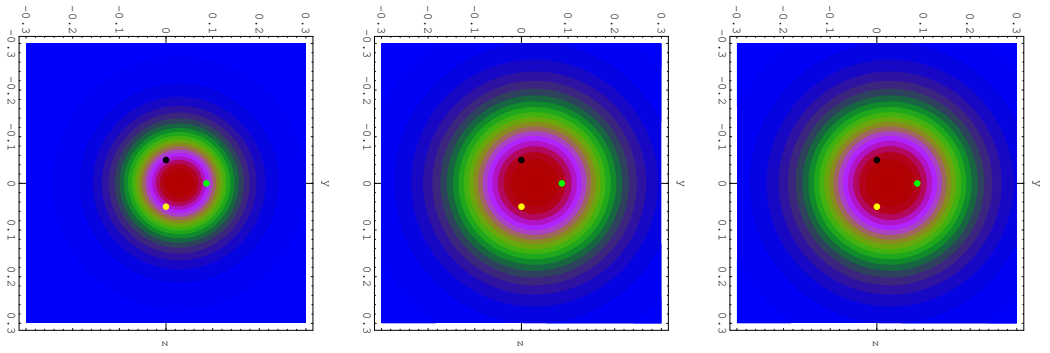

Figure 5.4: Contour plots of the periodic zero-mode densities at the $t = x = 0$ plane for gauge group SU(3) and the equal mass case. The zero-modes have been constructed from orthogonal combinations of the $\Psi^{(a)}$ described in Eq. 5.141. The plot on the left corresponds to the supersymmetric mode, the ones on the right display the other two orthogonal modes. Monopoles are localised on the vertices of an equilateral triangle of side 0.1, on the $x = t = 0$ plane. The small filled circles indicate the monopole positions, starting from the top monopole in each plot and in clockwise sense: $\vec{X}^1$-green, $\vec{X}^2$-yellow, $\vec{X}^3$-black.

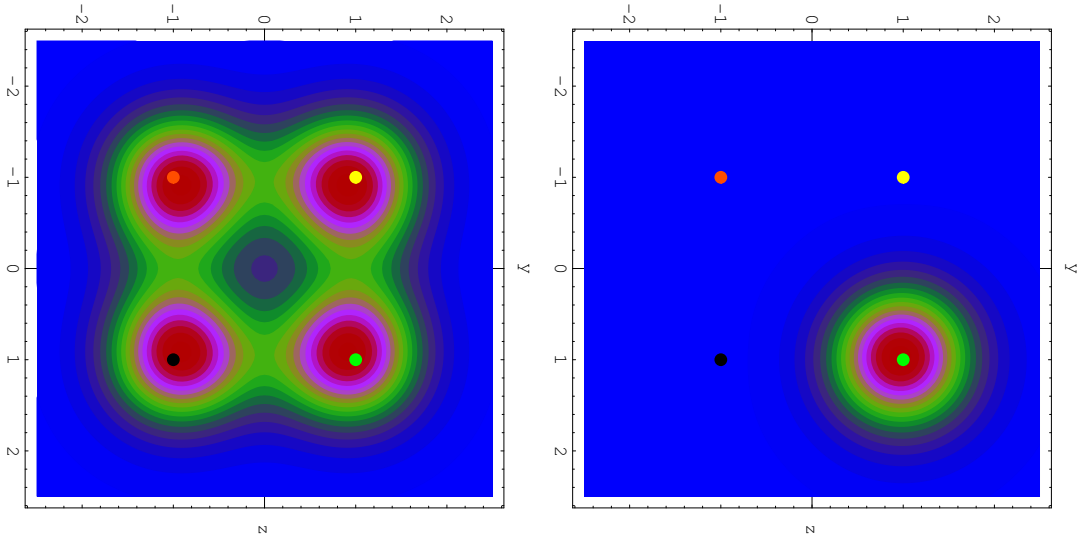

Figure 5.5: Contour plots of the supersymmetric (left) and non-supersymmetric (right) periodic zero-mode densities on the $x = t = 0$ plane for gauge group SU(4) and the equal mass case. We only show one of the non-supersymmetric zero-modes, $\Psi^{(1)}$. The rest look alike but rotated by 90, 180 and 270 degrees along the x symmetry axis. Monopoles are localised on the vertices of a square of side 2, on the $x = t = 0$ plane. The small filled circles indicate the monopole positions, starting from the top-right monopole in each plot and in clockwise sense: $\vec{X}^1$-green, $\vec{X}^2$-black, $\vec{X}^3$-red, $\vec{X}^4$-yellow.

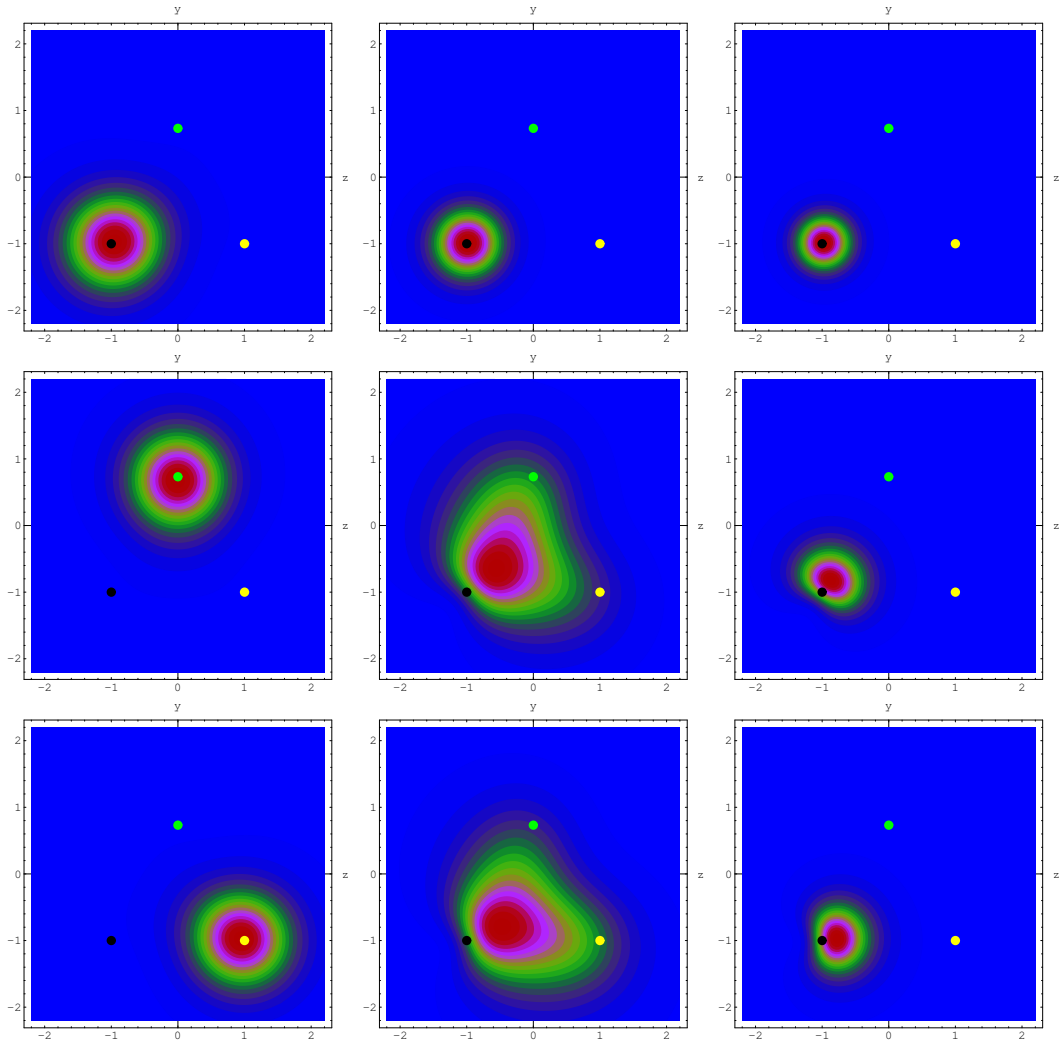

Figure 5.6: Contour plots of the anti-periodic zero-mode densities on the $x = t = 0$ plane for gauge group SU(3). The three columns display, from left to right, the zero-modes corresponding to monopole masses: $m_1 = m_2 = m_3 = 2\pi/3$; $m_1 = m_2 = \pi/2$, $m_3 = \pi$; and $m_1 = m_2 = \pi/3$, $m_3 = 4\pi/3$. The three rows display the modes corresponding to $\delta A_\mu^{(\bar{a})}$ as in Eqs. (5.116)-(5.119), with, from top to bottom, $a = 1, 2, 3$. Monopoles are localised on the vertices of an equilateral triangle of side 2, on the $x = t = 0$ plane. The small filled circles indicate the monopole positions, starting from the top monopole in each plots and in clockwise sense: $\vec{X}^1$-green, $\vec{X}^2$-yellow, $\vec{X}^3$-black.

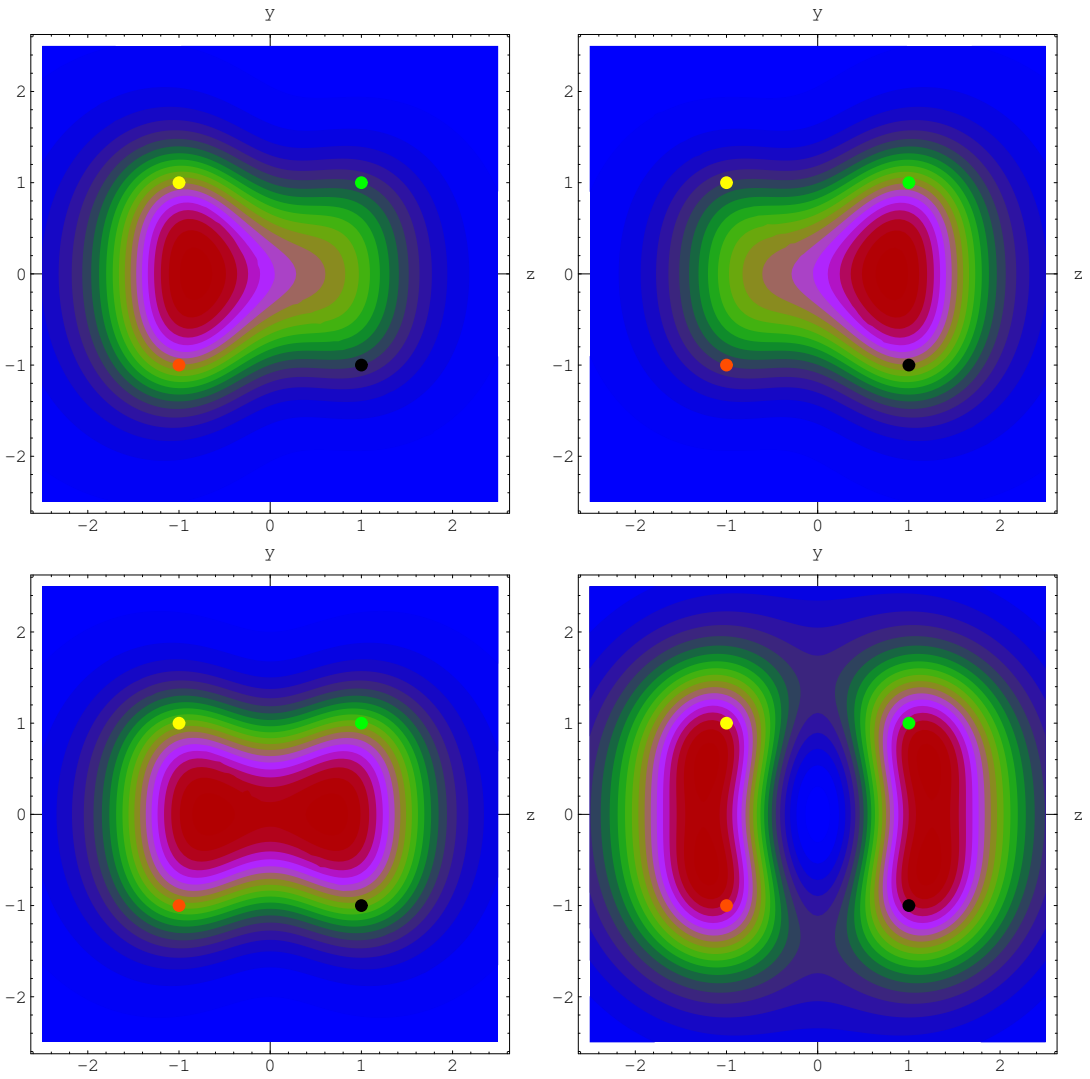

Figure 5.7: Contour plots of the anti-periodic zero-mode densities on the $x = t = 0$ plane for SU(4) and the equal mass case. The relative positions of the monopoles are such that $\Delta\vec{X}^2 = -\Delta\vec{X}^4 = -2\hat{k}$. The upper plots display $\Psi^{(\bar{1})}$ (left) and $\Psi^{(\bar{3})}$ (right). The lower plots display the linear combinations $\Psi^{(\bar{1})} - \Psi^{(\bar{3})}$ (left) and $\Psi^{(\bar{1})} + \Psi^{(\bar{3})}$ (right). The remaining modes can be obtained by rotating each of these plots by 90 degrees. Monopoles are localised on the vertices of a square of side 2, on the $x = t = 0$ plane. The small filled circles indicate the monopole positions, starting from the top-right monopole in each plot and in clockwise sense: $\vec{X}^1$-green, $\vec{X}^2$-black, $\vec{X}^3$-red, $\vec{X}^4$-yellow.

as compared to periodic zero-modes is their localisation with respect to the constituent monopole positions. For well separated monopoles the $\Psi^{(\bar{a})}$ CP-pair of zero-modes has support on the monopole attached to the interval $[Z_{b-1}, Z_b]$ containing $Z_{\bar{a}} = Z_a + \frac{1}{2}$. This gives rise to different possibilities depending on the monopole masses. Fig. 5.6 displays three characteristic cases corresponding to: $m_1 = m_2 = m_3 = 2\pi/3$; $m_1 = m_2 = \pi/2$, $m_3 = \pi$; and $m_1 = m_2 = \pi/3$, $m_3 = 4\pi/3$. The first one is analogous to the periodic case (Fig. 5.3) in that each monopole supports one CP-pair of zero-modes. This changes, however, when one of the monopole masses exceeds π. In that case the more massive monopole *attracts* the full set of anti-periodic zero-modes and the rest support none. The intermediate case is a limit between the two situations in which two of the zero-modes become delocalised. These results match the predictions of the index theorem for SU(N) self-dual configurations on $R^3 \times S^1$. We will make here a brief interlude, following Ref. [83, 84], to show that this is indeed the case. We will not give the general formula for the index but we will directly analyse the case for SU(3), relevant for the discussion of Figs. 5.3 and 5.6. The reader is referred to Ref. [83, 84] for the general treatment.

The index in the adjoint representation can be written in terms of the topological charge Q, the eigenvalues of the holonomy Z_a (equivalently the monopole masses) and the magnetic charges $(M_1, \cdots, M_{N-1})$. The latter are derived from the asymptotic behaviour of the magnetic field at spatial infinity, i.e.

$$\vec{B}(|\vec{x}| \to \infty) = \frac{\vec{x}}{|\vec{x}|^3} \, \mathrm{diag}(n_1 - n_N, n_2 - n_1, \cdots, n_N - n_{N-1}) \,, \tag{5.141}$$

with magnetic charges given by $M_i = n_i - n_N$. Note that one can fit both calorons and BPS monopoles into this description. For the latter, there are N elementary types of monopoles obtained by setting $n_i = 1$, with $n_{j \neq i} = 0$ and $i = 1, \cdots, N$. The monopole that corresponds to taking $i = N$ is usually called the Kaluza-Klein monopole and has magnetic charges $(-1, \cdots, -1)$. Calorons with topological charge $Q = 1$ have zero magnetic charge and are obtained by setting all n_i equal to one, reproducing therefore the picture of the caloron as a composite of N BPS monopoles.

In terms of the n_i and the monopole masses the index in the adjoint representation of SU(3), giving the number of periodic zero-modes, is [83, 84]:

$$I_{\mathrm{adj}}(Q, n_1, n_2, n_3) = 2NQ\, n_3 - \sum_{i=1}^{3} n_i \, \Big(2\,[-v_i] - 2\,[v_i] - \sum_{i \neq j} ([-v_j] - [v_j]) \Big) \tag{5.142}$$

where $v_i = m_i/2\pi$, for $i = 1, 2$, $v_3 = m_3/2\pi - 1$, and $[v] \equiv \max\{n \in \mathcal{Z} \,|\, n \leq v\}$. Note that the Kaluza-Klein monopole is peculiar in that it receives a contribution from the topological charge term. It is easy to check from the formula that, for monopole masses smaller than 2π and $Q = 1$, each monopole supports 2 periodic zero-modes in agreement with the index theorem by Callias. The formula also gives a correct counting of the number of periodic zero-modes for the $Q = 1$ caloron, i.e. 2N. To compute the number of anti-periodic zero-modes we have to resort again to the replica trick. After replicating once in time we obtain that $Q \to 2Q$ and $v_i \to 2v_i$. Accordingly the number of zero-modes for the replicated caloron is $4N$, out of which $2N$ are periodic and $2N$ anti-periodic on the

original torus. In what refers to monopoles, it is easy to check that the formula for the index in the replicated torus gives:

- If $m_1 = m_2 = m_3 = 2\pi/3$, then: $I^R_{\rm adj}(Q = 2, n_1, n_2, n_3) = 4n_1 + 4n_2 + (4N - 8)n_3$. Each monopole supports 4 periodic zero-modes in the replicated torus. This implies two periodic plus two anti-periodic zero-modes in the original configuration as observed in the corresponding plots of Figs. 5.3 and 5.6.

- If $m_1 = m_2 = \pi/3$, $m_3 = 4\pi/3$, then: $I^R_{\rm adj}(Q = 2, n_1, n_2, n_3) = 2n_1 + 2n_2 + (4N-4)\, n_3$. Monopoles 1 and 2 have only two zero-modes in the replicated torus, while the more massive monopole, attached to n_3, has 8 zero-modes. Out of those 2 for each monopole correspond to periodic zero-modes of the original configuration. We obtain therefore the result advanced in Figs. 5.3 and 5.6: monopoles 1 and 2 support no anti-periodic zero-modes, while monopole 3 carries 6 anti-periodic zero-modes.

More general situations can also be analysed using the expression for the index given in Eq. (5.142).

We proceed now to present results for the gauge group SU(4). We will restrict the discussion to the case of equal mass monopoles localised on the vertices of a square. Given that the monopole relative positions are coplanar this admits special solutions as the ones discussed in section 5.5.2. However, we will only consider the case having $\Delta\vec{X}^2 = -\Delta\vec{X}^4 = -2\hat{k}$, which belongs to the generic situation in which $\mathbf{I} - W_1^\star W_1$ is invertible. Thus, the zero-modes are given by Eqs. (5.116)-(5.119). The alternative choice having $\Delta\vec{X}^2 = \Delta\vec{X}^4 = -2\hat{k}$, gives rise to $W_1^\star W_1 = \mathbf{I}$. The solutions can be obtained by the construction following Eqs. (5.122), (5.123), but will not be presented here.

Figure 5.7 displays the invertible case with monopoles localised on the vertices of a square of side 2. The fact that zero-modes are not attached to a single BPS monopole is related to a singularity of the equal mass case for SU(4). It happens that every $Z_{\bar{a}}$ coincides with one of the eigenvalues of the holonomy (Z_b for some b). Consequently it lies between two monopole intervals and the zero-mode density spreads among both. The $a = 1$ case for instance has the singularity at $Z_{\bar{1}} = Z_3$, therefore the density profile should be attached to monopoles 3 and 4 and aligned with the 3-4 relative position: $\Delta\vec{X}^4 = 2\hat{k}$. The upper-left plot of Fig. 5.7 shows that this is indeed the case. Note in addition that the anti-parallelism of $\Delta\vec{X}^2$ and $\Delta\vec{X}^4$ corresponds to the condition for the existence of spurious solutions with modified periodicity described at the end of section 5.5.1. According to the discussion presented there whenever this condition holds it should be possible to find a pair of zero-modes for which $\hat{\Psi}_{11} = 0$ and only the term in $\delta\tilde{q}$ survives. As already discussed, for equal mass monopoles these spurious solutions do give rise to anti-periodic zero-modes. Indeed, two such solutions can be obtained from the linear combinations $\Psi^{(\bar{2})} + \Psi^{(\bar{4})}$ and $\Psi^{(\bar{1})} + \Psi^{(\bar{3})}$. The latter and the alternative combination $\Psi^{(\bar{1})} - \Psi^{(\bar{3})}$ are displayed in Fig. 5.7.

5.7 Summary and Outlook

In this chapter we have addressed the analytical construction of adjoint zero-modes of the Dirac equation in the background field of SU(N) $Q = 1$ calorons. We have covered

both periodic and anti-periodic boundary conditions in time. The latter is useful for the semi-classical study of $\mathcal{N} = 1$ SUSY Yang-Mills at finite temperature and the longstanding issues of Supersymmetry breaking. In this chapter we have made an effort to make a complete study of the problem of adjoint zero-modes in SU(N) Yang-Mills theory, presenting general formulas and derivations for the ADHM construction, the Nahm transform on the torus, and, finally, for the caloron case. Thus, we hope this solutions could serve as a useful reference for researchers interested in gluino zero-modes.

Although the formulas for SU(N) contain those for the SU(2) case, it is found out that the latter case is quite exceptional in several aspects, so that the generalisation is far from being trivial. Ultimately, given the generality of our formulas, we hope that they will be instrumental in addressing several open issues, including theoretical problems about higher charge calorons, the finite temperature behaviour of SUSY Yang-Mills theory, which we intend to address themselves in future publications, and other applications of adjoint zero-modes mentioned in the Introduction of this chapter.

Chapter 6

Probing Yang-Mills vacuum

In the past years a considerable effort has been devoted to the analysis of the topological structure of pure Yangs-Mills theory on the lattice. These studies encompass from global quantities, like the topological susceptibility, to local ones, in an attempt to link topology to models of chiral symmetry breaking and confinement. For that one has to deal with the roughness of lattice Monte-Carlo configurations, which are generally plagued with ultraviolet fluctuations. Several cooling and smearing algorithms have been proposed in order to obtain a smoother image of these configurations. Although these methods are useful in order to compute global quantities, they are criticized as a tool to analyse local properties. An alternative, claimed to distort less the original ensemble, is to use filtering methods based on the Dirac operator (see for example [91] and references therein). The main idea is the relation between fermions and topology given by the Atiyah-Singer index theorem and the correlation between the gauge action density and the local density of the eigenstates of the Dirac operator. As will be described below, this relation is particularly neat for fermions in the adjoint representation.

In the following we will present a review of smoothing and filtering methods commonly used to explore the Yang-Mills vacuum. Section 6.1 focuses in standard smoothing techniques, paying special attention to the improved cooling algorithm, used to generate the smooth configurations analysed in section 6.3. A new filtering method based on the use of the adjoint representation of the Dirac operator advocated in [89] is presented in section 6.2. This method relies on finding an adjoint fermion zero-mode, called Supersymmetric Mode (SSM), whose density corresponds directly with the gauge action density. Two methods were proposed in [89] to find the SSM. In section 6.2 they are explained as well as their lattice implementation using the Neuberger operator. The construction of the SSM in [89] is exact for classical solutions of the equations of motion and relies on the existence of zero-modes of the Dirac operator. In practice, however, non-classical configurations are involved in most interesting situations and we will analyse how the method performs in such cases.

6.1 Smoothing and Filtering Methods

The analysis of topological structures hidden in Monte Carlo configurations is crucial to try to connect the results obtained in lattice calculations with the semi-classical approximation. In the gauge action, high momentum fluctuations of A_μ are amplified, so the gauge action density of Monte Carlo configuration is too rough to be explored directly. This problem can be treated by two methods: modifying the configuration by removing the high momentum fluctuations or using an operator where these fluctuations will be suppressed. In the spirit of the first method, smearing and cooling algorithms have been proposed. These methods are based on replacing each link by a combination of staples, reducing the noise of the configurations. Let the gauge action density be written as

$$S = \mathrm{Tr}(U_\mu(n) U'^{\dagger}_{\mu}(n)) + ... \tag{6.1}$$

where $U'(n)$ is a complex matrix. Both algorithms update each link as

$$U_\mu(x) \to P_{SU(N)} \left(\alpha U_\mu(x) + (1-\alpha) U'_\mu \right) \tag{6.2}$$

where $\alpha \in (0,1)$. Smearing replaces simultaneously all links of the lattice. In the cooling algorithms, however, the replacement is done sequentially guaranteeing that the action is minimized at every step. Thus, using cooling algorithms the configuration is driven to a local minimum of the action. The main property of both smearing and cooling algorithms is that they reduce ultraviolet modes faster than the infrared ones. So it is expected that extended objects are not altered too much. The problem of these methods comes from the possible modification of the positions and sizes of topological objects in the updating process. For small objects, this modification could destroy them. Improved implementations of these methods can be used to minimize these effects.

In order to avoid this problem it would be desirable to have a method that does not modify the initial configuration. Within this framework fall the filtering methods. The main idea is analyse Monte Carlo configurations through differential operators. In the spectrum of these operators high-momentum fluctuation are suppressed. Thus, it is expected that the lower part of the spectrum is dominated by large structures contained in the gauge fields. The operator mostly used is the Dirac operator, although others like the Laplacian operator [92] have been proposed.

In order to extract information about local structures, it is necessary to know how to relate the eigenvectors of the filtering operators with the gauge action density. The Atiyah-Singer index theorem [7, 8] relates the topological charge with the number of zero-modes of the Dirac operator in each chirality. The explicit relation depends on the SU(N) representation of fermionic fields. We are interested in two cases

$$Q = n_+ - n_- \quad \textbf{Fundamental representation}, \tag{6.3}$$

$$2NQ = n_+ - n_- \quad \textbf{Adjoint representation}. \tag{6.4}$$

The GW relation, Eq. 3.12, allows to define an index theorem on the lattice [93] as

$$Q = tr(\gamma_5 D) \tag{6.5}$$

In this framework, the topological charge density can be defined in terms of the GW operator

$$q(x) = tr\left[\gamma_5\left(1 - \frac{a}{2}D(0,x,x)\right)\right]. \tag{6.6}$$

Several authors have used as filtering operator an expansion of this equation in terms of the GW eigenvectors [94]

$$q(x) = \sum_k \left(1 - \frac{\lambda_k}{2}\right) p_k^5(x) \tag{6.7}$$

where $p_k^5(x) = \psi_k^\dagger(x)\gamma_5\psi_k(x)$. The integration of this expansion satisfies the index theorem for any value of k due to the orthogonality relation $\langle\gamma_5\psi_k, \psi_k\rangle = 0$. Since large values of k are related with short distance fluctuations, it is expected that truncating the expansion 6.7 above a large enough value of λ_k, the information about large structures will not be affected. In this way, the value of k can be used to filter the higher frequency modes.

This method works in all representations. Since in the adjoint representation the number of zero-modes per unit of topological charge is $2N$ (remember Eq. 6.4) the fundamental representation is the cheaper computational candidate. Then, what is the motivation for using the adjoint representation? As mentioned in the introduction of this chapter, there is a special mode whose density corresponds directly with a filtered gauge action density. From this viewpoint, only one mode should be computed, so the computational cost could be much lower than in the case of the fundamental representation.

6.1.1 ϵ-Cooling

To end this section, we will pay special attention to the description of an improved cooling algorithm proposed in [95]. This method has been widely used by us to generate the smooth configurations analysed in section 6.3, as well as to check the results obtained with the method based on the SSM.

Let us define an improved lattice action as

$$S(\epsilon) = \sum_{n,\mu\neq\nu}\left(\frac{4-\epsilon}{3}\mathrm{Tr}\left(1 - P_{\mu\nu}(n)\right) + \frac{\epsilon - 1}{48}\mathrm{Tr}\left(1 - \Pi_{\mu\nu}(n)\right)\right), \tag{6.8}$$

where $\Pi_{\mu\nu}(n)$ is the 2×2 plaquette in the plane $\mu - \nu$. The ϵ parameter allows us to control the $O(a^2)$ corrections on the continuum limit. Expanding Eq. 6.8 in terms of the lattice spacing we obtain [95]

$$S(\epsilon) = \sum_{n,\mu,\nu} Tr\left(-\frac{a^4}{2}F_{\mu\nu}^2(n) + \frac{\epsilon a^6}{24}\left((D_\mu F_{\mu\nu}(n))^2 + (D_\nu F_{\mu\nu}(n))^2\right)\right) + O(a^8). \tag{6.9}$$

So, for $\epsilon = 0$ the first correction to the action vanishes. Applying the previous formulate to an instanton and taking the limits $a \ll \rho \ll L$ gives [95]:

$$S(\epsilon) = 8\pi^2\left(1 - \frac{\epsilon}{5}\frac{a}{\rho}^2 - O\left(\frac{a^4}{\rho^4}\right)\right). \tag{6.10}$$

From here it is clear that the fate of instantons under a minimization algorithm based in this action leads the instantons to small sizes, for $\epsilon > 0$. Since in the lattice there is a minimal size, the cooling algorithm with $\epsilon > 0$ will eventually destroy topological charge. On the other side, negative values of ϵ produce growing instanton sizes. In our work cooling is used to both erase high momentum fluctuations and generate smooth configurations with different sizes. The most appropriated value of ϵ will be taken in each case.

6.2 Supersymmetric Mode

The second part of this thesis is based in analysing the filtering method proposed in Ref. [89]. The main idea is based on the fact that for classical solutions of the Euclidean equations of motion (not necessarily anti(self-dual)) there is a zero-mode of the adjoint Dirac operator, $\psi(x)$, whose density is equal to the gauge action density. The mode, called Supersymmetric zero-mode (SSM), is given by [96, 97]:

$$\psi^a(x) = \frac{1}{8}\, F^a_{\mu\nu}(x)\, [\gamma_\mu, \gamma_\nu]\, V\,, \tag{6.11}$$

where $F_{\mu\nu}(x)$ is the gauge field strength, V a constant four-spinor, γ_μ are the Dirac matrices and $a = 1, ..., N^2 - 1$ is the colour index. From Eq. 6.11, two positive and two negative chirality zero modes are obtained. The densities of these zero-modes give respectively the self-dual and anti-self-dual parts of the action density. Taking, for instance, $V^+ = (1, 0, 0, 0)$, the corresponding positive chirality zero mode in Eq. (6.11) becomes

$$\psi^a_+(x) \propto \begin{pmatrix} E^a_3(x) + B^a_3(x) \\ E^a_1(x) + B^a_1(x) - i(E^a_2(x) + B^a_2(x)) \\ 0 \\ 0 \end{pmatrix}, \tag{6.12}$$

selecting only the self-dual part of the action density. There is one peculiarity of ψ^a_+ that allows to single it out from the subspace of zero-modes: the imaginary part of the first component is zero at every point x and for all components in colour space. We call this fact: reality condition. So the problem is reduced to finding this mode in the spectrum of the Dirac operator. For the case of smooth self-dual configurations with charge Q, the SSM defines a subspace of dimension one in the $2QN$ zero-modes subspace. When the configuration is not a classical solution, the SSM is no longer a zero-mode of the Dirac operator. In that case, the SSM should be found as a linear combination of the lower eigenvectors of the Dirac operator. The rule to select the SSM is that the reality condition is fulfilled. Hence, the main problem is how to impose the reality condition that selects the SSM. We have explored two possibilities to obtain the SSM.

6.2.1 Projecting onto the supersymmetric zero-mode

In order to obtain the SSM, two methods have been employed in terms of the Dirac operator. In this section we present both, as well as their lattice implementation.

Method 1. Analytic version

Although the SSM is not necessarily a zero-mode, it is expected that for small deformations of the classical solution, the correction to the eigenvalue will be small. Therefore, the SSM should remain in the lower part of the spectrum. The strategy is to compute the eigenvectors associated to the lower part of the spectrum and single out the SSM by imposing the reality condition. For example, within the space of low modes with positive (negative) chirality, the reality condition is imposed by minimizing

$$\sum_{x,a}[\text{Im } \psi_+^{1,a}(x)]^2, \tag{6.13}$$

$$\sum_{x,a}[\text{Im } \psi_-^{3,a}(x)]^2. \tag{6.14}$$

where 1 and 3 denotes the first and the third spinor coordinate. From here, the density of the mode in each chirality ($|\psi_+(x)|^2$ and $|\psi_-(x)|^2$) corresponds to the self-dual and anti-self-dual part of the gauge action density. If the number of modes necessary to find the SSM is small, this method is computationally cheaper than those based on the use of the fundamental representation.

Although it is expected to find the SSM in the low-lying part of the spectrum, it is unclear how many eigenvectors must be computed to obtain a good approximation of the gauge action density. A stability criterion is that the linear combination, Eq. 6.14, remains essentially unchanged when more modes are added.

Method 1. Lattice implementation

This method was implemented in Ref. [89] by using the Wilson-Dirac operator. In that case, chirality should be imposed in addition to reality, so that Eq. 6.14 should be modified to include the Wilson term correction. This fact complicates the definition of the SSM. A better option is to use the Neuberger-Dirac operator [30, 31] presented in chapter 3.1:

$$D_{ov} = \frac{1}{2}\left(1 + \gamma_5 \epsilon(H_{WD})\right). \tag{6.15}$$

This operator has good chiral properties and the condition Eq. 6.14 can be imposed without problems.

The low-lying part of the spectrum of the adjoint Neuberger-Dirac operator is computed by the conjugate gradient algorithm presented in Appendix B. In order to obtain a hermitian and positive definite operator, $(\gamma_5 D_{ov})^2$ will be used. This operator is hermitian and positive definite. For the Neuberger-Dirac operator, it is possible to compute each chirality independently by diagonalising the operators $H_\pm^2$ defined in Eq. 3.18. The eigenvectors of D can be obtained from these by 4.22. Bearing in mind that $\epsilon^2 = 1$, these operators can be written as

$$H_\pm^2 = \frac{1}{2} P_\pm \left(1 \pm \epsilon\right) P_\pm \,. \tag{6.16}$$

In this projection the ϵ operator should be computed only once in each iteration.

Method 2. Supersymmetric Operator (SSO)

An alternative method that fulfils the reality condition was proposed in [89], and had been implemented for the first time in this work. The main idea is to replace the Dirac operator by its projection to the reality condition. So, the lowest eigenvector of the projected operator, should correspond with the SSM. This method should match with the Method 1, when Eq. 6.14 is imposed over the whole spectrum. The main advantage of this methods is that only one mode must be computed.

Let us explain how to build the projected operator. The first step is to rewrite the SSM in quaternionic notation as described in section 4

$$\Psi^a(x) = \frac{1}{8} F^a_{\mu\nu}(x) \left[\gamma_\mu, \gamma_\nu\right] \equiv \begin{pmatrix} \Psi^{a\mu}_+(x)\bar{\sigma}_\mu \\ \Psi^{a\mu}_-(x)\bar{\sigma}_\mu \end{pmatrix}, \tag{6.17}$$

where $\Psi^{a\mu}_\pm(x)$ are real functions. The reality condition can be imposed by taking $\Psi^0_\pm = 0$. Both Weyl operators defined by Eq. 4.9 can be written as operators acting over quaternionic fields. For example,

$$-D\bar{D} = -D_\mu D_\nu \sigma_\nu \bar{\sigma}_\nu = -\eta^{\mu\nu}_\alpha D_\mu D_\nu \bar{\sigma}_\alpha. \tag{6.18}$$

As we are interested in finding a zero-mode with the component $\psi^0_\pm = 0$, we can restrict the operator $-D\bar{D}$ to the subspace of σ_i matrices. Then, we are interested in operators acting over a 3-dimensional space, the projection can be done using

$$\bar{\sigma}_\alpha \tau_k = \bar{\eta}^{\alpha k}_j \tau_j. \tag{6.19}$$

Hence finally the operator becomes

$$O^+_{jk} = -D_\mu D_\nu \eta^{\mu\nu}_\alpha \bar{\eta}^{\alpha k}_j, \tag{6.20}$$

The expression can be expanded and we get

$$O^+_{ij} = -\delta_{ij} D^2_\mu - \epsilon_{ijk} \eta^{\mu\nu}_j D_\mu D_\nu = -\delta_{ij} D^2_\mu + i\epsilon_{ijk}(E_k + B_k), \tag{6.21}$$

where E_i and B_i are the electric and magnetic field components. In the adjoint representation the generators of SU(N) are pure imaginary matrices, so the operator O^+ is real. The same can be done for the other chirality obtaining

$$O^-_{ij} = -\delta_{ij} D^2_\mu - i\epsilon_{ijk}(E_k - B_k). \tag{6.22}$$

Method 2. Supersymmetric Operator (SSO). Lattice version

Eqs. 6.21,6.22 are useful for an analytic approach to the SSO. The lattice implementation starts from the $(\gamma_5 D_{ov})^2$ written in terms of quaternions as explained in Appendix B. The projection to the reality condition can be imposed as

$$O^\pm_L = P_0 H^2_\pm P_0, \tag{6.23}$$

where σ_0 is projected out, $P_0\Psi = \Psi - \frac{1}{2}\sigma_0 Tr(\sigma_0\Psi)$, and $H^2_\pm$ are the operator defined in Eq. 6.16. It is important to remember that this operator acts over a real 3-dimensional vector space. So the conjugate gradient algorithm (section B) must be computed for a real operator. As shown in Eq. 3.15, the continuum limit of the Neuberger-Dirac operator is given by

$$D_{ov} = \not{D} + \frac{a}{2}H^2 + O(a^2). \tag{6.24}$$

The zero-modes of D are zero-modes of H^2 too, so the lattice corrections to the zero-modes are expected to be order a^2.

6.3 Testing the performance

In this section, we present a detailed analysis of the SSO lattice implementation. Before doing an analysis of a Monte Carlo ensemble, it is necessary to know the limitations of the numerical implementation. Four situations are going to be explored for this purpose:

- Classical solutions with one lump in the action density: the first test is done over a set of prepared smooth $Q = 1$ instanton configurations. This is the simplest case, and a deep understanding of it will be crucial for facing more complicated cases. We test if the SSM mode reproduces the gauge action density. In addition, we are interested in analysing the behaviour of the spectrum in terms of the instanton parameters. It is known that there are no $Q = 1$ classical solutions on a periodic torus [22], so important finite-volume effects are expected to be found. In order to improve this situation, we analyse the effect of imposing twisted boundary conditions in the timelike planes. Lattice spacing effects are expected when the instantons are small in lattice units.

- Classical solutions with more than one lump: It is interesting to analyse smooth configurations with more than one object, when both objects are very far away from each other. The reality condition could be satisfied separately in each region independently and the SSM could be degenerate. Since this problem appears in the continuum theory when the distance tends to infinity, we are interested in the numerical corrections due to finite volume and the discretization. SU(2) calorons and two-instanton configuration have been prepared for this purpose.

- Smooth Non-classical solutions: the third part refers to smooth configurations composed by structures in both chiral sectors. Here we test the capacity of the method to extract the information from each chirality. The set of configurations analysed are instanton-antiinstanton pairs at varying separations.

- Heated configurations: finally, the filtering properties of the operator are tested. In order to do that, the smooth configurations of the first part of this section are subject to a heat-bath algorithm. The β parameter of the heat-bath algorithm allows us to control the amplitude of the noise added. Two aspects will be treated in this

BC	L/a	# Confs	ρ_{max}/a	ρ_{min}/a
Periodic ($\vec{k}=\vec{m}=0$)	14	19	3.64	2.45
Periodic ($\vec{k}=\vec{m}=0$)	16	30	4.23	2.10
Time-Twist ($\vec{k}=1$, $\vec{m}=0$)	14	19	4.29	2.83
Time-Twist ($\vec{k}=1$, $\vec{m}=0$)	16	19	4.06	2.84

Table 6.1: Ensembles of smooth $Q=1$ instantons configurations generated.

case: the modification of the spectrum of the operator and the filtering power of the algorithm.

6.3.1 Classical solutions with one action density lump

Gauge Configurations

We generate smooth $Q=1$ instanton configurations with different sizes. Four ensembles of instantons are generated with different lattice volumes and boundary conditions (BC), as summarized in Table 6.1. In order to do this, the ϵ-cooling algorithm explained in section 6.1.1 is used. Starting from a smooth instanton, the ϵ-cooling algorithm is applied in order to modify the size of the object. Intermediate configurations are stored obtaining a set of instantons with different sizes. The four lowest eigenvalues and eigenvectors of the $O^{\pm}$ operators are computed for each of the previous configurations.

Density profile

In this case, the SSM mode corresponds to the lowest eigenvector of the O^{+} operator. As a first check, the SSM density and the gauge action density are compared. The SSM density is computed as

$$S_{ss}(n)=\sum_{i,a}|\Psi_{+}^{ai}(n)|^2, \tag{6.25}$$

and the gauge action density is computed from two different definitions as

$$S_{Cl}(n) = \sum_{\mu\neq\nu} Tr\left(1-P_{\mu\nu}^{Cl}(n)\right), \tag{6.26}$$

$$S_{Q}(n) = -\frac{1}{4}Tr\left(F_{\mu\nu}^{CL}(n)\tilde{F}_{\mu\nu}^{Cl}(n)\right), \tag{6.27}$$

where

$$P_{\mu\nu}^{Cl}(n) = \frac{1}{4}\left(P_{\mu\nu}(n)+P_{\nu\bar{\mu}}(n)+P_{\bar{\mu}\bar{\nu}}(n)+P_{\bar{\nu}\mu}(n)\right), \tag{6.28}$$

$$F_{\mu\nu}^{Cl}(n) = \frac{i}{2}\left(P_{\mu\nu}^{Cl}(n)-P_{\nu\mu}^{Cl}(n)\right) \tag{6.29}$$

$$\tilde{F}_{\mu\nu}^{Cl}(n) = \frac{1}{2}F_{\mu\nu}^{Cl} \tag{6.30}$$

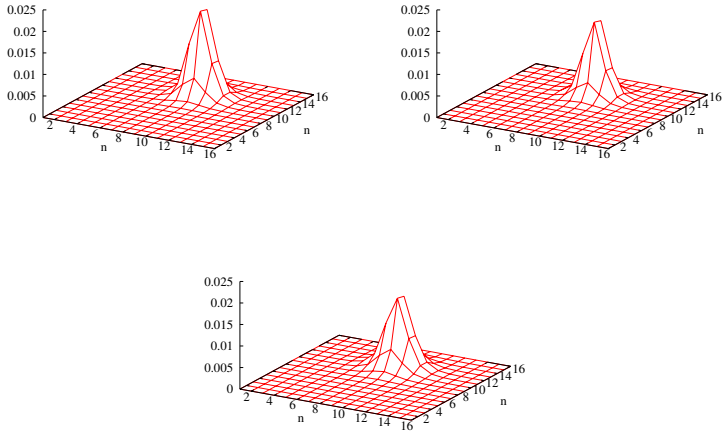

Figure 6.1: The upper plots show the gauge action densities: S_{Cl} (left) and S_F (right). The lower plot is the SSM density. Two dimensional slices of the densities are displayed. The configuration corresponds with the smaller instanton of the periodic $L = 16a$ ensemble. The fit to the instanton parameters can be found in Table 6.2

	x_0/a	y_0/a	z_0/a	t_0/a	ρ_c/a
S_{Cl}	8.19	10.42	14.86	16.48	2.26
S_Q	8.17	10.42	14.87	16.48	2.09
S_{ss}	8.17	10.41	14.87	16.48	2.47

Table 6.2: Fits corresponding to Fig. 6.1

and $\bar{\mu}$ denotes a displacement in the negative direction.

In Figs. 6.1-6.6 the densities obtained from each definition are displayed. The gauge configurations correspond with the largest, the lowest and an intermediate instanton for lattice size $L = 16a$ in both periodic and twisted BC. The positions and the sizes of the instanton obtained for each method are fitted to the instanton density (Eq. 2.34).The results are presented in Tables 6.2-6.7. The positions are obtained with an agreement larger than 99% in all cases. The size determination presents a small hierarchy, $\rho_Q < \rho_{Cl} < \rho_{ss}$. The worst situation appears for small instantons ($\rho/a \approx 2$) where the discrepancy is around 10% between ρ_{Cl} and ρ_{ss} and around 20% between ρ_Q and ρ_{ss}. Small instantons are not well defined on the lattice so this deviation is expected. In conclusion, for a smooth instanton, the density of the SSM can reproduce the gauge action density with similar errors to those due to different lattice gauge action definitions.

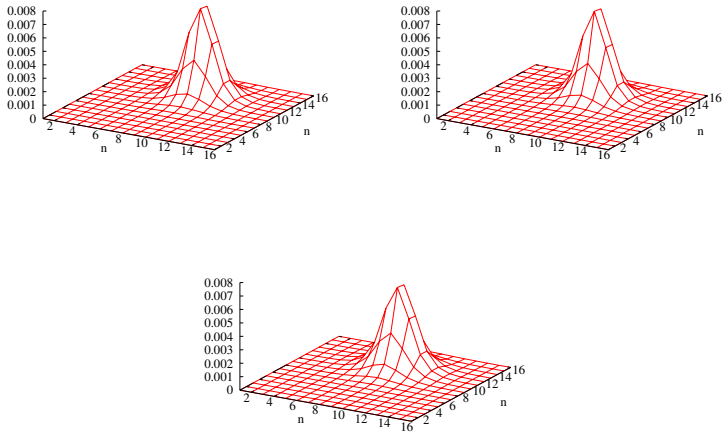

Figure 6.2: As in Fig.6.1 for the intermediate instanton of the periodic $L = 16a$ ensemble. The fit to the instanton parameters can be found in Table 6.3

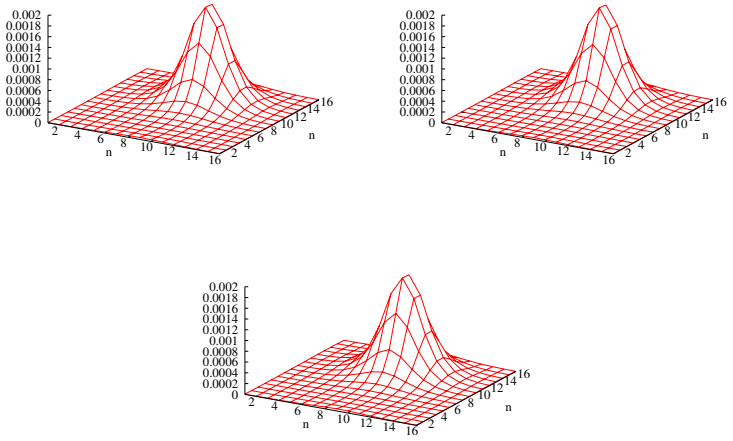

Figure 6.3: As in Fig.6.1 for the larger instanton of the periodic $L = 16a$ ensemble. The fit to the instanton parameters can be found in Table 6.4

	x_0	y_0	z_0	t_0	ρ_c
S_{Cl}	8.13	10.38	14.92	16.49	3.12
S_Q	8.13	10.38	14.92	16.49	2.95
S_{ss}	8.12	10.38	14.92	16.49	3.24

Table 6.3: Fits corresponding to Fig. 6.2

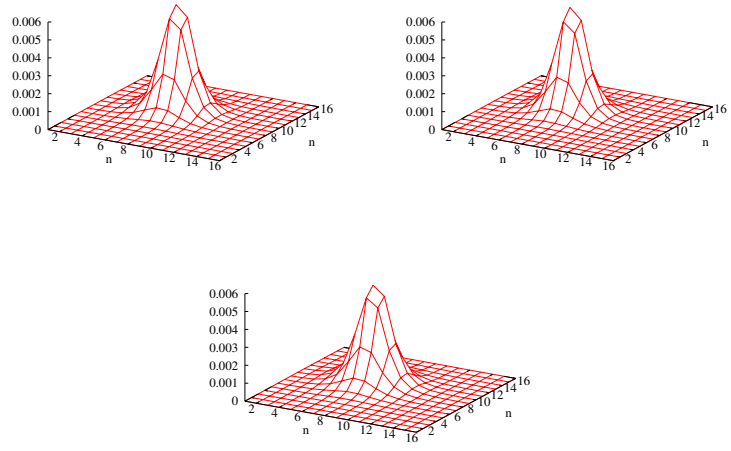

Figure 6.4: As in Fig.6.1 for the smaller instanton of the twisted $L = 16a$ ensemble. The fit to the instanton parameters can be found in Table 6.5

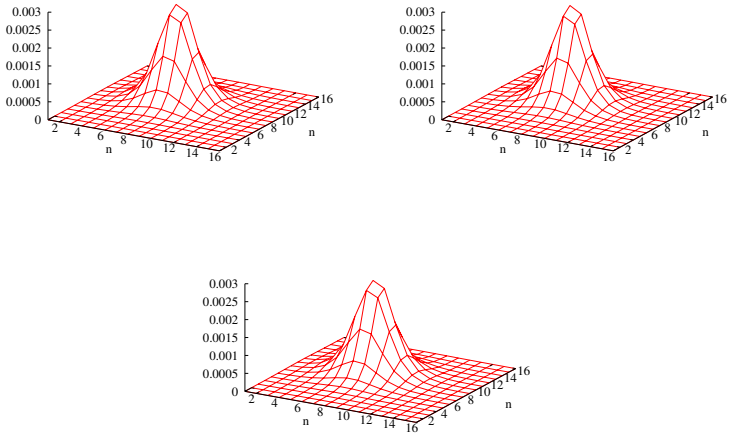

Figure 6.5: As in Fig.6.1 for the intermediate instanton of the twisted $L = 16a$ ensemble. The fit to the instanton parameters can be found in Table 6.6

	x_0	y_0	z_0	t_0	ρ_c
S_{Cl}	8.11	10.33	14.99	16.48	4.36
S_Q	8.11	10.33	14.99	16.49	4.27
S_{ss}	8.11	10.33	14.99	16.49	4.48

Table 6.4: Fits corresponding to Fig. 6.3

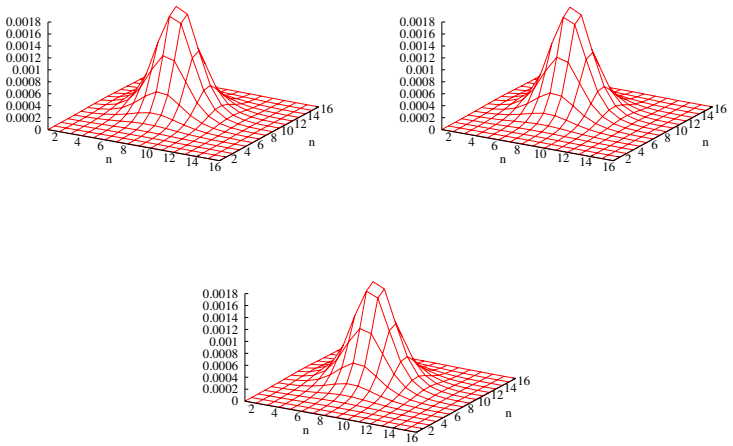

Figure 6.6: As in Fig.6.1 for the largest instanton of the twisted $L = 16a$ ensemble. The fit to the instanton parameters can be found in Table 6.7

	x_0	y_0	z_0	t_0	ρ_c
S_{Cl}	11.41	10.03	14.36	0.63	3.22
S_Q	11.41	10.03	14.36	0.63	3.05
S_{ss}	11.41	10.03	14.36	0.64	3.32

Table 6.5: Fits corresponding to Fig. 6.4

	x_0	y_0	z_0	t_0	ρ_c
S_{Cl}	11.42	10.03	14.36	0.64	3.94
S_Q	11.41	10.03	14.36	0.64	3.80
S_{ss}	11.41	10.03	14.36	0.64	4.02

Table 6.6: Fits corresponding to Fig. 6.5

	x_0	y_0	z_0	t_0	ρ_c
S_{Cl}	11.42	10.03	14.36	0.65	4.39
S_Q	11.41	10.03	14.36	0.65	4.26
S_{ss}	11.41	10.03	14.36	0.65	4.46

Table 6.7: Fits corresponding to Fig. 6.6

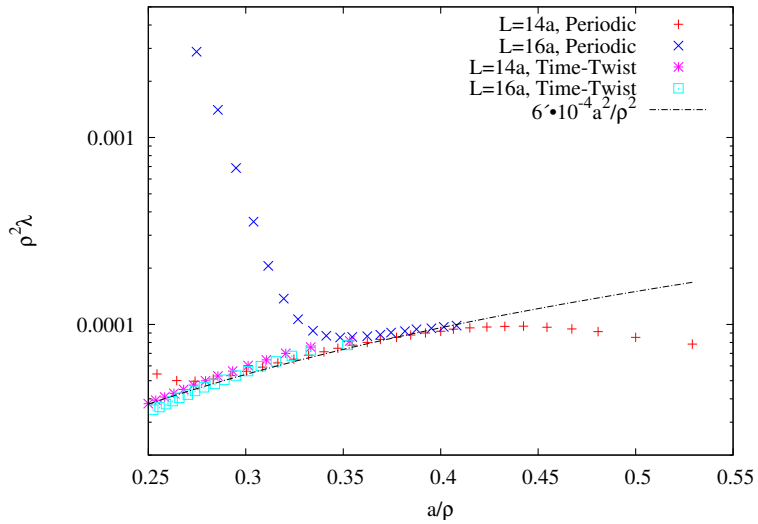

Figure 6.7: The lowest eigenvalue of the O^+ operator is displayed in terms of a/ρ. As expected, in the purely periodic case the finite-volume effects become sizable when $L/\rho < 4$, increasing the value of the lowest eigenvalue. For the time-twisted boundary conditions $(k = (1,1,1), \quad m = (0,0,0))$, this finite-volume effect disappears, as can be seen in the left part of the plot.

Spectrum of the O^+ operator on an instanton background

Our method to find the SSM is based on the fact that these modes correspond to the lowest eigenvalue of the $O^{\pm}$ operators. We are going to test how the numerical implementation affects this condition.

The first question is related with the value of the lowest mode. Is it compatible with zero? Two effects could modify the zero-mode condition: the discretization and the finite volume. The first ones are expected to be important for small enough instantons compared with the lattice spacing. The correction to the lowest eigenvalue should depend on the size of the instanton in lattice units as

$$\lambda_1 = \frac{1}{\rho^2} f_1(a/\rho). \tag{6.31}$$

Fig. 6.7 displays the lowest eigenvalue of the O^+ operator computed for all the configurations in Table 6.1. The lowest eigenvalue can be fitted as

$$\lambda_1 = 6 \cdot 10^{-4} \frac{a^2}{\rho^4} + O\left(\frac{a^4}{\rho^4}\right), \tag{6.32}$$

for $\rho/a > 2.5$. The corrections are order a^2 as was expected. For very small instantons ($\rho/a \sim 2$) there are additional problems related with the locality properties of the Neuberger-Dirac operator. These problems are analysed in Appendix C.

The finite-volume effects appear when periodic boundary conditions are imposed. They are due to the non existence of $Q = 1$ classical solutions in this case. For large enough instantons compared with the torus size, corrections to the lowest eigenvalue are expected. In the time-twisted case, these solutions exist and the corrections should disappear. The difference between both cases is shown in Fig. 6.7. For periodic BC there is a large deviation to Eq. 6.32 for $L/\rho \lesssim 4$, while in the twisted case, the deviation is not observed, as expected.

There is an additional problem related to the fact that the gap between the lowest mode and the other ones disappears in the infinite volume limit. It is expected that the second eigenvalue, λ_2, decreases with the volume. The only scale of the instanton solution is its size (ρ), so the behaviour of the second eigenvalue can be parametrized by

$$\lambda_2 = \frac{1}{L^2} f_2(\rho/L). \tag{6.33}$$

In Fig. 6.8 the eigenvalues λ_2, λ_3 and λ_4 of the configurations in Table 6.1 are displayed. A different behaviour appears between periodic and twisted BC. In each case, the function $f_2(\rho/L)$ can be fitted for large volumes to:

$$\lambda_2^P = \frac{\pi^2}{L^2}\left(0.28\frac{\rho^2}{L^2} + O(\frac{\rho^4}{L^4})\right), \tag{6.34}$$

$$\lambda_2^T = \frac{\pi^2}{L^2}\left(1 - 8.14\frac{\rho^2}{L^2} + O(\frac{\rho^4}{L^4})\right). \tag{6.35}$$

In the twisted case, the first correction is $1/L^2$. This is due to the zero frequency is not presented in the spectrum of the vacuum state with these boundary conditions.

For the method to work there should be a gap in the spectrum. Defining $\rho_l = \rho/a$, and using expression Eq. 6.32 and Eqs. 6.35,6.35 the gap λ_2/λ_1 can be written as

$$\frac{\lambda_2^P}{\lambda_1} \approx 4606\frac{\rho_l^6}{n^4}(1 + O(\rho^2/L^2)), \tag{6.36}$$

$$\frac{\lambda_2^T}{\lambda_1} \approx 16449\frac{\rho_l^4}{n^2}(1 + O(\rho^2/L^2)), \tag{6.37}$$

where $n = \frac{L}{a}$ is the number of lattice points in one direction. For example, if the limit for small instantons is taken ($\rho_l = 2.5$), the gap disappears for lattice volumes $n \approx 32$ in the periodic case, and $n \approx 800$ for the twisted case. For larger volumes, the eigenvalues could cross and it is not guaranteed that the lowest eigenvector corresponds with the SSM. If periodic BC are used, another limit appears, due to the finite volume effects for $L/\rho < 4$.

6.3.2 Classical solutions with more than one action density lump

When there are more than one lumps in the same chiral sector, some problems could appear related with degeneracy of the SSM. If the distance between the objects is very large, there could be more than one mode satisfying the reality condition. We expect a decreasing of the values of these new modes with the distance between the objects. As

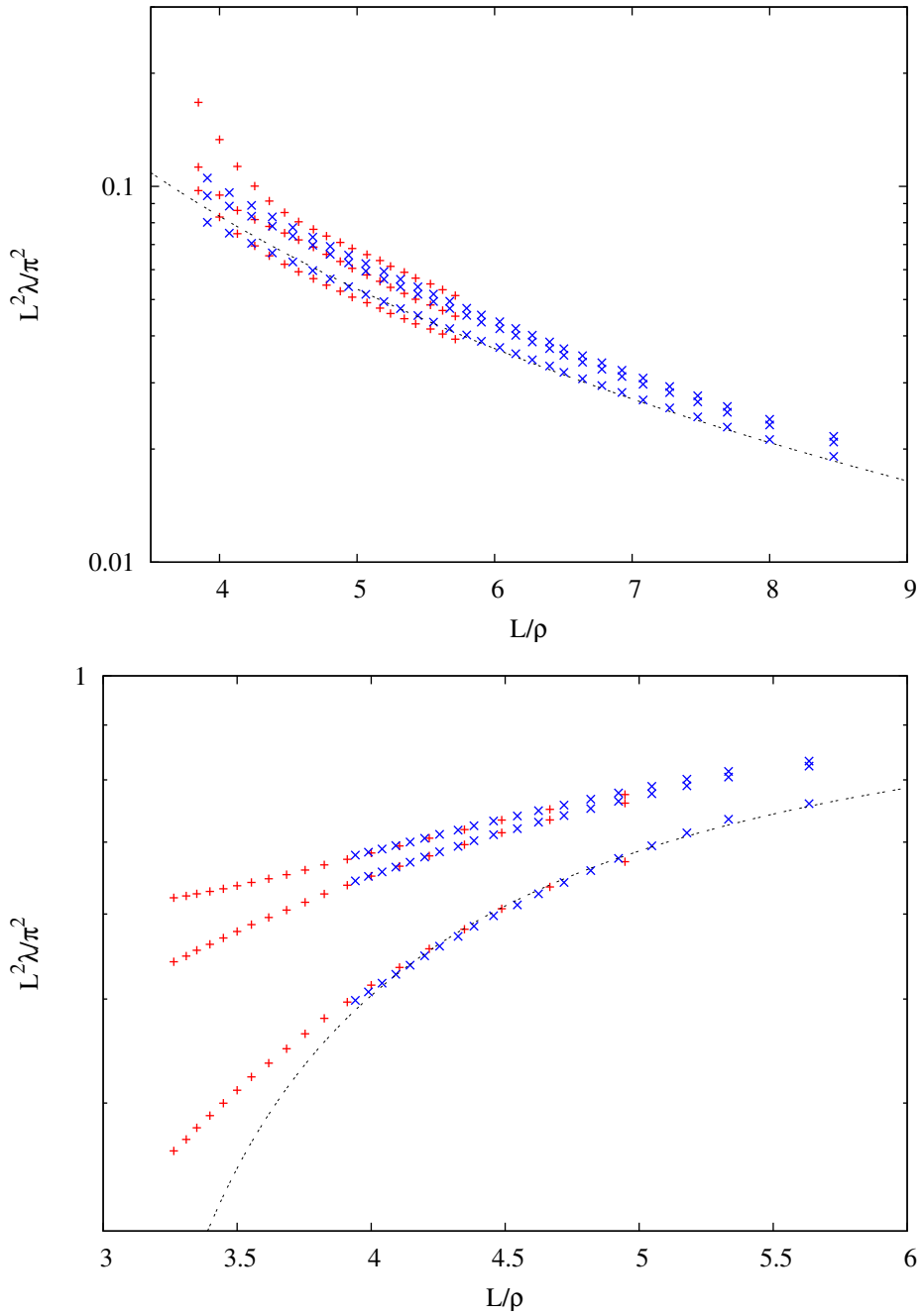

Figure 6.8: The eigenvalues λ_2, λ_3 and λ_4 of the operator O^+ are displayed in terms of L/ρ. Red points corresponds to a box $(14a)^4$ and the blue ones to a box $(16a)^4$. The upper plot corresponds with the periodic case, and the lower plot is refereed to the twisted case. The dotted lines is the fit to Eqs. 6.35 and 6.35.

BC	$V = (L_s/a)^3 \times L_t/a$	# Confs	δ_1	$(d/a)_{max}$	$(d/a)_{min}$
$(k = 0, m = 1)$	$24^3 \times 4$	19		12.35	3.47

Table 6.8: Parameters of the $Q = 1$ SU(2) caloron configurations.

BC	$V = (L_s/a)^3 \times L_t/a$	# Confs	$(d/\rho)_{max}$	$(d/\rho)_{min}$
$(k = 0, m = 0)$	$16^3 \times 32$	5	4.27	1.76

Table 6.9: Parameters of the two instanton configurations analysed ($\delta = 0.22$).

it was showed in the previous test, the value of the SSM depends as a function of a^2/ρ^2. Then, there could be a set of parameter where the value of the SSM and the previous ones have the same order and the level crossing occurs. Whether this happens or not is the question that will be addressed in this section.

Gauge configurations

We generate two kind of solutions with two lumps: $Q = 1$ SU(2) calorons, and two-instanton configurations. The first ones are generated on an asymmetric box ($(24a)^3 \times 4a$) modifying the distance between the constituent monopoles with fixed holonomy. The holonomy is fixed by selecting the appropriated twisted boundary condition, and the monopole distance can be modified by using the ϵ-cooling algorithm. More details about introducing calorons on the lattice can be found in [74]. The information about the parameters of these configurations is shown in Table 6.8.

The $Q = 2$ configurations are generated from the $Q = 1$ solutions of section 6.3.1. In order to do this, an asymmetric lattice ($L^3 \times 2L$) is used. The $Q = 2$ configurations are obtained by gluing two of the previous $Q = 1$ configurations in the x_4 direction. In order to obtain instanton pairs at different distances, both instanton configurations are shifted in opposite directions before gluing them by

$$U^1_\mu(n) \to U^1_\mu(n + \hat{4}), \;\; U^2_\mu(n) \to U^2_\mu(n - \hat{4}). \tag{6.38}$$

The overlap region is cooled in order to obtain a smooth configuration. When the instantons are near enough, their parameters can be modified. For this reason, the size of the instantons could present some modifications. The parameters of the $Q = 2$ configurations obtained in this way are presented in Table 6.9.

Caloron case

In this case, the lowest eigenvalue is compatible with a zero-mode and the gap is maintained approximately constant in all the range analysed. The gauge action density is recovered by the SSM as depicted in Fig. 6.9.

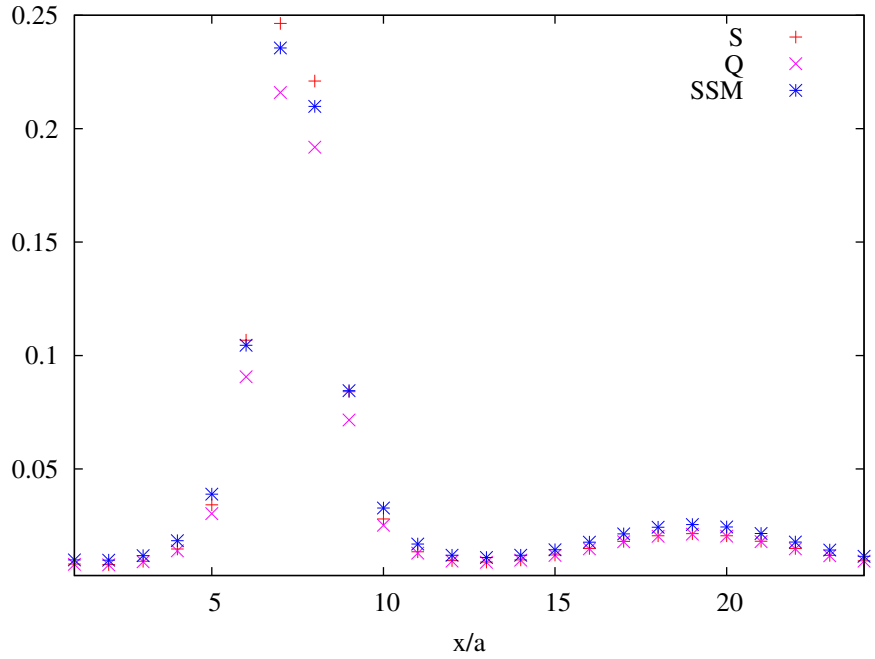

Figure 6.9: The integral of the densities over three dimensions is displayed for the SSM, S_{Cl} and S_Q ($d/a = 13.2$,$\delta = 0.22$)

Two instantons case. Density profiles

In this case, it is expected that, for large separation, the profile of the second eigenvector will be related with the gauge action density. In Figs. 6.10-6.14 the densities of these eigenvectors, the gauge action density and the sum of the two lowest eigenvector densities are displayed. For small separations ($L/\rho < 2$) only the lowest eigenvector is related with the gauge action density. When the distance is larger than 2, both eigenvectors density are related with the gauge action density. The eigenvectors combine both instantons with a wrong weight. We find that the best combination in order to reproduce the gauge action density is the sum of both eigenvectors densities.

Two instantons case. Spectrum of the O^+ operator

In this case, we expect to find two small eigenvalues when the instanton distance is large. In Fig. 6.15 the three lowest eigenvalues of the O^+ operator are displayed. The λ_2 eigenvalues decrease with the instanton distance. For distances $L/\rho > 2$ this eigenvalue can be fitted by

$$\lambda_2 = \frac{\pi^2}{L^2} e^{-\frac{3d}{2\rho}}. \tag{6.39}$$

This behaviour explains the density profile of the second eigenvector observed in the densities analysis. In this sense, when Monte Carlo configurations will be analysed, it is necessary to compute more the one eigenvalue. A new criterion in order select how many

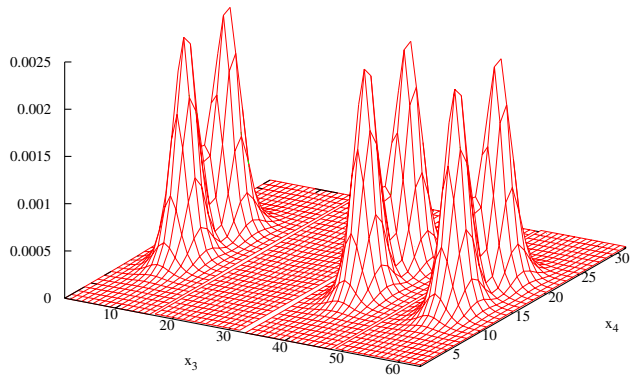

Figure 6.10: Density slices of two-instanton configurations, separated by $d/\rho = 1.76$, are displayed. In the x_3 direction are ordered the density of the two lowest eigenvectors (λ_1, λ_2), the gauge action density and the average of the two eigenvectors densities.

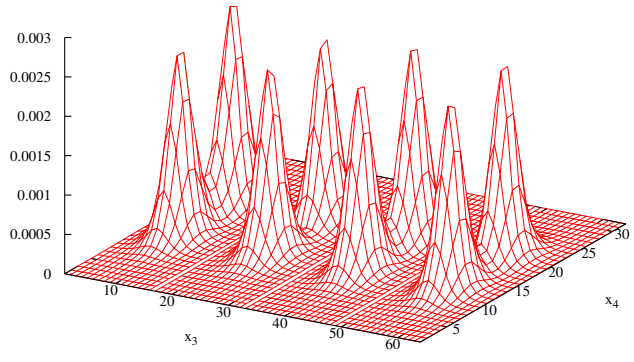

Figure 6.11: As in 6.10 for $d/\rho = 2.30$.

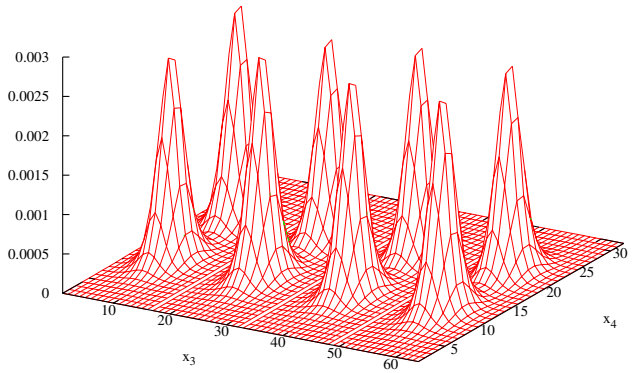

Figure 6.12: As in 6.10 for $d/\rho = 3.07$.

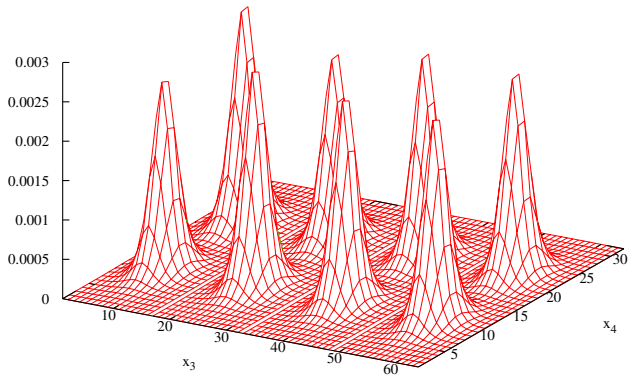

Figure 6.13: As in 6.10 for $d/\rho = 3.68$.

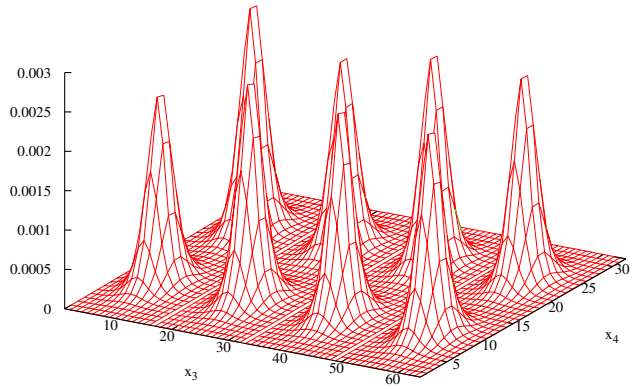

Figure 6.14: As in 6.10 for $d/\rho = 4.27$.

eigenvectors are necessary. A way to defined this criterion can be based in the fact that the density of the eigenvectors not related with the SSM is very flat. Then, the Fourier spectrum of the density or the IPR can be used as stopping criteria.

6.3.3 Non-Classical smooth configurations

Gauge configurations

In this section, we generate an ensemble of instanton-antiinstanton (IA) configurations with different IA separation. We start with a IA configuration on a lattice volume $(12a)^3 \times 24a$ lattice. The size of the objects is $\rho_i/a = 2.7$ and $\rho_{ia}/a = 3.0$ and they are separated by a distance $L/a = 12$. The distance is modified by using ϵ-cooling algorithm ($\epsilon = 0$). The objects come closer until they are destroyed, when the distance is approximately $L/\rho \sim 1$. In Table 6.10 the parameters of the configurations are showed.

BC	$V = (L_s/a)^3 \times L_t/a$	# Confs	$(L/\rho)_{max}$	$(L/\rho)_{min}$
$(k = 0, m = 0)$	$12^3 \times 24$	50	4.3	1

Table 6.10: Parameters of the IA configurations.

Density profiles

In this case, there are objects in both chiralities. Then, the SSM of each operator $O^{\pm}$ must be analysed. In this case, the density of the SSM is compared with the (anti)self-dual part of the gauge action density defined by

$$S_{\pm}(n) = \frac{1}{8} Tr \left(F^{CL}_{\mu\nu}(n) F^{Cl}_{\mu\nu}(n) \pm F^{CL}_{\mu\nu}(n) \tilde{F}^{Cl}_{\mu\nu}(n) \right). \tag{6.40}$$

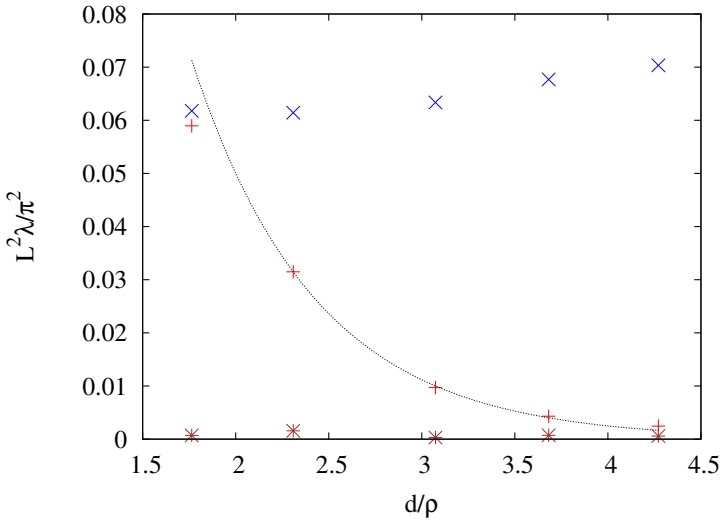

Figure 6.15: The three lowest eigenvalues of the operator O^+ for the two instanton configurations are displayed. The second eigenvalue, λ_2, decrease with the instanton distance. The behaviour of this eigenvalue can be fitted by an exponential term, Eq. 6.39.

In Figs. 6.16-6.20 the destruction process by comparing the SSM densities and the densities obtained from Eq.6.40 is displayed. As it was expected, the SSM is only sensitive to objects with the appropriated chirality. This separation is maintained until the distance is smaller than $L/\rho \sim 2$. For smaller distance, the SSMs do not correspond with the lowest eigenvalue.

In order to obtain a more quantitative relation between both densities, the size of the (anti)instanton is computed for each method. In Fig. 6.21 the ratio ρ_{ss}/ρ_g is displayed. The difference between both methods is 5% until 40 sweeps. From 40 to 48 sweeps a small deviation is observed between both methods.

Spectrum of the $O^{\pm}$ operators

In this case, we are interested in monitoring the lowest eigenvalue in terms of the IA distance. The Dirac operator has no zero-modes for these configurations. But it is expected that the lowest eigenvalue in each chiral sector goes to zero when the distance between the objects is increased.

In Fig. 6.22 the three lowest eigenvalues of the O^+ operator are displayed in terms of the cooling sweeps (an analogous figure is obtained for the spectrum of the operator O^-). Three regimes appear in the plot. In the first one (0-40), a clear gap between the lowest eigenvalues and the next one is maintained. In the second one, a fast growing of the SSM is observed and a level crossing occurs. This point corresponds with a distance $L/\rho \sim 1.8$. Finally, the three modes go to zero. After the destruction, the configuration is led to the classical vacuum ($U_\mu(n) = 1$) by the cooling algorithm. For this configuration, 9 zero-modes are expected for the operators $O^{\pm}$. These explain the vanishing of the eigenvalues

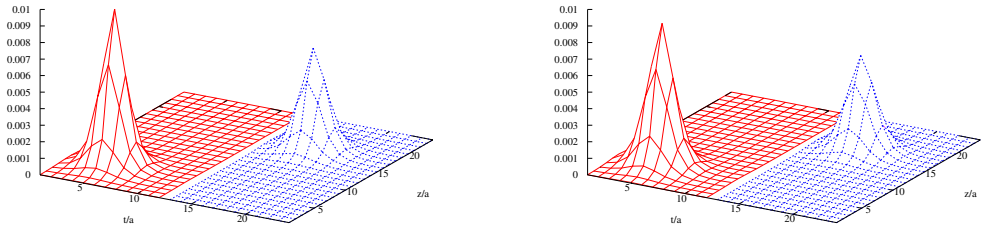

Figure 6.16: In the left part the S_+ density (red) and the S_- density (blue) are displayed. In the right part the SSM corresponding to the positive chiraliy (red) and the negative chirality (blue) are displayed. The IA are separated $d/\rho = 4.28$

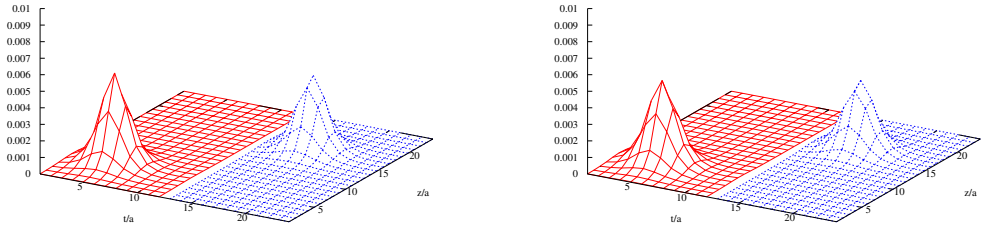

Figure 6.17: As in Fig. 6.16 for IA separation $d/\rho = 3.92$

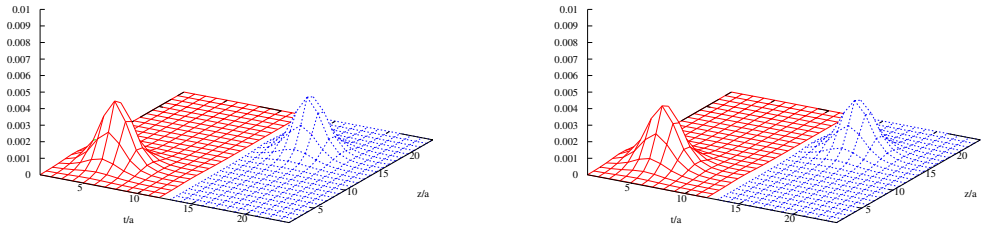

Figure 6.18: As in Fig. 6.16 for IA separation $d/\rho = 3.51$

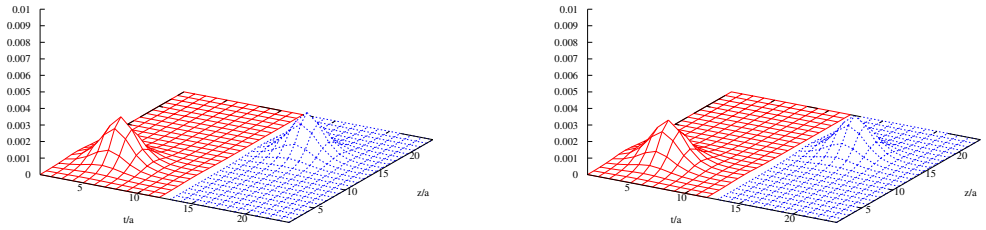

Figure 6.19: As in Fig. 6.16 for IA separation $d/\rho = 2.90$

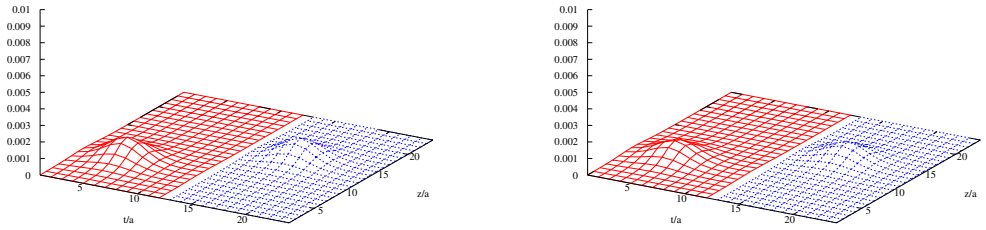

Figure 6.20: As in Fig. 6.16 for IA separation $d/\rho = 1.80$

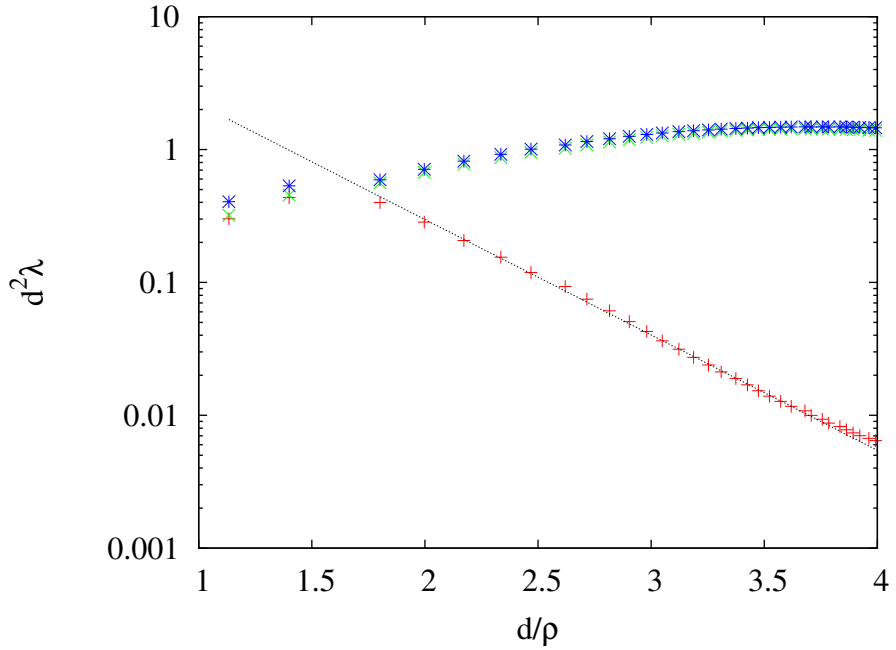

Figure 6.21: The determination of the (anti)instanton size for the $S_{\pm}$ densities and for the SSMs is compared in terms of the number of cooling sweeps.

after the IA destruction. In Fig. 6.23 the three lowest eigenvalues are displayed in terms of the IA distance. The lowest eigenvalue can be fitted as

$$\lambda_1 = \frac{16}{d^2} \exp^{-\frac{2d}{\rho}} . \tag{6.41}$$

In $d/\rho \sim 2$ a level crossing appears. Then, the operators $O^{\pm}$ can distinguish an IA pair separated by a distance lager than $d/\rho > 2$.

6.3.4 Heated solutions

Gauge configurations

We generate twenty ensembles of configurations for different values of β ($\beta = 30, 20, 8, 7, 6, 5, 4, 2.8, 2.6, 2.4$) with periodic and time-twisted boundary conditions on a lattice volume $(14a)^4$. Each ensemble is generated by starting from a smooth instanton configuration ($\rho/a = 3.39$). A fixed number of heat-bath sweeps are applied to this configuration. The same process is repeated with ten different seeds for each value of β. For the smaller values of β ($\beta < 3$), the number of heat-bath sweeps applied is lower in order to prevent the destruction of the instanton could be destroyed. In addition, two sweeps of ϵ-cooling ($\epsilon = 0$) are applied before computing the eigenvectors in these cases. This is due to problems with the Neuberber-Dirac operator. More details can be found in Appendix C. In Table 6.11 the parameters of the configurations generated are summarized. The four lowest eigenvalues

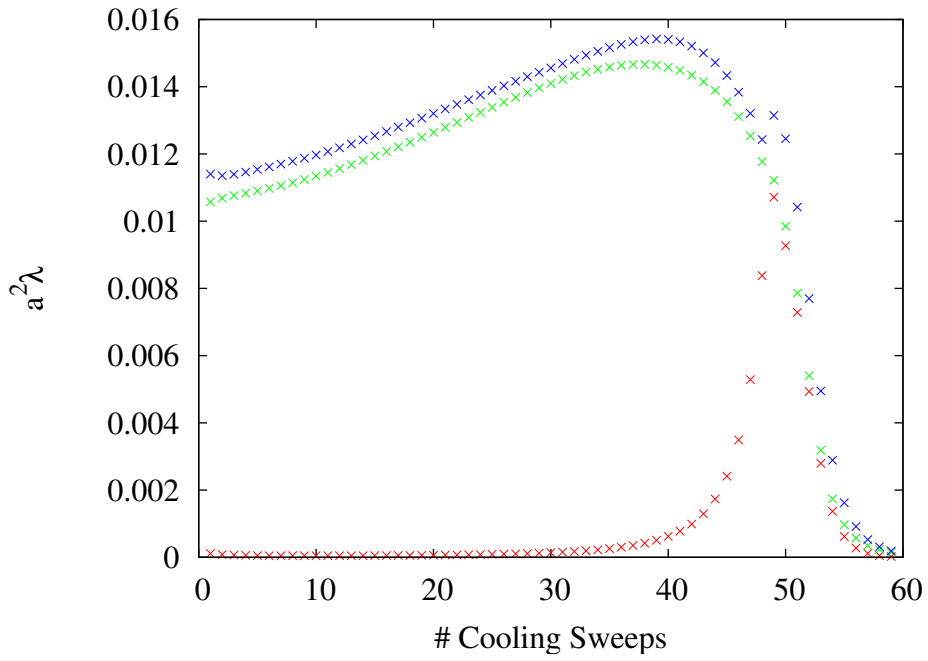

Figure 6.22: The three lowest eigenvalues of the operator O^+ are displayed in terms of the number of cooling sweeps. Level crossing appears in the step 49.

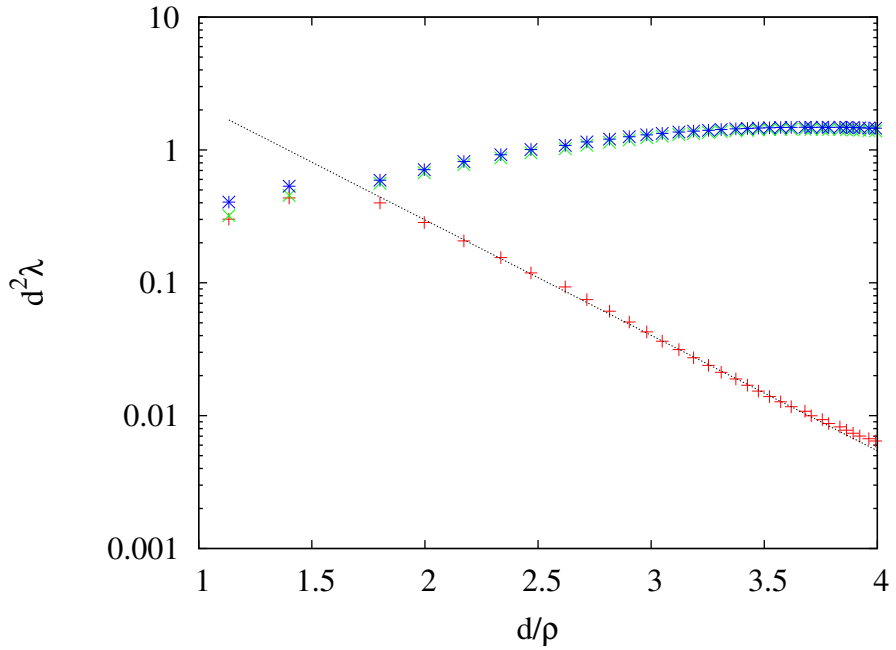

Figure 6.23: The three lowest eigenvalues of the operator O^+ are displayed in terms of the IA distance. Level crossing appears at a distance $L/\rho \sim 1.8$.

β	# Configurations	# Heat-bath sweeps	# Cooling Sweeps
30	10	10	0
20	10	10	0
8	10	10	0
7	10	10	0
6	10	10	0
5	10	10	0
4	10	10	0
2.8	10	4	2
2.6	10	4	2
2.4	10	4	2

Table 6.11: Configurations generated by applying heat-bath sweeps to a smooth instanton configuration. Configurations are generated on a lattice $(14a)^4$. The same configurations are generated for periodic and time-twisted boundary conditions.

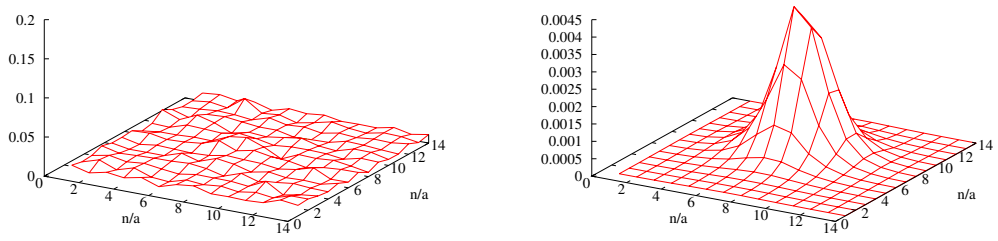

Figure 6.24: Gauge action density and SSM density are compared. The configuration is generated by applying ten heat-bath sweeps ($\beta = 30$) to a smooth instanton configuration.

are computed in each chirality.

Density profiles

We expect the eigenevectors of the operators $O^{\pm}$ will be less sensible to the high frequency modes than the gauge action density. In Figs. 6.24-6.33 the SSM density and the gauge action density are displayed for all β values in the periodic case for the first configuration of each ensemble. The gauge action density becomes rough and the instanton structure is lost. In the SSM density a smooth object compatible with an instanton appears in all cases. The same thing occurs for the twisted case.

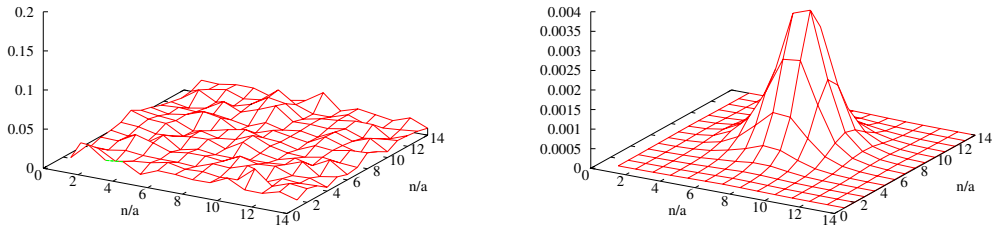

Figure 6.25: As in Fig.6.24 for ($\beta = 20$).

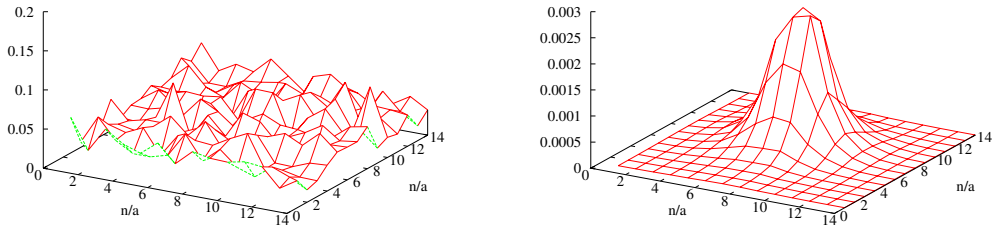

Figure 6.26: As in Fig.6.24 for ($\beta = 8$).

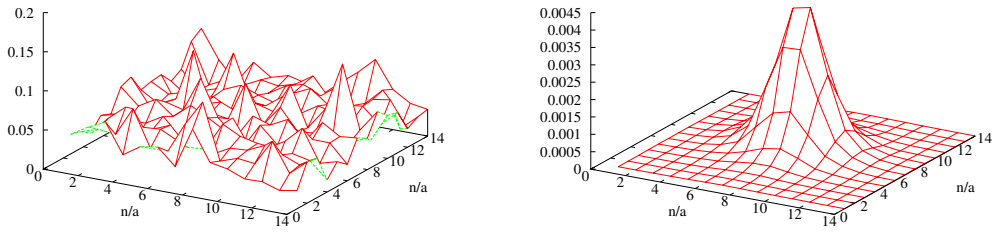

Figure 6.27: As in Fig.6.24 for ($\beta = 7$).

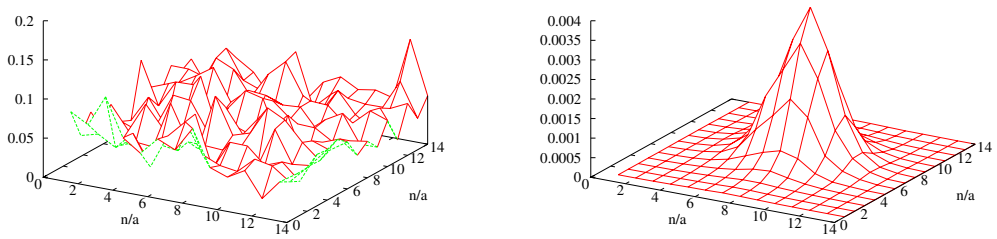

Figure 6.28: As in Fig.6.24 for ($\beta = 6$).

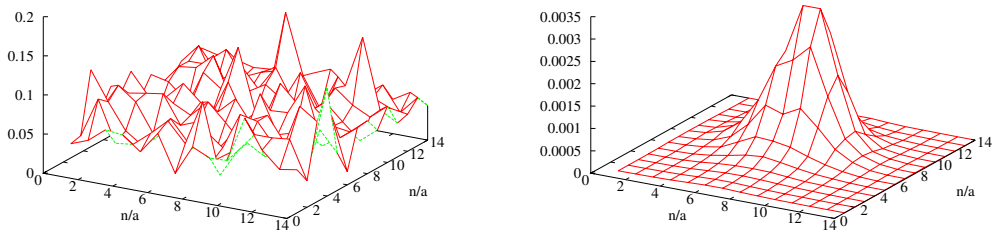

Figure 6.29: As in Fig.6.24 for ($\beta = 5$).

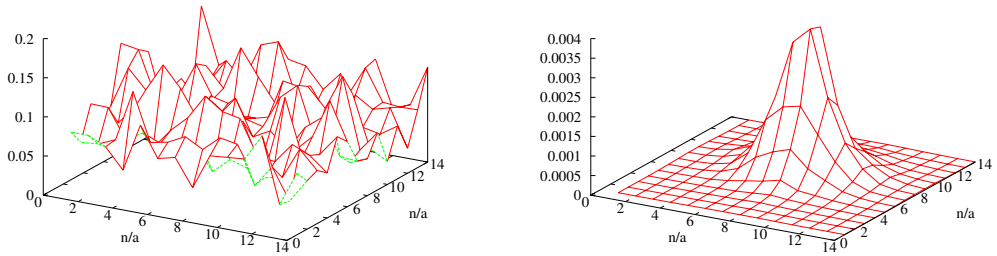

Figure 6.30: As in Fig.6.24 for ($\beta = 4$).

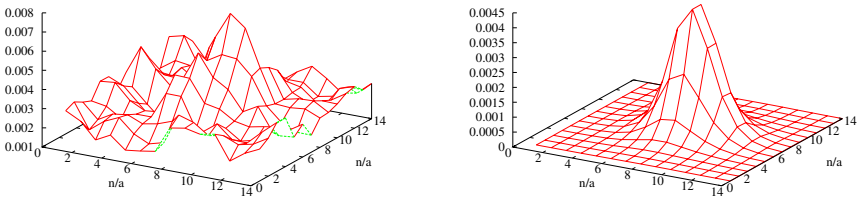

Figure 6.31: Gauge action density and SSM density are compared. The configuration is generated by applying four heat-bath sweeps ($\beta = 2.8$) to a smooth instanton configuration and two ϵ-cooling ($\epsilon = 0$) sweeps.

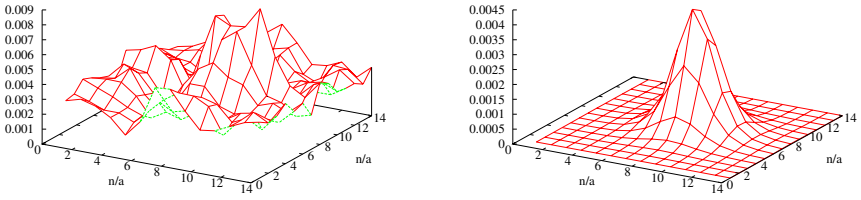

Figure 6.32: As in Fig.6.31 for ($\beta = 2.6$).

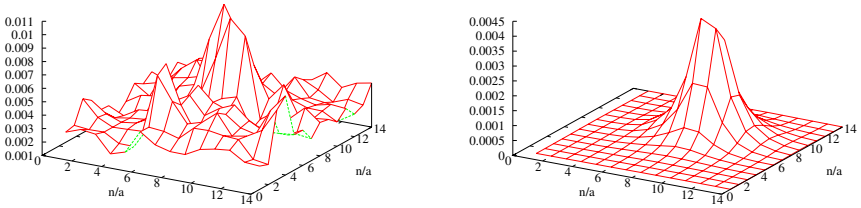

Figure 6.33: As in Fig.6.31 for ($\beta = 2.4$).

Spectrum analysis

Rough configurations are not classical solutions. Hence, the SSM will not appear as a zero-mode. The roughness can be added in a *controlled* way, leading a smooth growth of the lowest eigenvalue. The main difficulty could be the occurrence of level crossing when noise is added to the configuration. In the left part of Fig. 6.34 the spectrum of the heated configuration is displayed, in terms of the β^{-1} value. The same process has been repeated by imposing time-twisted boundary conditions, just as the instanton case, Fig. 6.34 right. The two lowest eigenvalues are fitted for large values of β ($\beta > 4$) as

$$\begin{aligned} \lambda_1^P &= 3.27 \cdot 10^{-5} + 0.15\beta^{-1} + 0.55\beta^{-2}, \\ \lambda_2^P &= 3.49 \cdot 10^{-3} + 0.16\beta^{-1} + 0.63\beta^{-2}, \\ \lambda_1^T &= 7.19 \cdot 10^{-6} + 0.15\beta^{-1} + 0.56\beta^{-2}, \\ \lambda_2^T &= 3.04 \cdot 10^{-2} + 0.17\beta^{-1} + 0.77\beta^{-2}. \end{aligned} \tag{6.42}$$

The constants terms are fixed by the value of corresponding modes of the smooth configurations. The whole spectrum grows with the value of β^{-1} and no level crossing is observed. For periodic and twisted BC, the behaviour of the eigenvalue corresponding to the SSM is the same . The second eigenvalue grows a little faster, so the gap increases with β.

Finally, we study the effect of small values of β ($\beta = 2.8, 2.6, 2.4$). In these cases, some problems appear in the computation of the Neuberger-Dirac operator. We observe these problems for $\beta < 3$ when the Wilson action is used (the same problem appears at $\beta < 6.2$ for SU(3)). These problems can be partially solved by using improved actions in the heat-bath algorithm [91]. In our case, we apply two sweeps of ϵ-cooling ($\epsilon = 0$) to the configuration before computing the spectrum. This is equivalent to a redefinition of the Neuberger-Dirac operator. Cooling with $\epsilon = 0$ produces a minimal modification of the objects presented in the initial field, and we expect that it reduces the high frequency noise. In the Fig. 6.35 we show how the gap is recovered when the cooling is applied.

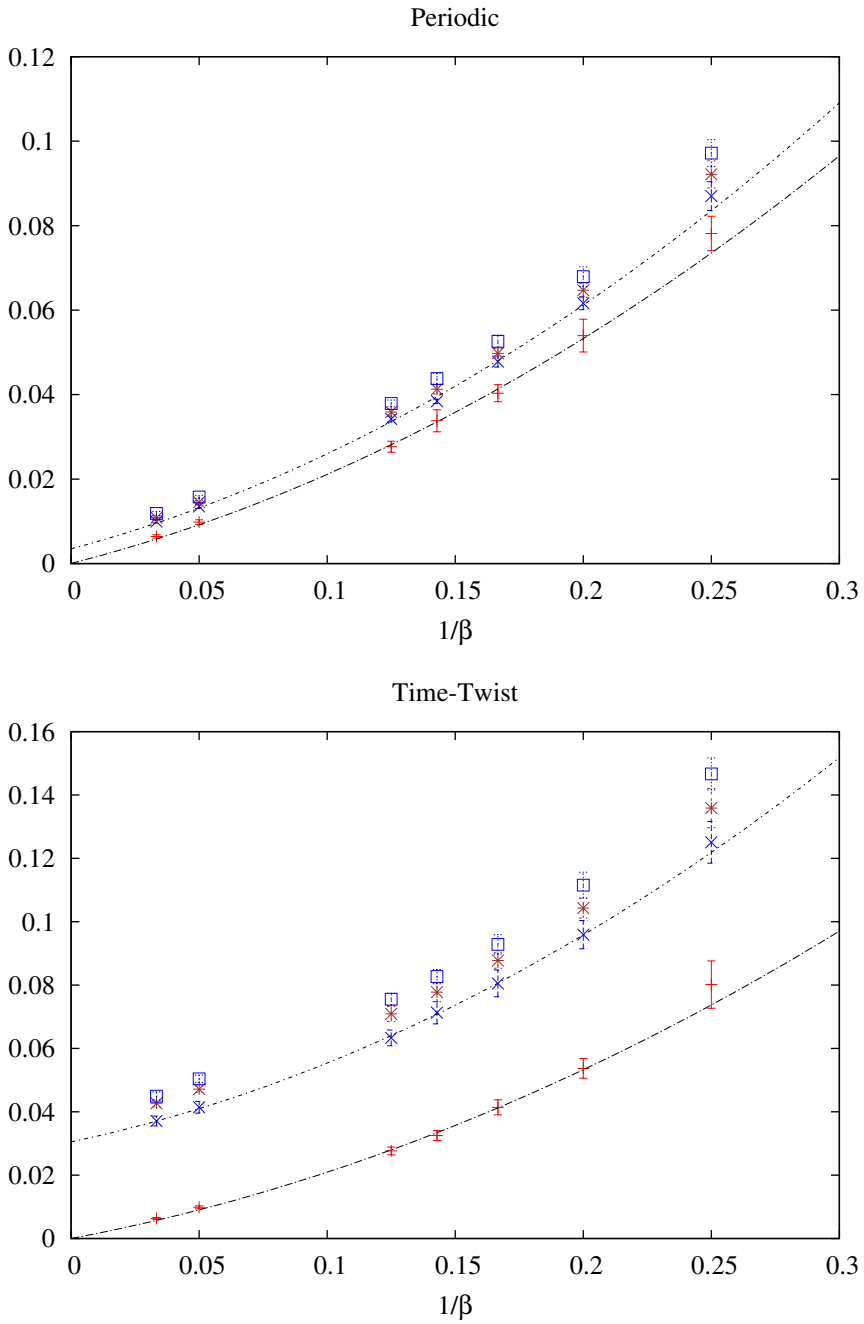

Figure 6.34: The three lowest eigenvalues of the configurations defined in Table 6.11 ($\beta > 3$) are displayed. For each value of β the average of the eigenvalues is plotted. The error bars correspond with standard deviation. The behaviour of the two lowest ones is fitted by Eqs. 6.43.

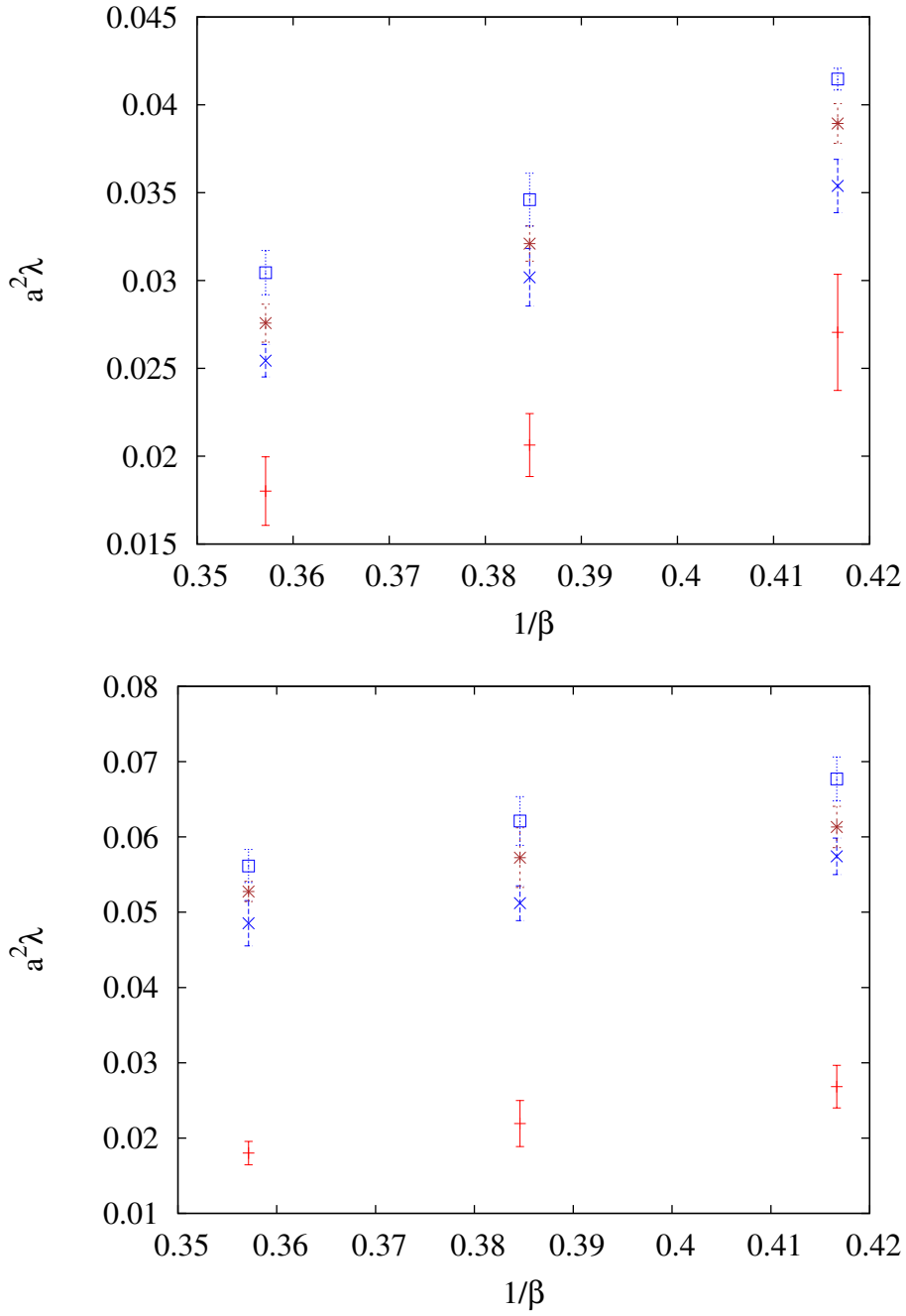

Figure 6.35: The three lowest eigenvalues of the configurations defined in Table 6.11 ($\beta < 3$) are displayed. For each value of β the average of the eigenvalues is plotted. The error bars correspond with standard deviation.

6.4 A brief note about Monte Carlo Configurations

In the analysis of Monte Carlo configurations, all the problems studied in the previous section are mixed:

- The SSM does not correspond with a zero-mode due to the high frequency noise.
- The gap between the lowest eigenvalue and the next one can be suppressed by the presence of other particles.
- The SSM should be constructed by using more than one eigenvector if there are well separated objects.

In addition, there is an extra problem in this case: we do not know the topological charge present in each chiral sector, so we do not know the appropriate normalization of the SSM.

In order to analyse this kind of configurations we are going to use two results obtained in the previous section:

- The SSM can always be obtained from the lowest eigenvectors.
- The density of the eigenvectors that do not correspond to the SSM is very flat.

We present preliminary results in order to reproduce the gauge action density.

6.4.1 Gauge configurations

We have generated two ensembles of $SU(2)$ Monte Carlo configurations by using the Wilson action. The ensembles are generated with two different physical volumes ($V_{\beta=2.468} = (1.4fm)^4$, $V_{\beta=2.518} = (1.22fm)^4$) on a 14^4 lattice. Two ϵ-cooling ($\epsilon = 0$) sweeps are applied to the configurations before computing the spectrum. We compute the eight lowest eigenvalues and eigenvectors of $O^{\pm}$ for each configuration.

6.4.2 Analysis of the configurations

In order to obtain the SSM, we must define how many eigenvectors are necessary to compute it. We expect that the density of the eigenvectors not related with the SSM will be very flat. This fact can be analysed by using the IPR, defined by:

$$IPR = N \sum_n \rho^2(n) \tag{6.43}$$

where ρ is the density of the zero-mode and $\sum_n \rho(n) = 1$ and N is the number of lattice points. The IPR is bounded between 1 (for constant configurations) and N (for $\rho(n) = \delta_{in}$). In Fig. 6.36 the mean values of IPR for each eigenvector density are displayed. In both volumes, the largest value of the IPR corresponds with the lowest eigenvector. For the largest volume the value of the IPR of the second eigenvector is considerably large too. The IPR decreases very fast for the other eigenvector densities. From this, we expect that only the lowest eigenvectors contain information about the gauge action density.

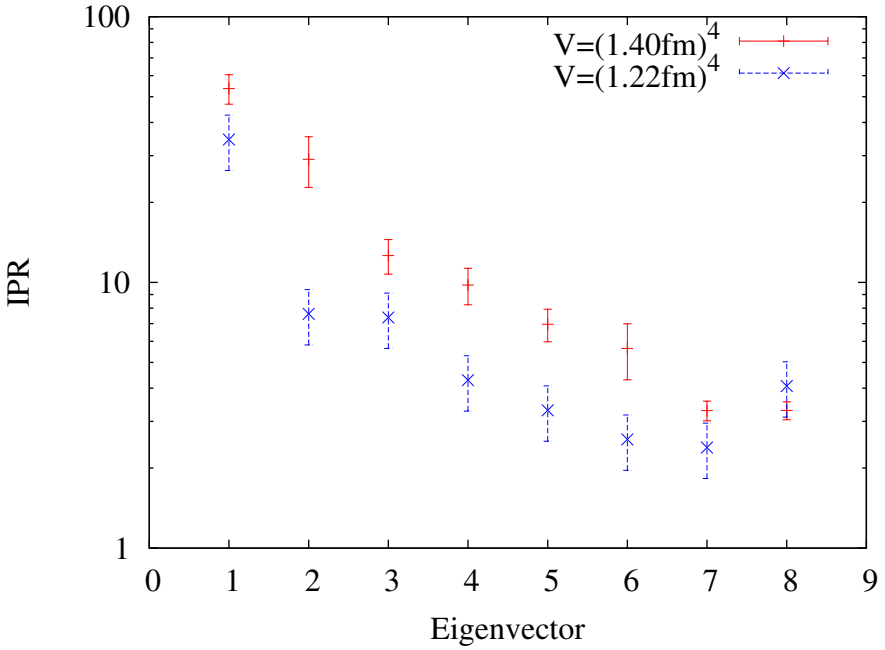

Figure 6.36: The mean of the IPR is displayed for the eight lowest eigenvectors densities. Two different physical volumes are presented.

As first check we propose to construct the SSM as the sum of the eigenvectors densities computed. In Figs. 6.37-6.39, three typical examples of structures present in the SSM are compared with the structures present in the same position of the (anti)self-dual part of the gauge action density. The gauge action densities are computed before applying 10 and 20 cooling sweeps to the original configuration. The first one corresponds with an isolated object, in this case an isolated object is clearly identified both in the cooled densities and in the SSM density. In the second example, a complex structure is observed. The same structures are present in all densities. Finally, in the third example, two objects are well identified in the SSM density and in the 12-cooled configuration, since these structures are remove in the 22-cooled configuration.

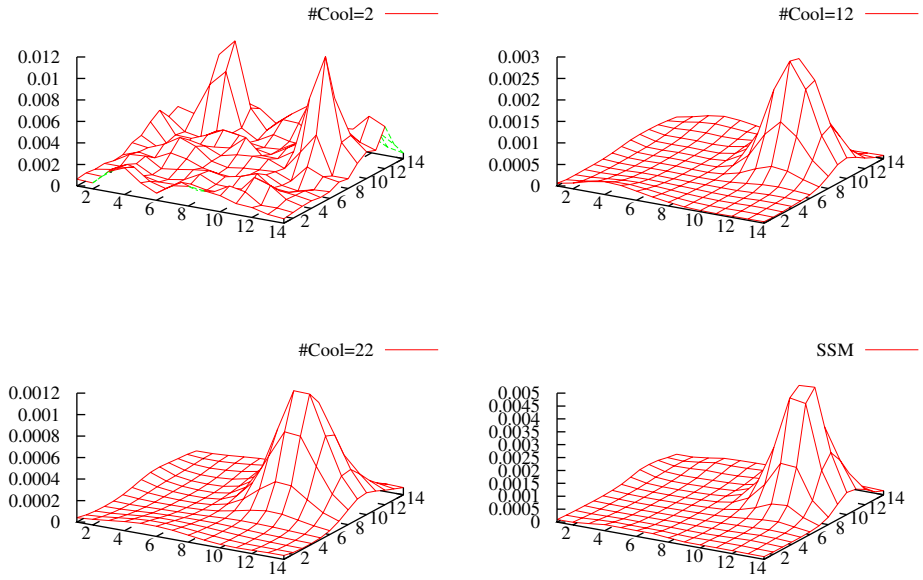

Figure 6.37: Self-dual part of the gauge action density for three different number of cooling sweeps and the SSM density are displayed. The position corresponds to an isolated peak of of the SSM density.

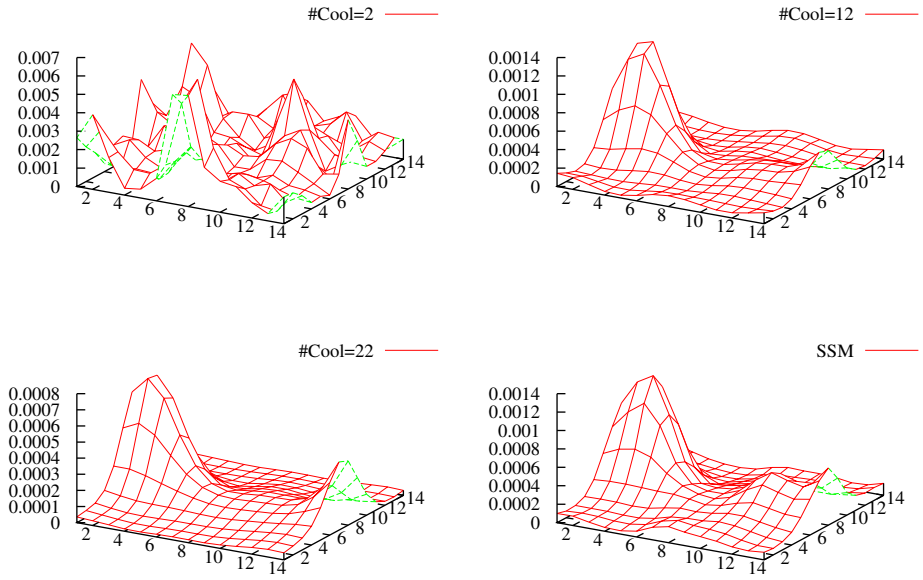

Figure 6.38: Other example similar to Fig.6.37. In this case two peaks appear.

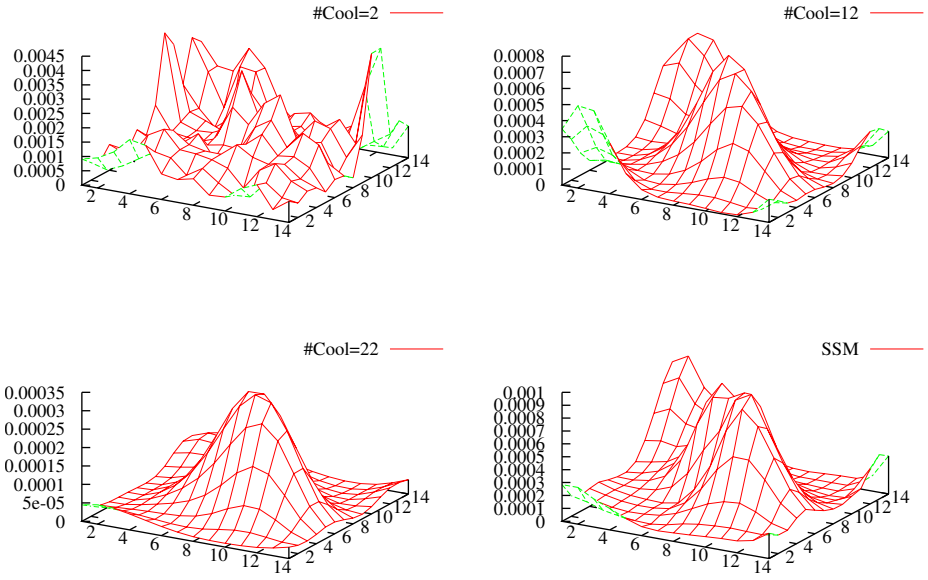

Figure 6.39: Other example similar to Fig.6.37. In this configuration, a more complex structure is found. Part of the structure is removed for 22 cooling sweeps.

Chapter 7

Conclusiones

En la primera parte de la tesis estudiamos las soluciones clásicas del operador de Dirac en la representación adjunta en presencia de un Calorón. Hemos deducido una base de soluciones de la ecuación de Dirac para el grupo SU(N) con distintas condiciones de periodicidad en la dirección temporal del fermión.

Para condiciones periódicas encontramos N soluciones linealmente independientes para el grupo SU(N), de acuerdo con el Teorema del Índice. Estas soluciones pueden ser agrupadas en una base, en la que cada una de ellas esta asociada a uno de los monopolos de definen las configuración Calorón.

Con condiciones anti-periódicas encontramos también N soluciones linealmente independientes. La estructuras en este caso son mucho mas complicadas. Hemos encontrado desde soluciones centradas en los monopolos, hasta soluciones extensas que unen varios de los monopolos, pudiendo formar estructuras muy extendidas. En el límite en que los monopolos se separan una distancia infinita, el Teorema del Índice predice una numero de modos cero que depende del valor de la masa de los monopolos. Hemos comprobado que nuestras soluciones funcionan también en ese límite.

Finalmente hemos deducido las soluciones para condiciones de periodicidad dadas por una fase compleja. En este caso aparecen también N soluciones.

Nuestros soluciones extienden el conjunto de las solución analíticas del operador de Dirac conocidas para los campos de Yang-Mills. Las técnicas desarrollas para encontrar estas soluciones son de carácter general, por lo que creemos pueden ser utilizadas para encontrar soluciones en presencia de otras configuraciones gauge.

Esperamos que esta soluciones jueguen un papel importante en el estudio semi-clásico de $\mathcal{N} = 1$ SUSY Yang-Mills a temperatura finita, así como para tratar de entender la ruptura de la Supersimetría.

En la segunda parte, utilizamos la representación adjunta del operador de Dirac para identificar las estructuras topológicas contenidas en configuraciones Monte Carlo. Para ello utilizamos, el hecho de que existe de una solución del operador de Dirac en la representación adjunta capaz de reproducir la densidad de acción gauge, el modo Supersimétrico.

Dos operadores, $O^{\pm}$, son construidos para encontrar esta solución en cada quiralidad. Los operadores de definen proyectando el operador de Dirac, al subespacio de soluciones que satisfacen la condición de realidad. El modo Supersimétrico corresponde con el auto-estado de autovalor mínimo de estos operadores y reproduce la densidad gauge de las partes auto-dual y anti-auto-dual de la acción gauge.

Estos operadores han sido implementados en el Retículo mediante el operador de Neuberger. Hemos analizado el espectro del operador en diversas configuraciones para estudiar el comportamiento del auto-estado más bajo en situaciones en la que la configuración gauge no es una solución clásica. Los resultados obtenidos son los siguientes:

- Las correcciones debidas a la discretización, modifican el autovalor mínimo, que no corresponde con un modo cero. Cuyas correciones van como:

$$\lambda_1 = \frac{6 \cdot 10^{-4}}{\rho^2} \frac{a^2}{\rho^2} + O(\frac{a^2}{\rho^4}) \tag{7.1}$$

- Las correcciones de volumen finito, son apreciables en el autovalor mínimo cuando el objeto es de un tamaño comparable al de la caja ($L/\rho < 4$). Este tipo de corrección desaparece al imponer condiciones de contorno tipo Twist en los planos espacio-temporales.

- En el caso de configuraciones suaves que no son soluciones clásicas (por ejemplo un par instanton-antiinstanton), el modo fundamental no es un modo cero y su valor depende exponencialmente de la distancia entre los objetos.

- En el caso de configuraciones dominadas por modos altos de Fourier, todo el espectro es desplazado. Hemos observado que la inclusión de ruido mantiene la jerarquía de autovalores, sin producir cruces de niveles.

Una vez controlados los errores de la implementación, nuestros resultados muestran que el modo Supersimétrico es capaz de:

- Reproducir la densidad de acción gauge con errores del orden de los que provienen de la definición de la acción gauge en el Retículo.

- Separar las estructuras presentes en cada sector quiral.

- Filtrar los modos de Fourier altos que impiden la identificación directa de los objetos en la densidad de acción gauge.

Un estudio exhaustivo de configuraciones Monte Carlo se deja para futuros trabajos. En estas configuraciones podrían aparecer nuevos problemas como: determinar el número de modos necesarios para obtener el modo Supersimétrico. En una primera aproximación a este problema, hemos obtenido resultados prometedores, encontrando una rica estructura en el estudio de la densidad del modo Supersimétrico. Esperamos que este método sea una buena herramienta para entender mejor las estructuras que dominan el vacío de QCD.

Bibliography

[1] Richard Phillips Feynman. The principle of least action in quantum mechanics.

[2] Kenneth G. Wilson. CONFINEMENT OF QUARKS. *Phys. Rev.*, D10:2445–2459, 1974.

[3] Gerard 't Hooft. Computation of the quantum effects due to a four- dimensional pseudoparticle. *Phys. Rev.*, D14:3432–3450, 1976.

[4] Chen-Ning Yang and Robert L. Mills. Conservation of isotopic spin and isotopic gauge invariance. *Phys. Rev.*, 96:191–195, 1954.

[5] A. A. Belavin, Alexander M. Polyakov, A. S. Schwartz, and Yu. S. Tyupkin. Pseudoparticle solutions of the Yang-Mills equations. *Phys. Lett.*, B59:85–87, 1975.

[6] Tom Banks and A. Casher. Chiral Symmetry Breaking in Confining Theories. *Nucl. Phys.*, B169:103, 1980.

[7] M. F. Atiyah and I. M. Singer. The Index of elliptic operators. 1. *Annals Math.*, 87:484–530, 1968.

[8] M. F. Atiyah and I. M. Singer. The Index of elliptic operators. 4. *Annals Math.*, 93:119–138, 1971.

[9] Edward V. Shuryak. Hadrons Containing a Heavy Quark and QCD Sum Rules. *Nucl. Phys.*, B198:83, 1982.

[10] Dmitri Diakonov and V. Yu. Petrov. Instanton Based Vacuum from Feynman Variational Principle. *Nucl. Phys.*, B245:259, 1984.

[11] Thomas Schafer and Edward V. Shuryak. Instantons in QCD. *Rev. Mod. Phys.*, 70:323–426, 1998.

[12] Barry J. Harrington and Harvey K. Shepard. Periodic Euclidean Solutions and the Finite Temperature Yang-Mills Gas. *Phys. Rev.*, D17:2122, 1978.

[13] Barry J. Harrington and Harvey K. Shepard. THERMODYNAMICS OF THE YANG-MILLS GAS. *Phys. Rev.*, D18:2990, 1978.

[14] Thomas C. Kraan and Pierre van Baal. Exact T-duality between calorons and Taub - NUT spaces. *Phys. Lett.*, B428:268–276, 1998.

[15] Thomas C. Kraan and Pierre van Baal. Periodic instantons with non-trivial holonomy. *Nucl. Phys.*, B533:627–659, 1998.

[16] Ki-Myeong Lee. Instantons and magnetic monopoles on R**3 x S(1) with arbitrary simple gauge groups. *Phys. Lett.*, B426:323–328, 1998.

[17] Thomas C. Kraan and Pierre van Baal. Monopole constituents inside SU(n) calorons. *Phys. Lett.*, B435:389–395, 1998.

[18] E. Corrigan, D. B. Fairlie, S. Templeton, and P. Goddard. A Green's Function for the General Selfdual Gauge Field. *Nucl. Phys.*, B140:31, 1978.

[19] H. Osborn. SOLUTIONS OF THE DIRAC EQUATION FOR GENERAL INSTANTON SOLUTIONS. *Nucl. Phys.*, B140:45, 1978.

[20] Gerard 't Hooft. Some Twisted Selfdual Solutions for the Yang-Mills Equations on a Hypertorus. *Commun. Math. Phys.*, 81:267–275, 1981.

[21] Antonio Gonzalez-Arroyo. Yang-Mills fields on the 4-dimensional torus. (Classical theory). 1997.

[22] Peter J. Braam and Pierre van Baal. NAHM'S TRANSFORMATION FOR INSTANTONS. *Commun. Math. Phys.*, 122:267, 1989.

[23] Antonio Gonzalez-Arroyo. On Nahm's transformation with twisted boundary conditions. *Nucl. Phys.*, B548:626–636, 1999.

[24] W. Nahm. ALL SELFDUAL MULTI - MONOPOLES FOR ARBITRARY GAUGE GROUPS. Presented at Int. Summer Inst. on Theoretical Physics, Freiburg, West Germany, Aug 31 - Sep 11, 1981.

[25] David J. Gross, Robert D. Pisarski, and Laurence G. Yaffe. QCD and Instantons at Finite Temperature. *Rev. Mod. Phys.*, 53:43, 1981.

[26] Thomas C. Kraan. Instantons, monopoles and toric hyperKaehler manifolds. *Commun. Math. Phys.*, 212:503–533, 2000.

[27] M. Creutz. Monte Carlo Study of Quantized SU(2) Gauge Theory. *Phys. Rev.*, D21:2308–2315, 1980.

[28] Holger Bech Nielsen and M. Ninomiya. No Go Theorem for Regularizing Chiral Fermions. *Phys. Lett.*, B105:219, 1981.

[29] Paul H. Ginsparg and Kenneth G. Wilson. A Remnant of Chiral Symmetry on the Lattice. *Phys. Rev.*, D25:2649, 1982.

[30] Herbert Neuberger. More about exactly massless quarks on the lattice. *Phys. Lett.*, B427:353–355, 1998.

[31] Herbert Neuberger. Exactly massless quarks on the lattice. *Phys. Lett.*, B417:141–144, 1998.

[32] Pilar Hernandez, Karl Jansen, and Martin Luscher. Locality properties of Neuberger's lattice Dirac operator. *Nucl. Phys.*, B552:363–378, 1999.

[33] Herbert Neuberger. Minimizing storage in implementations of the overlap lattice-Dirac operator. *Int. J. Mod. Phys.*, C10:1051–1058, 1999.

[34] N. Michael Davies, Timothy J. Hollowood, Valentin V. Khoze, and Michael P. Mattis. Gluino condensate and magnetic monopoles in supersymmetric gluodynamics. *Nucl. Phys.*, B559:123–142, 1999.

[35] N. Michael Davies, Timothy J. Hollowood, and Valentin V. Khoze. Monopoles, affine algebras and the gluino condensate. *J. Math. Phys.*, 44:3640–3656, 2003.

[36] Guido Cossu and Massimo D'Elia. Finite size phase transitions in QCD with adjoint fermions. *JHEP*, 07:048, 2009.

[37] Joyce C. Myers and Michael C. Ogilvie. Phase diagrams of SU(N) gauge theories with fermions in various representations. *JHEP*, 07:095, 2009.

[38] Pavel Kovtun, Mithat Unsal, and Laurence G. Yaffe. Volume independence in large N(c) QCD-like gauge theories. *JHEP*, 06:019, 2007.

[39] Mithat Unsal and Laurence G. Yaffe. Center-stabilized Yang-Mills theory: confinement and large N volume independence. *Phys. Rev.*, D78:065035, 2008.

[40] Mithat Unsal. Abelian duality, confinement, and chiral symmetry breaking in QCD(adj). *Phys. Rev. Lett.*, 100:032005, 2008.

[41] Tohru Eguchi and Hikaru Kawai. Reduction of Dynamical Degrees of Freedom in the Large N Gauge Theory. *Phys. Rev. Lett.*, 48:1063, 1982.

[42] Antonio Gonzalez-Arroyo and M. Okawa. A TWISTED MODEL FOR LARGE N LATTICE GAUGE THEORY. *Phys. Lett.*, B120:174, 1983.

[43] Antonio Gonzalez-Arroyo and M. Okawa. The Twisted Eguchi-Kawai Model: A Reduced Model for Large N Lattice Gauge Theory. *Phys. Rev.*, D27:2397, 1983.

[44] Gyan Bhanot, Urs M. Heller, and Herbert Neuberger. The Quenched Eguchi-Kawai Model. *Phys. Lett.*, B113:47, 1982.

[45] Ki-Myeong Lee and Chang-hai Lu. SU(2) calorons and magnetic monopoles. *Phys. Rev.*, D58:025011, 1998.

[46] A. A Belavin, V. A. Fateev, Albert S. Schwarz, and Yu. S. Tyupkin. QUANTUM FLUCTUATIONS OF MULTI - INSTANTON SOLUTIONS. *Phys. Lett.*, B83:317–320, 1979.

[47] Curtis G. Callan, Jr., Roger F. Dashen, and David J. Gross. Toward a theory of the strong interactions. *Phys. Rev.*, D17:2717, 1978.

[48] M. Garcia Perez, Antonio Gonzalez-Arroyo, and P. Martinez. From perturbation theory to confinement: How the string tension is built up. *Nucl. Phys. Proc. Suppl.*, 34:228–230, 1994.

[49] Antonio Gonzalez-Arroyo and P. Martinez. Investigating Yang-Mills theory and confinement as a function of the spatial volume. *Nucl. Phys.*, B459:337–354, 1996.

[50] Antonio Gonzalez-Arroyo, P. Martinez, and A. Montero. Gauge invariant structures and confinement. *Phys. Lett.*, B359:159–165, 1995.

[51] Antonio Gonzalez-Arroyo and A. Montero. Do classical configurations produce Confinement? *Phys. Lett.*, B387:823–828, 1996.

[52] Dmitri Diakonov and Victor Petrov. Confining ensemble of dyons. *Phys. Rev.*, D76:056001, 2007.

[53] Dmitri Diakonov, Nikolay Gromov, Victor Petrov, and Sergey Slizovskiy. Quantum weights of dyons and of instantons with non- trivial holonomy. *Phys. Rev.*, D70:036003, 2004.

[54] Dmitri Diakonov. Statistical physics of dyons and confinement. *Acta Phys. Polon.*, B39:3365–3393, 2008.

[55] P. Gerhold, E. M. Ilgenfritz, and M. Muller-Preussker. An SU(2) KvBLL caloron gas model and confinement. *Nucl. Phys.*, B760:1–37, 2007.

[56] Christof Gattringer. Calorons, instantons and constituent monopoles in SU(3) lattice gauge theory. *Phys. Rev.*, D67:034507, 2003.

[57] Christof Gattringer and Stefan Schaefer. New findings for topological excitations in SU(3) lattice gauge theory. *Nucl. Phys.*, B654:30–60, 2003.

[58] Christof Gattringer and Rainer Pullirsch. Topological lumps and Dirac zero modes in SU(3) lattice gauge theory on the torus. *Phys. Rev.*, D69:094510, 2004.

[59] Ernst-Michael Ilgenfritz, B. V. Martemyanov, M. Muller-Preussker, S. Shcheredin, and A. I. Veselov. On the topological content of SU(2) gauge fields below T(c). *Phys. Rev.*, D66:074503, 2002.

[60] E. M. Ilgenfritz, B. V. Martemyanov, M. Muller-Preussker, and A. I. Veselov. The monopole content of topological clusters: Have KvB calorons been found? *Phys. Rev.*, D71:034505, 2005.

[61] Ernst-Michael Ilgenfritz, B. V. Martemyanov, M. Muller-Preussker, and A. I. Veselov. Recombination of dyons into calorons in SU(2) lattice fields at low temperatures. *Phys. Rev.*, D69:114505, 2004.

[62] E. M. Ilgenfritz, B. V. Martemyanov, M. Muller-Preussker, and A. I. Veselov. Calorons and monopoles from smeared SU(2) lattice fields at non-zero temperature. *Phys. Rev.*, D73:094509, 2006.

[63] E. M. Ilgenfritz, M. Muller-Preussker, and D. Peschka. Calorons in SU(3) lattice gauge theory. *Phys. Rev.*, D71:116003, 2005.

[64] V. G. Bornyakov et al. Calorons and dyons at the thermal phase transition analyzed by overlap fermions. *Phys. Rev.*, D76:054505, 2007.

[65] V. G. Bornyakov, E. M. Ilgenfritz, B. V. Martemyanov, and M. Muller-Preussker. The dyonic picture of topological objects in the deconfined phase. *Phys. Rev.*, D79:034506, 2009.

[66] Falk Bruckmann, Simon Dinter, Ernst-Michael Ilgenfritz, Michael Muller-Preussker, and Marc Wagner. Cautionary remarks on the moduli space metric for multi- dyon simulations. *Phys. Rev.*, D79:116007, 2009.

[67] Ashok K. Das and Michio Kaku. SUPERSYMMETRY AT HIGH TEMPERATURES. *Phys. Rev.*, D18:4540, 1978.

[68] L. Girardello, Marcus T. Grisaru, and P. Salomonson. Temperature and Supersymmetry. *Nucl. Phys.*, B178:331, 1981.

[69] L. Van Hove. SUPERSYMMETRY AND POSITIVE TEMPERATURE FOR SIMPLE SYSTEMS. *Nucl. Phys.*, B207:15, 1982.

[70] Hideaki Aoyama and Daniel Boyanovsky. GOLDSTONE FERMIONS IN SUPERSYMMETRIC THEORIES AT FINITE TEMPERATURE. *Phys. Rev.*, D30:1356, 1984.

[71] D. Boyanovsky. Supersymmetry breaking at finite temperature and the existence of the goldstone fermion. *Physica*, 15D:152–162, 1985.

[72] H. Matsumoto, M. Nakahara, Y. Nakano, and H. Umezawa. A NEW ZERO ENERGY MODE IN SUPERSYMMETRY AT FINITE TEMPERATURE. *Phys. Lett.*, B140:53–55, 1984.

[73] Detlev Buchholz and Izumi Ojima. Spontaneous collapse of supersymmetry. *Nucl. Phys.*, B498:228–242, 1997.

[74] Margarita Garcia Perez, Antonio Gonzalez-Arroyo, Carlos Pena, and Pierre van Baal. Weyl-Dirac zero-mode for calorons. *Phys. Rev.*, D60:031901, 1999.

[75] M. N. Chernodub, Thomas C. Kraan, and Pierre van Baal. Exact fermion zero-mode for the new calorons. *Nucl. Phys. Proc. Suppl.*, 83:556–558, 2000.

[76] Falk Bruckmann, Daniel Nogradi, and Pierre van Baal. Constituent monopoles through the eyes of fermion zero- modes. *Nucl. Phys.*, B666:197–229, 2003.

[77] Claude W. Bernard, Norman H. Christ, Alan H. Guth, and Erick J. Weinberg. Pseudoparticle parameters for arbitrary gauge groups. *Phys. Rev.*, D16:2967, 1977.

[78] Albert S. Schwarz. On Regular Solutions of Euclidean Yang-Mills Equations. *Phys. Lett.*, B67:172–174, 1977.

[79] M. F. Atiyah, Nigel J. Hitchin, and I. M. Singer. Selfduality in Four-Dimensional Riemannian Geometry. *Proc. Roy. Soc. Lond.*, A362:425–461, 1978.

[80] E. Corrigan, P. Goddard, and S. Templeton. Instanton Green functions and tensor products. *Nucl. Phys.*, B151:93, 1979.

[81] Norman H. Christ, Erick J. Weinberg, and Nancy K. Stanton. General self-dual Yang-Mills solutions. *Phys. Rev.*, D18:2013, 1978.

[82] Antonio Gonzalez-Arroyo. On Nahm's transformation with twisted boundary conditions. *Nucl. Phys.*, B548:626–636, 1999.

[83] Tom M. W. Nye and Michael A. Singer. An L^2-Index Theorem for Dirac Operators on $S^1 * R^3$. 2000.

[84] Erich Poppitz and Mithat Unsal. Index theorem for topological excitations on $R^3 * S^1$ and Chern-Simons theory. *JHEP.*, 0903:027, 2009.

[85] Margarita Garcia Perez and Antonio Gonzalez-Arroyo. Gluino zero-modes for non-trivial holonomy calorons. *JHEP*, 11:091, 2006.

[86] Erek Bilgici, Falk Bruckmann, Christof Gattringer, and Christian Hagen. Dual quark condensate and dressed Polyakov loops. *Phys. Rev.*, D77:094007, 2008.

[87] Erek Bilgici, Christof Gattringer, Ernst-Michael Ilgenfritz, and Axel Maas. Adjoint quarks and fermionic boundary conditions. *JHEP*, 11:035, 2009.

[88] Margarita Garcia Perez, Antonio Gonzalez-Arroyo, and Alfonso Sastre. Adjoint zero-modes as a tool to understand the Yang-Mills vacuum. *PoS*, LAT2007:328, 2007.

[89] Antonio Gonzalez-Arroyo and Robert Kirchner. Adjoint modes as probes of gauge field structure. *JHEP*, 01:029, 2006.

[90] Constantine Callias. Index Theorems on Open Spaces. *Commun. Math. Phys.*, 62:213–234, 1978.

[91] E. M. Ilgenfritz et al. Exploring the structure of the quenched QCD vacuum with overlap fermions. *Phys. Rev.*, D76:034506, 2007.

[92] Falk Bruckmann and Ernst-Michael Ilgenfritz. Laplacian modes probing gauge fields. *Phys. Rev.*, D72:114502, 2005.

[93] Peter Hasenfratz, Victor Laliena, and Ferenc Niedermayer. The index theorem in QCD with a finite cut-off. *Phys. Lett.*, B427:125–131, 1998.

[94] I. Horváth, S. J. Dong, T. Draper, F. X. Lee, K. F. Liu, H. B. Thacker, and J. B. Zhang. Local structure of topological charge fluctuations in qcd. *Phys. Rev. D*, 67(1):011501, Jan 2003.

[95] Margarita Garcia Perez, Antonio Gonzalez-Arroyo, Jeroen R. Snippe, and Pierre van Baal. Instantons from over - improved cooling. *Nucl. Phys.*, B413:535–552, 1994.

[96] S. Chadha, A. D'Adda, P. Di Vecchia, and F. Nicodemi. Fermions in the Background Pseudoparticle Field in an O(5) Formulation. In *Bielefeld 1976, Proceedings, Summer Institute Of Theoretical Physics, Vol.2*, New York 1978, 417-446 and Columbia Univ New York - COO-2271-91 (76,REC.OCT 77) 43p.

[97] R. Jackiw and C. Rebbi. Spinor analysis of Yang-Mills theory. *Phys. Rev.*, D16:1052, 1977.

[98] Thomas Kalkreuter and Hubert Simma. An Accelerated conjugate gradient algorithm to compute low lying eigenvalues: A Study for the Dirac operator in SU(2) lattice QCD. *Comput. Phys. Commun.*, 93:33–47, 1996.

[99] Urs M. Heller, Robert G. Edwards, and Rajamani Narayanan. Evidence for fractional topological charge in SU(2) pure Yang-Mills theory. *Nucl. Phys. Proc. Suppl.*, 73:497–499, 1999.

[100] D. J. R. Pugh and M. Teper. TOPOLOGICAL DISLOCATIONS IN THE CONTINUUM LIMIT OF SU(2) LATTICE GAUGE THEORY. *Phys. Lett.*, B224:159–165, 1989.

[101] Anna Hasenfratz, Roland Hoffmann, and Stefan Schaefer. Localized eigenmodes of the overlap operator and their impact on the eigenvalue distribution. *JHEP*, 11:071, 2007.

[102] Zoltan Fodor, Kieran Holland, Julius Kuti, Daniel Nogradi, and Chris Schroeder. Topology and higher dimensional representations. *JHEP*, 08:084, 2009.

[103] Roman Hollwieser, Manfried Faber, and Urs M. Heller. Lattice Index Theorem and Fractional Topological Charge. 2010.

Appendix A

$SU(N)$ ADHM-Nahm-data

In this appendix we will collect different formulas and calculations of a more technical type needed to complete the analytical computations of zero-modes described in the text. We will start by generalizing the calculation of u and ω for SU(N) calorons.

A.1 Computation of ω and u

In this subsection we derive explicit formulas for the basic ADHM quantities ω and u in terms of our Nahm data. Here we will follow the same procedure given in Ref. [85] for SU(2). Most of our formulas are generalised in a simple way, so we will be very sketchy in the derivation and invite the readers to consult that reference.

All interesting functions belong to the space of linear combinations of the following $2N$ functions:

$$\Psi_a^{\pm}(z) \equiv \Psi^{(\pm)}(z - Z_a^M, x - X^a, \frac{m_a}{4\pi}), \tag{A.1}$$

where m_a and X^a are the mass and position of the a-th constituent monopole, Z_a^M are the midpoints of the intervals in z, $Z_a^M = (Z_a + Z_{a-1})/2$, x is the space-time coordinate and

$$\Psi^{(+)}(z, x, \delta) = \chi(-\delta, \delta)\, e^{i2\pi\bar{x}z} \tag{A.2}$$

$$\Psi^{(-)}(z, x, \delta) = \chi(-\delta, \delta)\, e^{i2\pi\hat{x}z} \tag{A.3}$$

Using the form of the operator $\widetilde{M} \equiv \widetilde{A} - \hat{x}\, I\!I_Q$, see Eq. (2.71), and the equations fulfilled by the functions u and ω, i.e. Eqs. (5.29)-(5.32), it is easy to deduce that they can be expanded as:

$$u(z) = \sum_a u_a(z) = \sum_a (\Psi_a^+(z) A_a) \tag{A.4}$$

$$\omega(z) = \sum_a \omega_a(z) = \sum_a (\Psi_a^+(z) D_a^{(+)} + \Psi_a^-(z) D_a^{(-)}) \tag{A.5}$$

$$\hat{\partial}\omega = \sum_a (4\pi i (z - Z_a^M) \Psi_a^+(z) D_a^{(+)} + \Psi_a^+(z) S_a^{(+)} + \Psi_a^-(z) S_a^{(-)}) \tag{A.6}$$

where the coefficients (A_a, $D_a^{(\pm)}$, $S_a^{(\pm)}$) are $2 \times N$ matrix functions of space-time x. These can be determined by matching the value of the functions at the edges of the intervals to satisfy the delta function part of the equations. For that we would need to introduce the 2×2 matrix E' defined as:

$$E_a'^{\epsilon'\epsilon} = \Psi_a^{\epsilon}(z = Z_a^M + \epsilon' \frac{m_a}{4\pi}) \tag{A.7}$$

where ϵ and ϵ' take the values ± 1. The inverse matrix is given by

$$E_a'^{-1} = \frac{g(m_a r_a)\hat{n}_a}{2 m_a r_a} \times E_a^{\dagger} \tag{A.8}$$

where E_a is a new matrix. The symbol $\hat{n}_a$ stands for a hermitian unitary traceless matrix defined through the decomposition

$$(\vec{x} - \vec{X}^a)\vec{\tau} = r_a \hat{n}_a \tag{A.9}$$

where r_a is the distance to the corresponding constituent monopole. The expressions also contain the function g:

$$g(u) = u/\sinh(u) \tag{A.10}$$

evaluated at the product of the mass and the distance.

The first step in the determination of the coefficients $D_a^{(\pm)}$ and $S_a^{(\pm)}$ will be to express them in terms of the values of ω at the points separating the different intervals: $\omega(Z_a) \equiv \mathcal{W}_a$. Imposing the continuity in z of the function ω we obtain:

$$\mathcal{W}_a = \sum_{\epsilon} E_a'^{+\epsilon} D_a^{(\epsilon)} = \sum_{\epsilon} E_{a+1}'^{-\epsilon} D_{a+1}^{(\epsilon)} \tag{A.11}$$

$$\hat{\partial}\mathcal{W}_a = i m_a E_a'^{++} D_a^{(+)} + E_a'^{+\epsilon} S_a^{(\epsilon)} = -i m_{a+1} E_{a+1}'^{-+} D_{a+1}^{(+)} + E_{a+1}'^{-\epsilon} S_{a+1}^{(\epsilon)} \tag{A.12}$$

These equations can be rewritten as a vector equation allowing to solve for $D_a^{(\pm)}$ in terms of $\mathcal{W}_a$ and $\mathcal{W}_{a-1}$. Using our previous definitions of the matrices E_a and E_a' we can write:

$$D_a^{(\epsilon)} = \frac{\hat{n}_a g(m_a r_a)}{2 m_a r_a} (E_a^{\dagger})^{\epsilon\epsilon'} \mathcal{W}_{a+(\epsilon'-1)/2} \tag{A.13}$$

$$S_a^{(\epsilon)} = \frac{\hat{n}_a g(m_a r_a)}{2 m_a r_a} (E_a^{\dagger})^{\epsilon\epsilon'} \hat{\partial}\mathcal{W}_{a+(\epsilon'-1)/2} + \frac{i g^2(m_a r_a)}{2 m_a r_a^2} \widetilde{E}^{\epsilon} (E_a^{\dagger})^{+\epsilon'} \mathcal{W}_{a+(\epsilon'-1)/2} \tag{A.14}$$

where $\widetilde{E}^{+} = \cosh(m_a r_a)$ and $\widetilde{E}^{-} = -1$. The coefficient A_a appearing in the expansion of u can be related to $D_a^{(+)}$ by the equation $\widetilde{M}\omega = uF^{-1}$. Hence, we get

$$A_a = 2 i r_a \hat{n}_a D_a^{(+)} F \tag{A.15}$$

Notice that the functions u_a and ω_a can be regarded as the contribution of the a-th constituent monopole to the function u and ω, since they only depend on the distance r_a and the mass m_a of the corresponding monopole. Nonetheless, the mixing and interaction

among the constituent monopoles is hidden in the expression of $\mathcal{W}_a$, which we will now derive. The main equation satisfied by $\mathcal{W}_a$ comes from the equation:

$$q = \widetilde{M}^\dagger u \tag{A.16}$$

leading to

$$\zeta^a_\alpha P_a = \frac{-1}{2\pi i}(E'^{++}_a A_a - E'^{-+}_{a+1} A_{a+1}) \tag{A.17}$$

where P_a is an N-vector with components δ_{ai}. To write the previous equation in a more compact form we arrange the right hand side into an N-component column vector of $2 \times N$ matrices. The unknown $\mathcal{W}_a$ are also arranged as a column vector of the same kind. Finally, we introduce the N-component column vectors of quaternions e_a and $\widetilde{e}_a$ whose components are 2×2 matrices and such that the only non-zero components are the rows $a-1$ and a, given by

$$e^{a-1}_a = \quad E'^{-+}_a \; ; \quad e^a_a = -E'^{++}_a \tag{A.18}$$

$$\widetilde{e}^{a-1}_a = - \; E'^{--}_a \; ; \quad \widetilde{e}^a_a = \; E'^{+-}_a \tag{A.19}$$

Then the previous equations can be re-written as follows:

$$\zeta = \sum_a \frac{g(m_a r_a)}{2\pi m_a} e_a e_a^\dagger \mathcal{W} F \tag{A.20}$$

The projector $e_a e_a^\dagger$ is an $N \times N$ matrix of quaternions whose only non-zero components correspond to the $a-1$ and a rows and columns. Restricting to this non-zero 2×2 matrix we have The first term on the right-hand side can be completed (with zeroes) to an $N \times N$ complex matrix that we will call U_a. The second piece when summed over "a" can be rewritten in terms of the projector $\zeta\zeta^\dagger$. In this way Eq. (A.20) can be rewritten as

$$\zeta = V^{-1}\mathcal{W}F - \zeta\zeta^\dagger \mathcal{W} F \tag{A.21}$$

where

$$V^{-1} = \sum_a U_a + \frac{1}{2\pi}\mathrm{diag}(||\vec{X}^{a+1} - \vec{X}^a||) \tag{A.22}$$

Using the definition of F

$$F^{-1} = \mathbf{I} - \zeta^\dagger \mathcal{W} \tag{A.23}$$

we finally arrive to

$$\zeta = V^{-1}\mathcal{W} \tag{A.24}$$

whose solution is

$$\mathcal{W} = V\zeta \tag{A.25}$$

The matrix V is an $N \times N$ complex hermitian matrix. The elements of F^{-1} can be obtained in terms of this matrix

$$(F^{-1})_{ab} = \delta_{ab} - V_{ab}\zeta^\dagger_a \zeta_b \tag{A.26}$$

A.2 Field strength and periodic zero-modes

In section 5.5.1 we expressed the zero-modes in terms of 2 sets of functions $E_\mu^{(a)}$ and $\tilde{E}_\mu^{(a)}$ where the label a runs from 1 to N. With the aid of the formulas of the previous subsection one can compute these functions.

Let us start with the computation of $E_\mu^{(a)}$ defined in Eq. (5.101). Using the definitions of u_a and ω_a of the previous subsection it can be re-expressed as

$$E_\mu^{(a)} = \frac{i}{2} F^{-1/2} \int dz\, u_a^\dagger(z) \bar{\sigma}_\alpha \hat{\partial} \omega_a(z) F^{1/2} + \text{h.c.} \tag{A.27}$$

To obtain the corresponding expression one must perform the integration in z. Notice that all the z dependence of u_a and ω_a enters through the $\Psi_a^\pm$ functions. Their integrals can be performed analytically leading to the expression

$$I_\alpha^\pm = \int dz \Psi_b^{+\dagger} \bar{\sigma}_\alpha \Psi_a^\pm = \delta_{ab} \frac{m_a}{2\pi} (\mathcal{P}_\pm^{a\,\alpha} \frac{1}{g(m_a r_a)} + \mathcal{P}_\mp^{a\,\alpha}) \,, \tag{A.28}$$

One needs in addition the following integral

$$\widetilde{I}_\alpha = 4\pi i \int dz (z - Z_M^a) \Psi_b^{+\dagger} \bar{\sigma}_\alpha \Psi_a^+ = \delta_{ab} \frac{m_a^2}{2\pi} \left(\frac{g'(m_a r_a)}{g^2(m_a r_a)} \right) \mathcal{P}_+^{a\,\alpha}(i\hat{n}_a) \,, \tag{A.29}$$

In the final expressions we have introduced the quaternions

$$\mathcal{P}_\pm^{a\,\alpha} = \frac{1}{2} (\bar{\sigma}^\alpha \pm \hat{n}_a \bar{\sigma}^\alpha \hat{n}_a) \,, \tag{A.30}$$

where $\hat{n}_a$ and $g(u)$ have been defined in Eqs. (A.9) and (A.10).

Using the previous formulas and those of the first subsection of the appendix we arrive at

$$E_\mu^{(a)} = \frac{i}{2} F^{1/2} \mathcal{W}^\dagger \mathcal{L}_{a\alpha} \mathcal{W} F^{1/2} + \frac{i}{2} F^{1/2} \mathcal{W}^\dagger \widetilde{\mathcal{L}}_a \bar{\sigma}_\alpha \hat{\partial} \mathcal{W} F^{1/2} + \text{h.c.} \tag{A.31}$$

where

$$\mathcal{L}_{a\alpha} = -\frac{i m_a g(m_a r_a)}{2\pi} e_a \left(-i \frac{g^2(m_a r_a) - 1}{2 m_a^2 r_a^2} \mathcal{P}_+^{a\,\alpha} - i \frac{g'(m_a r_a)}{2 m_a r_a} \mathcal{P}_-^{a\,\alpha} \right) e_a^\dagger \tag{A.32}$$

and

$$\widetilde{\mathcal{L}}_a = \frac{-i g(m_a r_a)}{4\pi m_a r_a} e_a \hat{n}_a \left(g(m_a r_a) \tilde{e}_a^\dagger + e_a^\dagger \right) \tag{A.33}$$

Using the relation between the quantity inside parenthesis in Eq. (A.32) with the gauge field of a SU(2) BPS monopole we can write this first term as

$$\sum_a E_i^{\text{BPS}}(x - X^a; m_a) I_i^a \tag{A.34}$$

where we have introduced the $N \times N$ hermitian matrices I_i^a given by

$$I_i^a = \frac{g(m_a r_a)}{2\pi m_a} F^{1/2} \mathcal{W}^\dagger e_a \tau_i e_a^\dagger \mathcal{W} F^{1/2} \tag{A.35}$$

they provide an embedding of the SU(2) group in SU(N).

In this way all our formulas are expressed in terms of the values of $\omega(Z_b) = \mathcal{W}_b$. The latter can be expressed in terms of the matrix V defined in the first subsection of the appendix. The same quantities also appear in the expression of $\tilde{E}_\mu^{(a)}$, as shown in Eq. (5.103).

Notice that the electric field strength is a particular case of the previous formula, since $E_i = \sum_a E_i^{(a)}$.

A.3 Anti-periodic zero-mode formulas

The corresponding expressions for the anti-periodic zero-modes are considerably more involved, although again the integrals appearing in Eq. (5.119) can also be performed analytically. The main difference with respect to the periodic case is that in the latter each mode in the basis depends on a single region (Z_{a-1}, Z_a) associated to a given constituent monopole. The formula only depends on the remaining monopole positions through the matrix F. In the anti-periodic case, the expressions involve pairs of monopoles, namely those pairs such that

$$(Z_{a-1}, Z_a) \cap (Z_{b-1} + \frac{1}{2}, Z_b + \frac{1}{2}) \neq \emptyset \tag{A.36}$$

The condition can be easily implemented if we introduce $\chi_{\bar{b}}$ as the characteristic function of the interval $(Z_{b-1} + \frac{1}{2}, Z_b + \frac{1}{2})$. Then, one can rewrite

$$\hat{\Psi}_{12}^a(z) \equiv \sum_{b\,c} \hat{\Psi}_{12}^{abc}(z) = \sum_{b\,c} \chi_b \chi_{\bar{c}} \exp\{2\pi\tau_i (X_i^b - X_i^c) z\} \kappa_{abc} \tag{A.37}$$

where the coefficient matrices κ_{abc} follow from simple linear relations in terms of $\mathcal{U}_{AB}$ and $\kappa_\pm^A$. Notice then that, due to the characteristic functions, the integrals appearing in the expression of the anti-periodic zero-modes Eq. (5.119) only involve integrals of $\hat{\Psi}_{12}^{abc}(z)$ with u_b and ω_c. Using appropriate matrix projections, these integrals reduce to those of ordinary exponentials. The details are somewhat cumbersome and we will skip them here.

Appendix B

Computing the low-lying spectrum of the Dirac operator

Nowadays, the complete diagonalization of the overlap operator has a computational cost too expensive when the volumes are large. As it was pointed out in 6, many interesting problems are dominated by the low-lying part of the spectrum. There are several numerical techniques in order to compute only a few eigenvalues and eigenvectors. We are going to use the conjugate gradient method proposed in [98]. In this method, it is necessary to minimize the Ritz functional to be able to find the kth eigenvector,

$$\mu(z) = \frac{\langle z, Az\rangle}{\langle z, z\rangle}, \tag{B.1}$$

where $z \neq 0$ and orthogonal to the space of the $k-1$ lower eigenvectors. It is necessary to have an hermitian and positive defined operator, so we are going to use $(\gamma_5 \not{D})^2$. A detailed implementation can be found in [98]. We would like to remark some questions referent to its implementation in the adjoint representation. As described in section 4 in the adjoint representation, eigenvectors can be paired and written as 2-vector quaternions.

Firstly, it is taken the CP symmetry, Eq. 4.3, to group each eigenvector ψ_λ and its CP-transform ψ^C_λ in a pair as a 2-dimensional quaternion vector

$$\Psi = (\psi_\lambda, \psi^C_\lambda) = \begin{pmatrix} \psi^\mu_+ \sigma_\mu \\ \psi^\mu_- \sigma_\mu \end{pmatrix}. \tag{B.2}$$

where $\psi^a_\pm$ are real numbers. Writing the gamma matrices in terms of sigma matrices as

$$\not{D} = \begin{pmatrix} 0 & \sigma_\mu D_\mu \\ \bar{\sigma}_\mu D_\mu & 0 \end{pmatrix}, \tag{B.3}$$

the Dirac operator can be thoughted as a 2×2 quaternion operator over a 2-vector quaternion space. In our implementation the overlap operator is used as the lattice Dirac operator. The eigenvalues of GW operator are complex numbers, in this notation they appear

as quaternions. Since the product of quaternions is non commutative the eigenvector equations must be written in the correct order as

$$D\Psi_\lambda = \Psi_\lambda q_\lambda. \tag{B.4}$$

In the CG algorithm, it is necessary to compute dot products. In this case, we would like to remark our definition of the "dot product" in this case. We are working on the quaternionic field and in the complex field. So, our definition of dot product is an application

$$\langle , \rangle : Q^n \times Q^n \to Q. \tag{B.5}$$

Taken the σ_μ matrix representation for quaternions, the dot product of two quaternionic bi-spinors in the adjoint representation of the $SU(N)$ gauge group is done by

$$\langle A, B \rangle = a^{\mu a \alpha} b^{\nu a \alpha} \bar{\sigma}_\mu \sigma_\nu = c_\mu \sigma_\mu \tag{B.6}$$

where $A = a^{\mu a \alpha}\sigma_\mu$, $B = b^{\mu a \alpha}\sigma_\mu$, $\alpha = 1, 2$ and $a = 1, ..., N^2 - 1$.

This representation presents some computational advantages, an eigenvector and its CP-transform is computed and stored at the same time with only eight real numbers. Reminding that the adjoint representation of $SU(N)$ are real matrices, the gradient conjugate can be implemented completely with real numbers. Finally, in order to compute the $k - th$ eigenvector, an orthogonal base of the $k - 1 - th$ lower eigenvectors must be done. In this sense, the usual method of Graham-Smith must be written in the correct order as

$$\Psi_n^\perp = \Psi_n - \sum_i^{n-1} \Psi_i q_i, \quad q_i = \langle \Psi_n, \Psi_i \rangle . \tag{B.7}$$

Appendix C

Locality properties of the spectrum of the Adjoint Neuberger-Dirac

In this Appendix, we test two cases where the computation of the spectrum of the Neuberger-Dirac operator presents some problems. The firs one is related with small instantons ($\rho/a < 2$). We observe that the number of zero-modes does not correspond with the index theorem in this case. In order to analyse this problem, a set of instantons with size between 2.3 and 1.5 are generated from a smooth instanton configuration and the cooling algorithm. The four lowest eigenvalues of the operator H_+^2 are is displayed in Fig. C.1 as a function of the instanton size. The Index Theorem predicts two quaternionic zero-modes for these configurations. As can be seen in Fig. C.1, when the instanton is smaller than $2a$ only one eigenvalues is compatible with a zero-mode. For instantons of size smaller than $1.6a$ no zero-modes are present. The size of the instanton where the first zero-mode disappears is a function of the mass used in the implementation of the Neuberger-Dirac operator. In Fig.C.3 are displayed the critical value of ρ/a as function of the Wilson mass. The optimal values are obtained in the range $m_{WD} \approx 1.4 - 1.5$. This mismatch in the number of zero-modes is clearly associated to the roughness of the configuration. This can be quantified through the admissibility condition that should be imposed in order to guarantee locality of the overlap operator [32]. This condition, written in terms of the plaquette $U(p)$, reads

$$\|1 - U(p)\| \leq \varepsilon(m_{WD})\,. \tag{C.1}$$

Fig. C.2 shows the number of plaquettes that violate Eq. C.1, as a function of instanton size for the configurations presented in Fig. C.3. There is a clear link between configurations with wrong number of zero-modes and those that violate the admissibility condition. To stress it further we have analysed the location of 'wrong plaquettes'. Fig. C.4 shows that they are localized around the maximum of the action density where the configuration becomes rougher for small instantons.

The second problem appears when the spectrum is computed for rough configurations.

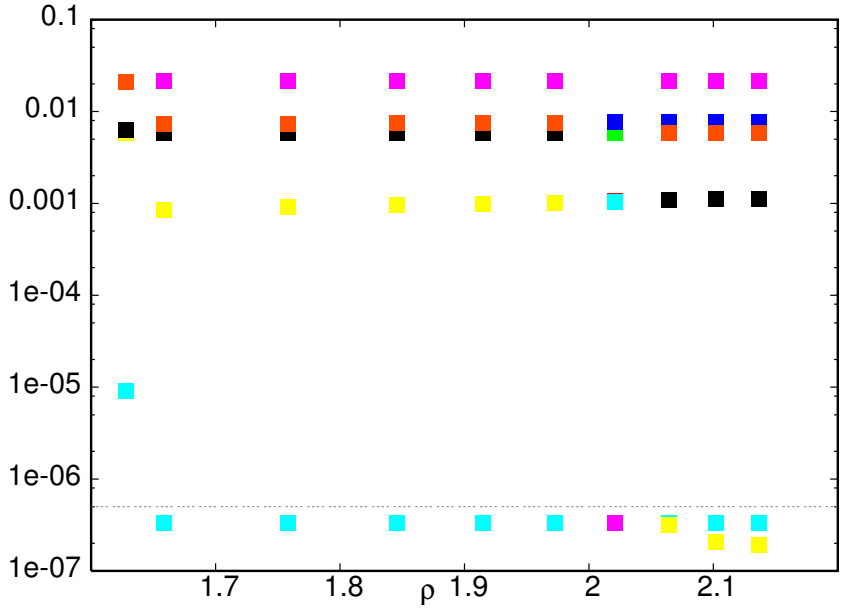

Figure C.1: Spectrum of $D_{ov}(m_{WD}=1.4)$ versus the instanton size in lattice units. Points below the line are doubly degenerate and compatible with zero.

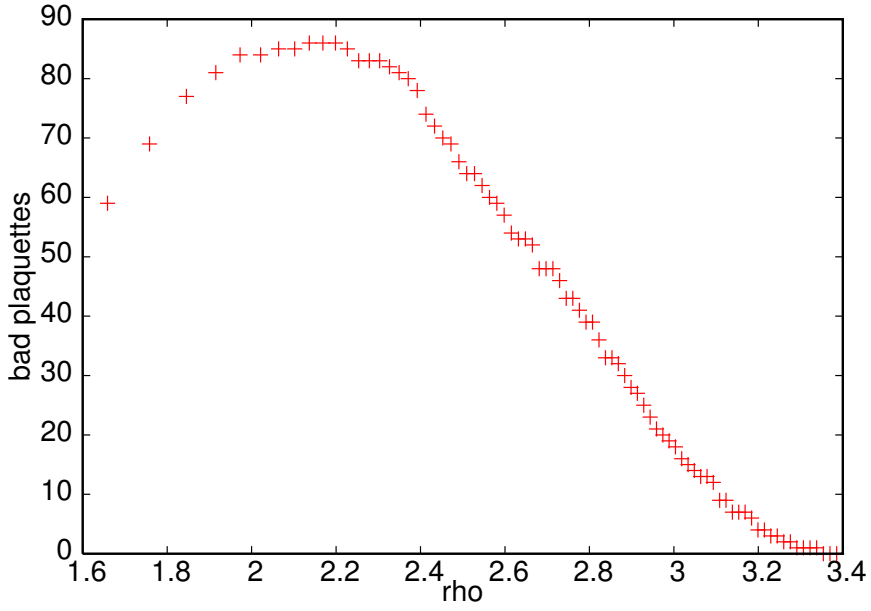

Figure C.2: Number of plaquettes that violate the admissibility condition Eq. (4.1) in terms of the instanton size. $\epsilon(1) = 1/30$.

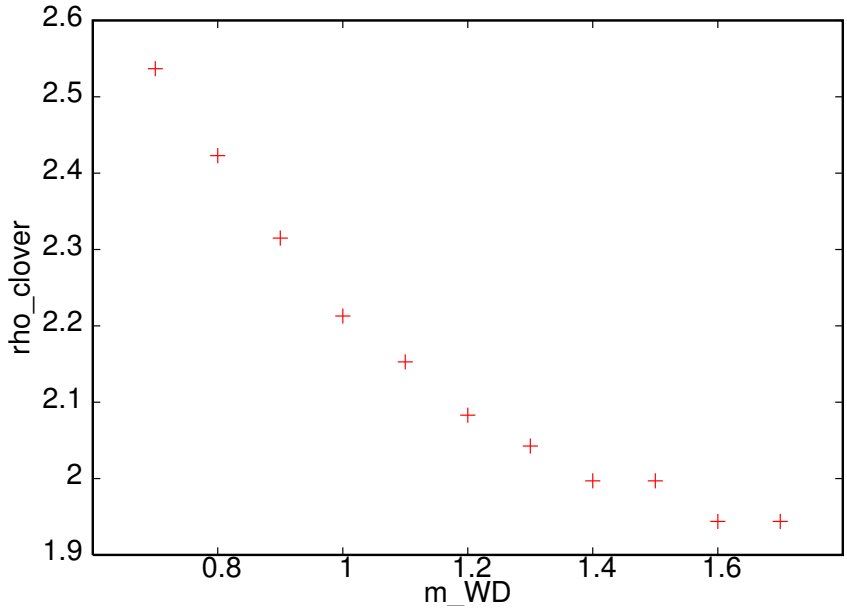

Figure C.3: Dependence of ρ_c on the mass of the overlap operator. ρ_c is the critical size (in lattice units) below which the spectrum has 2 zero modes.

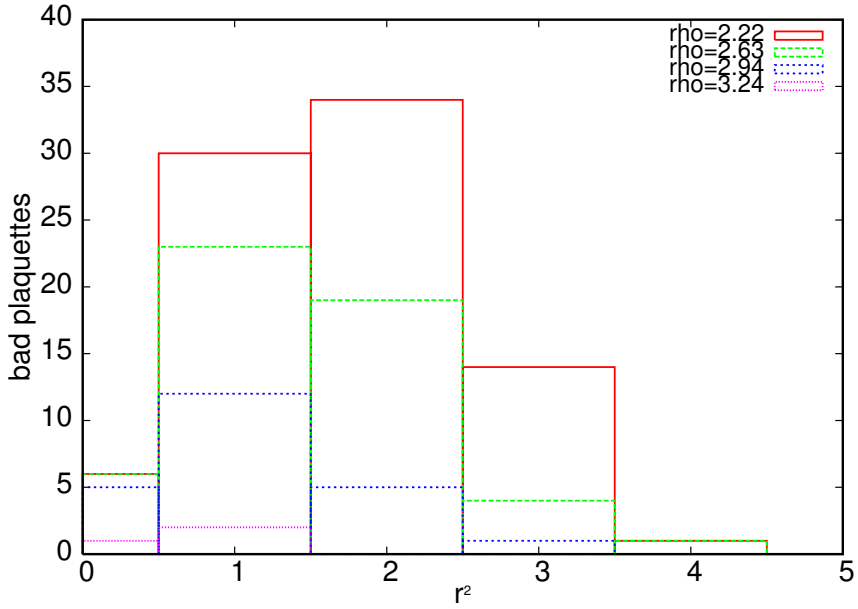

Figure C.4: Number of plaquettes that violate the admissibility condition vs distance from the maximum of the action density, for several instanton sizes.

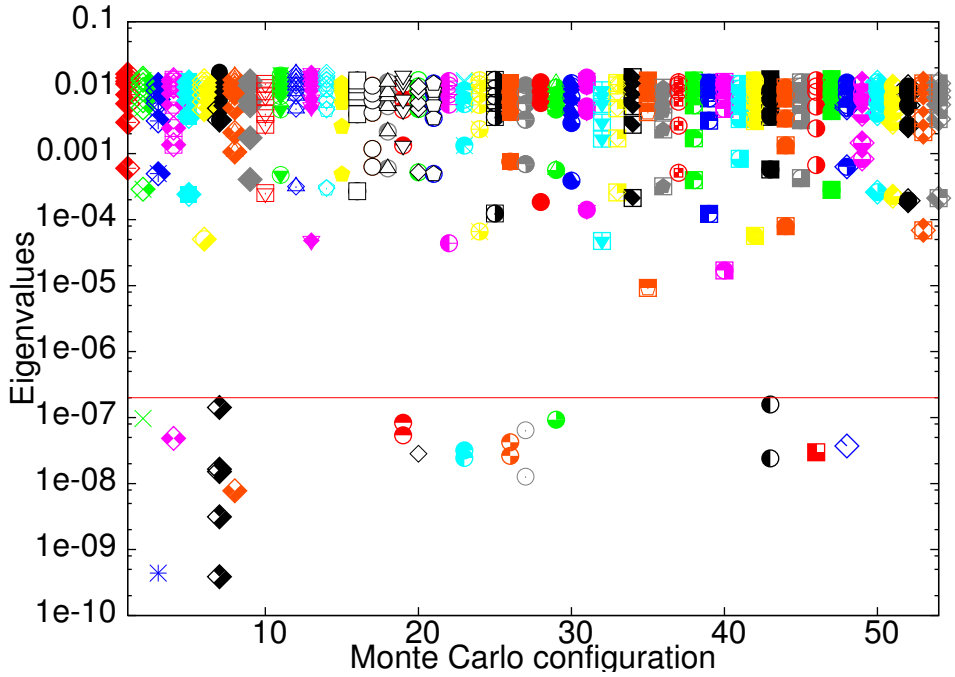

Figure C.5: Spectra of $D_{ov}(m_{WD}=1.4)$ for the Monte Carlo configurations. Points below the straight line are compatible with zero.

We have started analysing configurations extracted from a $SU(2)$ thermalized ensemble. They have been generated with the Wilson plaquette action, on a 12^4 lattice for $\beta = 2.57$ ($a = 0.08$ fm). Two sweeps of cooling are applied before compute the spectrum. For fifty Monte-Carlo configurations we have extracted the twelve lowest eigenvalues and eigenvectors. The eigenvalues are collected in Fig. C.5, showing a clear gap between zero and non-zero-modes. A histogram of the number of zero-modes is presented in Fig. C.6. Surprisingly, a significant fraction of the configurations shows only two zero modes, while the continuum index theorem predicts $4N$, $N \in \mathbb{Z}$. This mismatch was previously reported by Edwards, Heller and Narayanan [99], who interpreted it as an evidence for fractional topological charge (not expected on the continuum for the periodic boundary conditions used). Contrary to their belief, we will argue that this effect is an artefact associated to the roughness of the lattice configurations. Note that this mismatch is irrelevant if the set of rough configurations has zero measure in the continuum limit. Our $\beta = 2.57$ set has been generated with the SU(2) Wilson action. Indeed for this action, general arguments, due to Pugh and Teper [100], indicate a divergent contribution of small instantons in the continuum limit. The problem can be avoided by using an improved action for the Monte-Carlo generation and by tuning the mass in the overlap operator. Similar artefacts in the spectrum of the overlap Dirac operator in the fundamental representation have been reported in [101, 64]. All this is an indication that the use of improved actions might be essential even for the computation of global quantities as the topological susceptibility.

In the last two years, two works [102, 103] have been published about the presence of

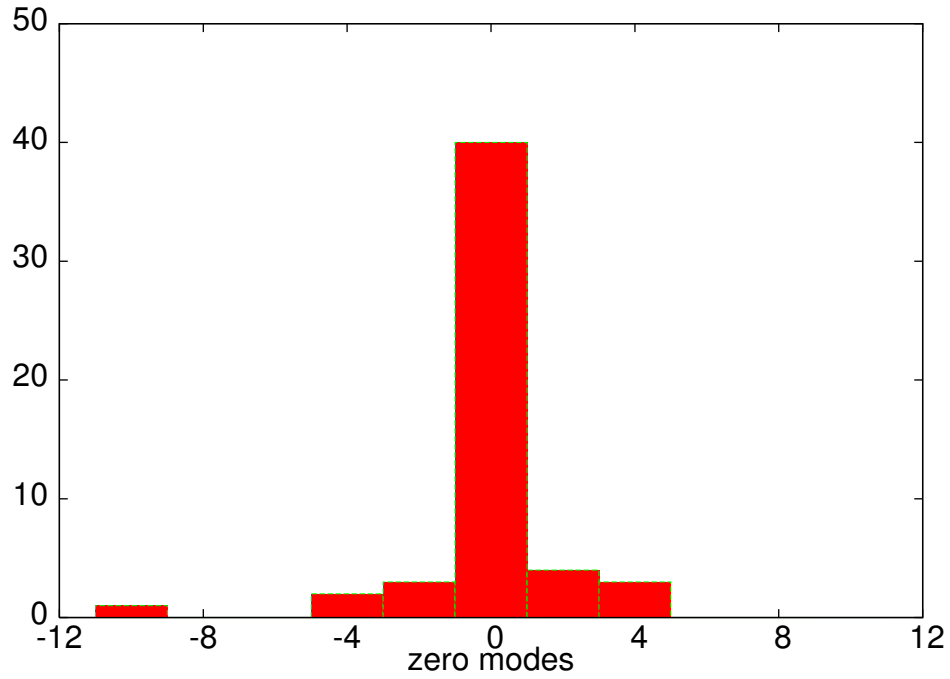

Figure C.6: Histogram of the number of configurations with a given number of zero modes. Negative number corresponds to negative chirality.

objects with topological fractional charge in Monte Carlo simulations. In the first one, the authors found that the configurations with a incorrect number of zero-modes vanishing when the β value increase, so this mismatch corresponds with a lattice artefact. Finally from this result they concluded that objects with fractional topological charge are present in the continuum limit. We do not agree with this part, since there are configurations like calorons composed by objects with fractional charge that fulfil the Index Theorem. In the second paper, the authors claim that can build a smooth configuration with fractional topological charge and non-twisted boundary condition. This result violets the Index Theorem and we do not understand it.